Response to Review n.1

November 25, 2019

General comments

General comments: The abstract is very long and contains too many information. Suggest to re-write it in a more concise way. The same comment is valid for the chapter 3.3.1 Window of opportunities, here there are interesting observations, but sometimes slightly verbose. The authors indicate that the active sediments are influenced by "deep methane source", then at the end of the paper they define that the deep methane source is ca 3 m below the seafloor, which is not exactly very deep. Would it be possible to find another term instead of "deep"? In any case, this has to be better defined at the beginning of the manuscript

Response

We would like to thank the reviewer for the overall positive comment and suggestions. We will revise the abstract and the section 3.3.1 *Window of opportunity* for the final version of the paper.

In addition, we will also clarify the term "deep". We used the term "deep" to refer to methane sources below the simulated sediment column (*i.e.* > 3 m) not investigating the precise origin of this methane (permafrost/hydrates/thermogenic sources/in situ production) at the base of the sediment column (which could also come from even deeper depths). But we do agree that we must refer more clearly to the base of the sediment column.

Specific comments

1. Page 2 Lines 17-18: "Under these conditions, permafrost aggraded on the shelf and was subsequently submersed when rising sea level flooded the shelf during the Holocene sea transgression (12 and 5 kyr BP)". Reference is needed
   Response: We added a reference to Romanovskii and Hubberten, 2001; Romanovskii, Hubberten, et al., 2005, for the thickness after submersion and Bauch et al., 2001 for the sea transgression.

2. Page 2 Line 19: explain what is"gas hydrate"
Response: a state of matter in which a low molecular weight gas (like CH_4) is trapped in a "cage" of water molecules and whose structure is thermodynamically stable under specific temperature-pressure-salinity conditions that are found either in oceanic depths or beneath the permafrost (Sloan Jr et al., 2007). We will integrate a definition in the revised version of the manuscript..

3. Page 2 Lines 29-30:"The increasing influx of warmer Atlantic water into the Arctic Ocean - the so-called Atlantification". This term need to be explained and relevant papers need to be cited. In both "Zhang et al., 1998; Biastoch et al., 2011" the term Atlantification is not mentioned.
Response: the influence of warmer and saltier waters of Atlantic origins has been identified and brought up to the attention of the scientific community already in Biastoch et al., 2011; Carmack et al., 1995; Zhang et al., 1998, but the term "Atlantification" appears only in Polyakov et al., 2017 and Barton et al., 2018. These reference will be added in the revised version of the manuscript.

4. "Page 2 Line 2: what destabilize gas hydrate? Pressure changes or temperature increase? Or what?"
Response: both pressure and temperature change are responsible of gas hydrates destabilization as reported in paragraph 3.3 of Shakhova, Semiletov, and Chuvilin, 2019. It has been suggested that in the case of subsea permafrost associated gas hydrates, temperature plays a more important role gas hydrate destabilization (Chuvilin et al., 2018; Makogon et al., 2007).

5. Page 4 Line 6: which are the"changes in environmental condition" mentioned here?
Response: The transient change in lower CH_4 boundary conditions and, in case of the seasonal scenario n.2, also the change in the upper boundary conditions of SO_4^{2-}. We will clarify this point in the revised version of the manuscript.

6. Page 4 Line 12: for methane emissions and fractures, it might be useful to read a recently published paper in Biogeosciences "Yao et al., 2019". Biogeosciences, 16, 2221-2232, 2019.
Response: Thanks for the suggestion. The recommend paper indeed supports our understanding of methane transport and biogeochemistry in fracture-affected sediments and we will add a reference to the revised version of the manuscript.

7. Rage 4 Line 19: What are the "passive and active sediment"? Although there is some explanation later in the manuscript, these concepts need to be explained here, as soon as they are mentioned in the text.

Response: "Passive sediments" are sediments characterized by the absence of an advective water flow. In contrast, "active sediments" are subject to a non-zero water flow pointing upwards towards the sediment-water interface. The definition in the paper is reported at page 5, line 18-19. We will define these terms earlier in the revised version of the manuscript.

8. Page 6 Line 15: what about the anaerobic oxidation of methane?
Response: The aerobic and the anaerobic oxidation of methane have been regarded as secondary redox reaction, as they are not directly involved in the degradation of the organic matter. They are described in detail later on (page 6, line 32 and page 7).

9. Page 9 Line 10: why the authors have assumed both baseline scenarios a water depth of 30 m when the average water depth of the ESAS is ∼45 m (data from James et al., 2016)?
Response: mainly for two reasons:

   - **We do not expect a large difference in the results between 30 or 45 meters, as well as if we had used 60 m. The mechanisms we identify and the sensitivity we explore is expected to be largely unaffected by such small changes in the water depth. Results indicate that one of the main controls on non-turbulent methane escape is the sedimentation rate ω. Applying the formulation of Burwicz et al., 2011, ω has basically the same value for 30 m and 45 m water depth. The only factor which is sensitive to water depth is the saturation value of methane ($[CH_4]^*$). At a water depth of 30 m, $[CH_4]^* = 5.45$ μM as opposed to ~ 10 μM at 45 m. This last value might increase even more the efficiency of the biofilter, leading in case simply to a reduction of the maximum CH_4 we identified.**
   - **The observed increase in summer temperature (Dmitrenko et al., 2011) occurs at shallower depths (~ 10 m). We wanted to investigate even shallower shelves, as they are the ones expected to be more delicate and active from the biogeochemical point of view. For this reason we set a depth halfway between the average value of 45 m (which takes into account also deeper depths, not really important for methane emissions) and shallower shelves closer to the coast.**

10. Page 10 Line 28: is the trawling in the area affecting gas hydrate stability also? Is the gas hydrate close to the seafloor? Where is the real sediment depth? Which is the thickness of the sediments that is affected by trawling? Few cm or maybe 1 meter?
Response: On the Siberian shelf, gas hydrates are often associated with subsea permafrost (the so called subsea permafrost associated gas hydrates, Ruppel et al., 2017) and are located below the subsea

permafrost. Trawling can affect sediments: from centimeters to meters to a few meters (Shakhova, Semiletov, Gustafsson, et al., 2017) and, thus, is not expected to exert a significant effect on hydrate stability. In any case, we do not simulate subsea permafrost thawing or hydrate destabilization explicitly, but rather explore the fate of plausible methane fluxes from such deep sources and therefore do not make assumptions about release mechanisms and drivers.

11. Page 17 Line 13:"rapidely".
Response: Thanks. Typo corrected

12. Page 23 lines 26-29: Would it be possible to better explain this concept here? I found very difficult to follow the reasoning here and related gas saturation concentration with precipitation of authigenic carbonates.
Response: Thanks. We will revise this section to clarify these aspects.

13. Page 24 Line 28: Lena river and Moustakh Island in the Buor-Khaya Gulf need to be included in Figures and captions. As a general rule, all the locations that are mentioned in the main text need to be reported in location maps and relative captions.
Response: The revised version of the manuscript will include a map reporting the mentioned locations.

14. Page 26 Lines 16-17: The authors indicate that Additional physical reworking such as ice scouring or dredging, or the absence of bioirrigation, which is known to be patchy in Arctic sediments could even further reduce estimated methane efflux. I would assume that these processes might enhance the methane fluxes instead since they remobilize sediments. More elaboration is needed here.
Response: The effects of non-local mixing processes are complex. They can indeed increase fluxes by enhancing transport through the sediment. However, they can also reduce fluxes of methane (and other reduced species) by increasing the flux of oxygen and sulfate into the sediment. We will revise this section to clarify this point.

15. Page 26 Line 25: "Artic's".
Response: Thanks. Typo corrected

16. How does it happen that "increasing sedimentation rates occur through coastal erosion"? please clarify.
Response: Coastal erosion and the erosion of coastal ice complex provide an input of debris and sediments which are sink rapidly to the sea floor (Vonk et al., 2014). Areas close to the coast are affected by coastal erosion and will thus receive a higher input of terrigeneous material.

17. Page 28 Lines 33-34: "we show that methane from deep sources (ca. 3 m) reaches the sediment water interface within 7 to 20 years." A comment on the fact that

3 meters is considered deep has been previously reported.
Response: see comment above

18. Page 29 Line 29: wording "which is in turn is determined".
Response: Thanks. Corrected.

19. Chapter 3.3.1 this chapter is not very well organized and it is difficult to follow.
Response: We will carefully revise this section.

20. Page 33 Lines 25-26: "On the ESAS, AOM is a transport-limited process and transport parameters thus exert an important control on the efficiency of the AOM biofilter and, thus, on methane efflux". Please rewrite in a more clear way.
Response: Since AOM is a transport-limited process, transport processes and parameters exert a dominant control on the efficiency of the AOM biofilter and, ultimately, on the methane efflux at the SWI. We will revise the section accordingly.

21. Page 33 line27: what does "sedimentation and active fluid flow" in brackets mean respect the advective transport?
Response: We simply list the two possible types of advective transport considered.

References

Barton, Benjamin I, Yueng-Djern Lenn, and Camille Lique (2018). "Observed Atlantification of the Barents Sea causes the Polar Front to limit the expansion of winter sea ice". In: *Journal of Physical Oceanography* 48.8, pp. 1849–1866.

Bauch, Henning A, Thomas Mueller-Lupp, Ekaterina Taldenkova, Robert F Spielhagen, Heidemarie Kassens, Peter M Grootes, Jörn Thiede, J Heinemeier, and VV Petryashov (2001). "Chronology of the Holocene transgression at the North Siberian margin". In: *Global and Planetary Change* 31.1-4, pp. 125–139.

Biastoch, Arne, Tina Treude, Lars H Rüpke, Ulf Riebesell, Christina Roth, Ewa B Burwicz, Wonsun Park, Mojib Latif, Claus W Böning, Gurvan Madec, et al. (2011). "Rising Arctic Ocean temperatures cause gas hydrate destabilization and ocean acidification". In: *Geophysical Research Letters* 38.8.

Burwicz, Ewa B, LH Rüpke, and Klaus Wallmann (2011). "Estimation of the global amount of submarine gas hydrates formed via microbial methane formation based on numerical reaction-transport modeling and a novel parameterization of Holocene sedimentation". In: *Geochimica et Cosmochimica Acta* 75.16, pp. 4562–4576.

Carmack, Eddy C, Robie W Macdonald, Ronald G Perkin, Fiona A McLaughlin, and Richard J Pearson (1995). "Evidence for warming of Atlantic water in the southern Canadian Basin of the Arctic Ocean: Results from the Larsen-93 expedition". In: *Geophysical Research Letters* 22.9, pp. 1061–1064.

Chuvilin, Evgeny, Boris Bukhanov, Dinara Davletshina, Sergey Grebenkin, and Vladimir Istomin (2018). "Dissociation and self-preservation of gas hydrates in permafrost". In: *Geosciences (Switzerland)* 8.12. ISSN: 20763263. DOI: 10.3390/geosciences8120431. URL: https://www.mdpi.com/2076-3263/8/12/431.

Dmitrenko, Igor A, Sergey A Kirillov, L Bruno Tremblay, Heidemarie Kassens, Oleg A Anisimov, Sergey A Lavrov, Sergey O Razumov, and Mikhail N Grigoriev (2011). "Recent changes in shelf hydrography in the Siberian Arctic: Potential for subsea permafrost instability". In: *Journal of Geophysical Research: Oceans* 116.C10.

Makogon, Y. F., S. A. Holditch, and T. Y. Makogon (2007). "Natural gas-hydrates - A potential energy source for the 21st Century". In: *Journal of Petroleum Science and Engineering* 56.1-3, pp. 14–31. ISSN: 09204105. DOI: 10.1016/j.petrol.2005.10.009. URL: https://www.sciencedirect.com/science/article/pii/S0920410506001859.

Polyakov, Igor V, Andrey V Pnyushkov, Matthew B Alkire, Igor M Ashik, Till M Baumann, Eddy C Carmack, Ilona Goszczko, John Guthrie, Vladimir V Ivanov, Torsten Kanzow, et al. (2017). "Greater role for Atlantic inflows on sea-ice loss in the Eurasian Basin of the Arctic Ocean". In: *Science* 356.6335, pp. 285–291.

Romanovskii, Nikolai N and H-W Hubberten (2001). "Results of permafrost modelling of the lowlands and shelf of the Laptev Sea region, Russia". In: *Permafrost and periglacial processes* 12.2, pp. 191–202.

Romanovskii, Nikolai N, H-W Hubberten, AV Gavrilov, AA Eliseeva, and GS Tipenko (2005). "Offshore permafrost and gas hydrate stability zone on the shelf of East Siberian Seas". In: *Geo-marine letters* 25.2-3, pp. 167–182.

Ruppel, Carolyn D and John D Kessler (2017). "The interaction of climate change and methane hydrates". In: *Reviews of Geophysics* 55.1, pp. 126–168.

Shakhova, Natalia, Igor Semiletov, and Evgeny Chuvilin (2019). "Understanding the Permafrost–Hydrate System and Associated Methane Releases in the East Siberian Arctic Shelf". In: *Geosciences* 9.6, p. 251.

Shakhova, Natalia, Igor Semiletov, Orjan Gustafsson, Valentin Sergienko, Leopold Lobkovsky, Oleg Dudarev, Vladimir Tumskoy, Michael Grigoriev, Alexey Mazurov, Anatoly Salyuk, et al. (2017). "Current rates and mechanisms of subsea permafrost degradation in the East Siberian Arctic Shelf". In: *Nature communications* 8, p. 15872.

Sloan Jr, E Dendy and Carolyn Koh (2007). *Clathrate hydrates of natural gases*. CRC press.

Vonk, Jorien E, Igor P Semiletov, Oleg V Dudarev, Timothy I Eglinton, August Andersson, Natalia Shakhova, Alexander Charkin, Birgit Heim, and Örjan Gustafsson (2014). "Preferential burial of permafrost-derived organic carbon in S iberian-A rctic shelf waters". In: *Journal of Geophysical Research: Oceans* 119.12, pp. 8410–8421.

Zhang, Jinlun, D Andrew Rothrock, and Michael Steele (1998). "Warming of the Arctic Ocean by a strengthened Atlantic inflow: Model results". In: *Geophysical Research Letters* 25.10, pp. 1745–1748.

Response to Review n.2: Volker Brüchert

November 25, 2019

General comment

"I have a lot of respect for the sophisticated details of the diagenetic reaction-transport model BRNS described in the manuscript by Puglini et al. It is a sophisticated, well-established model framework and has been used in many important publications, not the least already in the sensitivity analysis of anaerobic oxidation of methane in many different marine settings. This study takes advantage of the long developmental work that has been done previously with respect to AOM with this model. Here it is used to simulate sediment methane cycling for one of the big hotspots for potential future marine methane emissions - the East Siberian shelf sea, with its potential for thawing submarine permafrost and the potential presence of gas hydrates (although the presence of both is often contested in the literature for good reasons)."

Response: We would like to thank the reviewer for his appreciative, extremely constructive and insightful comment that not only sheds light on some critical aspects of our manuscript and helps to improve the quality of the manuscript, but also provides an opportunity to provide important clarifications and/or further detail.

Here we would like to stress that we included in the model a methane source from below (assuming different methane concentration spanning the range from 0 to the saturation concentration) which is supposed to resemble any kind underlying source. Our focus is in the upper 3 m of the sediments and we do not investigate and/or specify any explicit origin of the methane coming from below nor the model is, in such a version, sensitive to this origin. Since the area of interest is the ESAS, we hypothesize that subsea permafrost or gas hydrates may be the origin of such methane, but no results rely on this specific assumption. In fact we just wanted to stress the potential character of the non-turbulent methane emissions we found.

"The model uses the conventional setup of a network of biogeochemical reactions directly or indirectly coupled to the degradation of organic matter deposited at the sea floor. The paper is mostly not about the Siberian shelf, but is a very thorough assessment of AOM dynamics with explicit treatment of upward flow, bioenergetics controls of AOM, and a complex reaction network of biogeochemical redox reactions

as they may occur in Siberian shelf sediment"
Response: While the reviewer is absolutely right in pointing out that the results of the comprehensive sensitivity study described in the manuscript are universally valid, we would like to stress that the model setup and the sensitivity study have been specifically designed with the aim of assessing the fate of dissolved methane released from a deep source (*e.g.* dissociating hydrates or thawing subsea permafrost) in warming Siberian Shelf sediments. More specifically:

- **The model is forced with a variable flux of dissolved methane potentially originating from dissociating methane hydrates and/or thawing permafrost in the deeper sediment. The methane flux is constrained by assuming lower model boundary methane concentrations ranging from 0 to a maximum concentration that is constrained by the saturation of dissolved CH_4 under pressure, temperature and salinity conditions encountered on the Siberian shelf.**

- **All model boundary conditions, forcings and parameters (Tables S5 and S6) are chosen to be representative of environmental conditions encountered on the Siberian shelf.**

- **The range of boundary conditions and parameters tested in the steady state sensitivity study are constrained based on data compiled for the Siberian shelf.**

As a consequence, the study presented here does not cover the entire range of possible conditions (*e.g.* methane fluxes, active fluid flow, organic carbon concentrations etc.) encountered at the global ocean seafloor, but is representative for conditions (likely) encountered on the present and future Siberian Shelf.

"The manuscript is well written up section 3.3.1., after which it deteriorates conspicuously"
Response: We agree that the logical structure of section 3.3.1 could be improved and have carefully revised this part.

"In principle, there were two objectives: 1. Broadscale simulation of AOM dynamics: It does a very good job at simulating a range of broadly set environmental conditions with direct impact on the filter efficiency of anaerobic methane-oxidizing microbial consortia that use methane and sulfate. The range of the environmental conditions is set broad enough to encompass conditions that may be encountered on the East Siberian shelf. However, this part is not very novel and AOM dynamics and filter efficiency have been reviewed by Regnier et al. (2011) previously. Therefore all sections of the manuscript that relate to the simulation tests should be significantly shortened."
Response: We strongly disagree with this comment. Regnier et al., 2011 present a comprehensive review of previously developed models that have

been applied to investigate a large employed to simulate a large set of diverse depositional environments affected by intense methane cycling, ranging from mud volcanoes and active seeps to passive sediments experiencing groundwater discharge or high organic matter inputs. The review explicitly explores how different model implementations/formulations (with increasing complexity of the biogeochemical network) perform in simulating methane-affected sediments, as well as explore simulated AOM efficiency in response to a discrete, non-specific set of environmental conditions considered in these models.

However, the analysis of AOM filter efficiency and CH_4 effluxes presented has a completely different focus and goes well beyond the analysis presented in Regnier et al., 2011. As pointed out above, the main aim of this model study is to specifically investigate the potential escape of dissolved methane released from a deep source (*e.g.* dissociating hydrates or thawing subsea permafrost) from warming Siberian Shelf sediments. It thus assesses the efficiency of the microbial AOM filter in attenuating potential dissolved permafrost/hydrate methane fluxes under a continuous and specifically chosen range of environmental conditions/scenarios (likely) encountered on the present and (idealized) future Siberian shelf using an identical model set-up and thus offering not only more robust theoretical consistency and comparability. The main focus of the presented sensitivity analysis lies on identifying environmental conditions (and thus potential areas on the Siberian Shelf) that favor non-turbulent dissolved methane fluxes across the sediment-water interface.

We further emphasized this point in the manuscript by modifying the introduction and abstract accordingly.

"2. Regional application: The second part of the manuscript is the application of the model to the East Siberian shelf. I found this part the more relevant one, given the title, but unfortunately also less well constrained due to the paucity of data used to constrain their model in face of the diversity and size of the targeted marine region. For reference, my guess is that the authors would certainly not model the whole of the North Sea or the Baltic Sea with this model, two marginal seas of similar size or even smaller than the Laptev Sea"

Response: We also disagree with this statement. One strength of a models is that it can provide the explorative means to assess dynamics at spatial/temporal scales that cannot easily be assessed by observations alone. In particular, transfer functions, simple look-up tables and/or neural networks that are derived from or trained on a large ensemble of individual model simulations over a broad range of plausible boundary conditions have been frequently and successfully used to investigate regional and even global dynamics.

For instance, Gypens et al., 2008, Dale, Nickelsen, et al., 2015, Dale, Graco, et al., 2017, Capet et al., 2016 use simple transfer functions derived from a large ensemble of 1D diagenetic model simulations to predict benthic

nutrient recycling fluxes for the coastal North Sea (Gypens et al., 2008), the Peruvian Upwelling system (Dale, Graco, et al., 2017), the entire global ocean (Bohlen et al., 2012; Dale, Nickelsen, et al., 2015) or the entire Black Sea (Capet et al., 2016). Marquardt et al., 2010 used a transfer function to estimate the global gas hydrate inventory in marine sediments. In addition, Bourgeois et al., 2017 used a generalized additive model to calculate oxygen fluxes through the sediment-water interface for the entire Arctic Ocean and Artificial Neural Networks have been used to estimate sulfate (Bowles et al., 2014) fluxes through the sediment-water interface on a global scale.

These approaches are similar to the regional assessment presented here and illustrate the power of such transfer functions. We now highlight this in the introduction.

"My specific critique relates to the following points, which to my opinion are important in controlling the biogeochemical rates and flux output of the model, but that are not or too poorly constrained in the model to substantially further our understanding of how efficient anaerobic methane oxidation is and will be in the Siberian shelf sediments. Even with the reduction of the investigated area to the Laptev Sea only, the depositional environments and geological settings are so much more variable that a simple sedimentation rate/bathymetry-based prediction of present-day organic carbon accumulation gives a starting condition for the model that is too simplifying to be acceptable."

Response: The results of the extensive sensitivity study presented here clearly indicate the sedimentation rate and active fluid flow exert the dominant control on the escape of methane derived from thawing permafrost and/or disintegrating methane gas hydrates through the Siberian shelf sea floor across a wide range of contrasting environmental conditions encountered in this depositional environment. Results show that additional environmental conditions, such as OM content or AOM efficiency (*i.e.* k_{AOM}) play a minor or negligible role. Sedimentation rate can thus be used to predict the non-turbulent of methane escape on the Siberian Shelf.

The extensive sensitivity study presented here, thus also confirms the general approach that underlies the ensemble of studies listed in the previous response: single benthic biogeochemical characteristics, such as seafloor fluxes, redox horizons or inventories are often controlled by a limited set (1-2) of dominant factors that can then be used to robustly predict these characteristics on a regional/global scale.

"For example, the authors rely on a selected handful of Pb-210 data (there are more available in the literature for better coverage (see Bröder et al., 201; Strobl et al., 1988) for sedimentation rates"

Response: We thank the reviewer for the suggestions. Bröder et al., 2016 reports values for two sites in the East Siberian Sea and can thus unfortunately not be used to improve data coverage in the Laptev Sea. However, the reported linear sedimentation rate ($0.14 - 0.15$ cm yr^{-1}) is not only sim-

ilar to the sedimentation rate used in our local model application (0.12 cm yr^{-1}), but would also not change flux calculations if applied (see sensitivity study). We now include the values reported by Strobl et al., 1998. They show that sedimentation rate in the Laptev sea is of the same order (0.15 cm yr^{-1})- a value that falls well in the range we explored.

"The model doesn't consider the regionally diverse sediment types, permeabilities and rates in the Siberian Shelf Sea (see for example Dudarev et al., 2006 Oceanology; Rekant et al., 2015). The model doesn't consider known clay/sand/sand grain size variation and their influence of carbon concentration, permeability, transport, and resulting biogeochemical rates."

Response: We would like to stress again that the presented study does account for the regional variability of sedimentation rate: 1) in the sensitivity study considering a large range spanning almost two orders of magnitude ($0.03 - 1.5$ cm yr^{-1}), and 2) in the regional analysis that applies a spatially variable sedimentation rate. In addition, the influence of the amount of degradable OM has also been tested in the sensitivity study and, because it is of secondary importance, is qualitatively discussed in the regional study.

It is however correct that we assume a porosity profile, which is representative for fine-grained shelf sediments. This is in agreement with Dudarev et al., 2006 (although they focus on the East Siberian Sea and not the Laptev Sea). They suggest that: "*The distribution of sediments demonstrates that they sustain fine-grained texture in the major part of the continental shelf regardless of the distance from the shore*". Considering that the overall geomorfological characteristics of the East Siberian Sea and Laptev Sea are similar, we can assume that a 3 m sediment column with a prescribed porosity (dependent on depth) and a uniform texture and sediment type might be a decent representative for a large setting of the ESAS. We added a comment to the methods section.

"The model assumes Barents Sea depositional conditions as a good analog, however, these are unlike those of the Siberian shelf, since the Barents Sea is much deeper, has higher marine productivity, less ice cover, and much less input of terrestrial organic matter. In addition, it does not have terrestrial permafrost underneath the recent Holocene sediments. It is therefore not a particularly good analog. If the authors are interested, I can provide porewater methane, sulfate and ammonium data from this region."

Response: We would like to thank the reviewer for this offer. We have been in contact with the reviewer for porewater methane, sulfate and ammonium data and now include an additional model test case for this Laptev Sea site. We would however also like to stress that we do not consider the Barents Sea shelf offshore Versterålen as a good analog for the ESAS. Due to the paucity of observational data from the Laptev Sea for model testing, we used this Arctic site to illustrate the performance of our model set-up in simulating biogeochemical dynamics in high-latitude shelf sediments.

"The reactive continuum approach employed here probably overestimates the reactive organic carbon amount that is available to organic carbon degradation at depth. In reality, the reactivity of the organic matter below the oxic horizons is one to two orders of magnitude lower than commonly observed in marine shelf sediments (see Figure 9, Brüchert et al., 2018). Given the very low reactivity of carbon in these sediments (See Brüchert al., 2018; Bröder et al., 2016; Tesi et al., 2014), sulfate is likely never exhausted and methanogenesis and AOM may not even take place in these sediments at all. I am therefore not surprised at all that the authors arrive at such low regional dissolved benthic methane fluxes, seemingly at odds with the broadly published claims of extensive methane emission from the Siberian shelf."

Response: This is a misunderstanding which we would like to clarify. First of all, we would also like to emphasize again that, according to our findings, the organic matter reactivity only exerts a secondary effect on our conclusions and therefore does not alter the overall picture of our results. In addition, we would like to stress again that the focus of the presented analysis centers on the fate of methane fluxes from thawing permafrost and/or disintegrating methane gas hydrates and not in-situ biogenically produced methane for which OM reactivity may play a more important role. The presence of a deep methane flux from thawing permafrost and/or disintegrating methane gas hydrates also ensures the presence of an AOM and the depletion of sulfates.

However, apart from this, we also disagree with the overall comment that the reactive continuum model (RCM) overestimates reactivity in these sediments. In fact, the RCM accounts for the decrease of OM reactivity with sediment depth/degradation state. Here, we test a wide range of RCM parametrizations (*i.e. a*) including those that result in a rapid decrease of OM reactivity by 1-2 orders of magnitude. Moreover the two papers cited actually support the use of a reactive-continuum model.

1. **Bröder et al., 2016 show that the half-life of the organic matter deposited at two sites in the East Siberian Sea is $19 - 27$ yr. These half-life are represented by our RCM parametrizations in the intermediate range. Assuming $\nu = 0.125$ the corresponding a for the two samples would be $a = 3.4 - 4.8$ yr - values that are well within the range explored in our sensitivity analysis.**

2. **Tesi et al., 2014 in their conclusions clearly state: "*Therefore our results suggest that TerrOC is made of several allocthonous pools each with distinct reactivity toward the oxidation (i.e., reactive continuum)*".**

We modified the method section to clarify this point and also added the two references.

"In fact, these fluxes confirm my own direct measurements of porewater methane concentrations and methane fluxes from a range of stations investigated in the summer of 2014 during the SWERUS expedition with the Swedish icebreaker Oden. If the authors are interested, I am willing to share these data with them to better constrain their model."
Response: We are really thankful for this offer and have been in contact with the reviewer.

"The model doesn't consider Holocene sealevel change to elaborate on the mass of sediment available for methane generation since the last glacial maximum, which is the time since reactive sedimentary organic carbon accumulation began."
Response: This is a misunderstanding. Again, the focus of the presented paper is on the fate of methane released from subsea permafrost/gas hydrates on the present-day and future Siberian shelf. We do not intend to simulate the historical evolution of the SSPF and of related historical methane emission, but only a plausible range of current/future ones. Furthermore, our model analysis is based on the simulation of the first 3 meters of sediment and the Holocene sedimentation rates we explored ($0.03 - 1.5$ cm yr^{-1}) indicate that the sediment layer overlying the subsea permafrost always exceeds 3 m.

"The model design relies on a sequence of thermodynamically regulated terminal electron acceptor reactions driven by fresh carbon accumulation at the top of the model domain. In reality, non-biogenic or old Pre-Holocene-produced methane transport from below (of thermogenic or Pleistocene age, i.e., terrestrial) is the key unique characteristic of the Siberian shelf with respect to methane cycling. This carbon is old and uncoupled to recent carbon accumulation. In addition, carbon accumulation varied greatly through time on the Siberian shelf. The model appears to assume continuity of recent depositional conditions back in time and space, which is most certainly incorrect."
Response: This is a misunderstanding. In fact, the model analysis focus on this "non-biogenic or old Pre-Holocene-produced methane transport from below (of thermogenic or Pleistocene age, i.e., terrestrial)" and not on the in-situ produced biogenic methane. Because it is impossible to reconstruct depositional conditions over the Holocene for the entire region, we indeed assume broadly similar depositional conditions during the Holocene. This is an acceptable simplification, in particular because:

1. **Early diagenetic rates are highest in the shallow, young sediment layers and decrease rapidly with depth. As a consequence, biogeochemical dynamics are mostly affected by recent depositional conditions. This is especially true in the light of the fast decrease in OM reactivity reported by broder 2016; Brüchert et al., 2018; Tesi et al., 2014.**

2. **Our comprehensive sensitivity study indicates that OM degradation and biogenic methane production in the Holocene sediment layer ex-**

erts a minor control on non-turbulent methane fluxes across the sediment-water interface. Holocene fluctuations in environmental conditions will thus exert a negligible effect on our results.

We clarify this throughout the manuscript (see previous replies).

"Only the section with the transient model scenarios therefore applies to the Siberian shelf and only scenarios with an explicit upward flux of methane are relevant for investigating AOM dynamics in these sediments. However, because of the difficulties in constraining the regional distribution of seeps, flux rates cannot be reliably extrapolated and one should refrain from a regional flux estimate."
Response: This is a misunderstanding. All steady-state simulations also apply an upward flux of methane (as outlined in the method section for details). They are thus relevant for investigating the fate of permafrost/hydrate derived methane in the Holocene sediment column and its possible escape through the sediment water interface. They also allow to derive the transfer function for possible non-turbulent methane escape that has been used to establish a regional estimate. We clarify this point throughout the manuscript (see previous replies).

Because our steady state analysis shows that AOM acts as an efficient biofilter and mostly prevents non-turbulent methane escape from the sediment, we also explored a number of plausible transient scenarios to explore if microbial dynamics could possibly create âĂIJwindows of opportunityâĂİ for methane escape and assess their importance. We further clarify this in the introduction and method section. in the transient analysis we performed we actually refrained from an upscale estimate and we just explained the result of the flux out of simulated sediment column.

"My objections to the present manuscript are therefore not whether the model's capabilities are useful to the scientific community in general, which it certainly is, but a critique of the attempt to mimic biogeochemical as well as recent and past depositional conditions on the Siberian shelf to better predict sediment methane emissions from this region."
Response: see responses above.

"I am fully aware of the infected discussion of the relevance of the Siberian shelf sea's role as a potentially huge methane source to the atmosphere put forward by Shakhova and co-authors. The outcome of the model simulations presented here, even in their most generous state (high advective upward flow and moderately to high sedimentation rates), would imply that the emissions proposed by Shakhova and coauthors are very hard to achieve without invoking massive gas emissions (which are not seen regionally in atmospheric measurements)."
Response: This is indeed one of the conclusions of our analysis.

"However, the inability of this 1D model to encapsulate environmental conditions

that are found in the Laptev and East Siberian Sea make it impossible to use its scaled model output to the current system or to use the model to make reliable assessments of how the shelf environment may change methane fluxes in the future. Particularly the latter requirement is key to the use of a reaction transport model such as this one in climate science. [...] The study and conclusions give the false impression that this particular model is capable, with certainty, to predict the non-gaseous methane flux emanating from this 1.5 million square kilometer large region, if one only knows the sedimentation rate and water depth. The authors may therefore consider a new title for their manuscript for the first section and resubmit it under this new title without much reference to dissolved methane emissions on the East Siberian shelf, since this is not what they can model reasonably with the data they have available. [...] Alternatively, the model simulations can be tested with actual data from the Siberian shelf, which I am willing to share. In this case, I would suggest to reduce the first part of the manuscript and focus on the application of the BRNS to the Siberian shelf sea rather than a broad treatment of the model's performance."

Response: This comment reflects a string of misunderstandings. We do not aim at quantifying, "*with certainty*" the exact evolution of present and future methane emissions from the Siberian shelf. As highlighted in the title, abstract, introduction, the presented study assesses the potential for non-turbulent methane escape (derived from deep sediment sources such as permafrost/gas hydrates) from Siberian shelf sediments. As pointed out in the results and conclusion section, it thus provides a robust, quantitative framework suitable to make first order estimates and draw conclusions with respect to present and potential future emissions, as well as methane gas emissions required to support previous estimates of Arctic Ocean methane emissions to the atmosphere. Given the urgent need to assess this potentially ticking time bomb, but the paucity of observational data, it represents a feasible and robust quantitative first step towards a better assessment of the threat methane emissions from thawing subsea permafrost/ disintegrating methane hydrates pose for our climate.

Therefore, we are convinced that the title, as well as the approach of the presented study adequately reflect its scope and do not give a false impression. However, we have adapted the abstract, introduction, method and conclusion sections to further clarify these points. In addition, we have also included a new case study for the Laptev sea site based on the data provided by the reviewer.

Specific comments

Page 8: "This is a crude overgeneralization. The authors must provide more references on the physical oceanography of the Laptev Sea and its sediment distribution and bathymetry to justify this comparison. The Norwegian setting has much higher primary productivity, is up to 8 times deeper and has substantially less ice cover over the year. If anything, the Vesterålen site shares very few similarities with the Laptev

Sea or the East Siberian Shelf Sea."
Response: This is a misunderstanding. As pointed out in the response to general comments, we used the Hola trough sediments merely to assess the ability of the model to simulated carbon and sulfur dynamics in high latitude shelf sediments porewater profiles in a Northern shelf. No calibration of the BRNS or other following results relies on the simulations performed to reproduce the Vesterålen site, nor do we claim any similarity with the shelf areas of the East Siberian Arctic shelf. However, we do agree that our statement could be misunderstood and have now modified this section accordingly.

Page 12: "Please correct, not for methane"
Response: "Simulation results show an overall satisfactory agreement with measurements except for methane."

Page 13:

- "It is not correct to make reference to the ESAS, since the range of the environmental conditions applied here is sufficiently broad to be applied to a wide range of shelf and slope margin settings with possible AOM. One condition worthwhile exploring and not done here is whether at low OM reactivities, the consumption of sulfate may not be completed for the time span of Holocene sediment accumulation on the ESAS (i.e., since ca 7000 years ago)."
  This is a misunderstanding. As stated earlier, we investigate the fate of methane from deep sources (permafrost/hydrate) rather than in-situ produced methane (although the model also accounts for biogenic production in the Holocene sediment layer). As a consequence, we apply a range of methane fluxes from below that ensure a consumption of sulfate. With respect to the comment on the environmental conditions, we would like to repeat our response to a similar general comment here.

  "***While the reviewer is absolutely right in pointing out that the results of the comprehensive sensitivity study described in the manuscript are universally valid, we would like to stress that the model setup and the sensitivity study have been specifically designed with the aim of assessing the fate of dissolved methane released from a deep source (e.g. dissociating hydrates or thawing subsea permafrost) in warming Siberian Shelf sediments. More specifically:***

  - ***The model is forced with a variable flux of dissolved methane potentially originating from dissociating methane hydrates and/or thawing permafrost in the deeper sediment. The methane flux is constrained by assuming lower model boundary methane concentrations ranging from*** 0 ***to a maximum concentration that is constrained by the saturation of dissolved*** CH_4 ***under pressure,***

temperature and salinity conditions encountered on the Siberian shelf.

- ***All model boundary conditions, forcings and parameters (Tables S5 and S6) are chosen to be representative of environmental conditions encountered on the Siberian shelf.***
- ***The range of boundary conditions and parameters tested in the steady state sensitivity study are constrained based on data compiled for the Siberian shelf.***

***As a consequence, the study presented here does not cover the entire range of possible conditions (e.g. methane fluxes, active fluid flow, organic carbon concentrations etc.) encountered at the global ocean seafloor, but is representative for conditions (likely) encountered on the present and future Siberian Shelf.*"**

- "Please correct to : 'to the SWI' The model does not provide any constraint on the SWI flux, i.e., the benthic flux itself, because here other processes play an important that are modelled here."
  Response: We are not sure which processes the reviewer refers to, but in addition to diffusion and advection, the model explicitly accounts for bioturbation and non-local transport (through bioirrigation or ice scouring). It thus provides a robust representation of transport through the SWI.

- "Referencing this study to other studies that show a range of 5 orders of magnitude in methane fluxes to justify its applicability seems odd. Please clarify how exactly each of the referenced studies supports the model findings in your simulation."
  Response: The referenced studies offer a comparison with respect to the fluxes, as well as the flux variability in response to different environmental conditions we simulated.

- "Which value was that? Not clear from the text. Apart from that, I deeply object to the use of one value to the whole of the ESAS. What is the purpose of this upscaled value? The original model value doesn't gain any more legitimacy from upscaling and the fact that the upscaled value may be in the range of expected values neither. Please delete this section"
  The maximum value we found was $27.48\ \mu\mathbf{mol}CH_4\ \mathbf{cm^{-2}\ yr^{-1}}$**. We added the exact value to the respective section. As pointed out in the earlier response, model results provide a robust quantitative framework to evaluate the potential for non-turbulent methane escape from the Siberian Shelf. The purpose of upscaling the maximum value to the ESAS is simply to offer an upper limit for this possible non-turbulent methane flux and show that, even if the most favorable conditions for methane escape were to be found over large shelf areas (note, this is**

different from claiming that they are), non-turbulent methane fluxes would still be negligible and would not be able to support earlier estimates of methane emissions to the atmosphere.

Page 14:

- "This is an interesting conclusion. How can one reconcile the observation that methane concentrations in the methanogenic zone generally tend to increase with depth, i.e., their transport away from the zone of formation is too slow relative to the methanogenesis rate?"
  Response: The Damköhler numbers are defined in such a way that the transport process considered occurs in the same region as the reaction, *i.e.* we considered the methane transport within the methanogenic zone for the evaluation of Da_{MG} and the SMTZ for the evaluation of the Da_{AOM} . Simulation results reveal that methane transport is efficient within the methanogenetic zone. However, comparison with Da_{AOM} shows that methane consumption within SMTZ is slower than its transport. In other words, methane can be efficiently transported to SMTZ but it is not quickly consumed there. As a consequence, methane accumulates below the SMTZ because at the SMTZ level it is not consumed and below the SMTZ no AOM occurs.

- "This is a curious assertion for the Siberian shelf system. It is wellknown that the sediments of the Siberian shelf are not reactive enough to yield significant methane. It is instead supposed that externally introduced methane from the thawing permafrost that serves as the methane source. The current model does not take external sources into account and this is the major flaw of this paper. It is actually not suited in the current version to model the processes on the Siberian shelf."
  Response: Deep (external) sources of methane are the main focus of the presented study. See response to general comments for details on biogenic methane production, methane fluxes from permafrost/hydrates.

- "This introduction paragraph is rather wordy and doesn't say much. Can it be shortened?"
  Response: we will shorten it in the finalized version of the paper, although we value the fact that an introduction might already provide the main message of what is described in detail later.

- "Please provide a reference to the 'traditional views'. The view proposed here is not new."
  Response: We replaced "traditional" with "intuitive". Our findings give further evidence of the dominant role of transport processes for non-turbulent methane effluxes also in modeling scenario compatible with ESAS settings.

Page 15:"What is meant by 'margin'?"
Response: the continental margin. We could replaced "margin" with "shelf" to avoid confusion.

Page 17: "The authors should avoid trivial sentences such as this one."
Response: it is not necessarily trivial, since a high methanogenesis might also be expected to foster a higher oxidation process and therefore accumulation of methane is not necessarily a triviality

Page 19: "I wonder whether the reactivity of organic matter in large parts of the Siberian Shelf isn't even lower than 100 years. More 1000 years."
Response: we also explored the $a \geq 100$ yr. As already stated in the reply to the general comment, the reactivity of the organic matter reported in other studies (*e.g.* Bröder et al., 2016) shows that a is < 5, not far from the value $a = 10$ yr we used for the baseline simulation. In addition, a-values $>$1000 years are characteristic for deep sea sediments underlying extremely oligotrophic gyres, such as the deep South Pacific. Shelf, slope and most deep sea environments are generally characterized by $a < 1000$ years.

Page 23: "The authors are conflating to independent processes into one."
It is not clear which processes the reviewer refers to. We guess they are, on one hand, the actual AOM and, on the other hand, the precipitation of authigenic carbonate. We do not claim or mix them up and we are aware that they are two different processes but it is well established that they are not independent, since the alkalinity produced during the AOM can drive precipitation of authigenic carbonates as reported in many site all over the globe (*e.g.* Aloisi et al., 2004; Crémière, Lepland, Chand, Sahy, Condon, et al., 2016; Crémière, Lepland, Chand, Sahy, Kirsimäe, et al., 2016; Karaca et al., 2010; Luff et al., 2005; Meister et al., 2018; Pierre et al., 2012). We are simply hinting at an indirect effect supporting our findings, aware that the two processes are however well distinct and not trivially connected.

Page 24: "These calculated active and passive fluxes are so low that they are empirically not verifiable with currently available measurement techniques."
Response: We are aware of this limit and acknowledge it in the study. However, we would also like to point out that the exact quantity of these small fluxes is of minor importance. What is important here is that the potential for non-turbulent methane fluxes from Siberian Shelf sediments, even under the most favorable environmental conditions, is extremely limited and previous estimates of methane emissions to the atmosphere would thus require the build up of large quantities of methane gas.

Page 26: "The question is more, whether biogenic methane ever forms in these sediments, as the authors likely overestimate the reactivity of the organic matter. Altogether I think that the authors arrive at the right conclusion for the wrong reasons."

As stated previsouly, we disagree with this comment. Please see reply to general comment for details.

Page 28: "From this section on the manuscript becomes distinctly less well written, more typographic errors and less succinct writing. At the same time, the discussion of transient conditions is most relevant to the Siberian shelf system. This section needs to be carefully revised and improved in its writing."
Response: We will carefully revise and improve this section.

Page 29: "A better way of explaining the discrepancy between the two methane fluxes at steady state and the transient condition would be to show the AOM rate for the two rate laws."
Thanks for the suggestion. We add the AOM rate profile to fig. 11.b

Page 31:

- "This is hard to understand. It should be possible to extract the instantaneous apparent kAOM value throughout the simulation. Ultimately of relevance is not what the kAOM is at the end of the simulation, but its time-integrated AOM rate throughout the modelled transient run."
  It is actually possible to extract the k_{AOM} at each simulated time step. However, here we wanted to explain why the final, new steady-state flux in the bioenergetic formulation is different from the simulation with the bimolecular formulation and that is the reason we focused on the final k_{AOM}, its shape and values.

- "Poor English makes this paragraph hard to understand, most importantly it is not clear how the authors arrive at their conclusion with this argument"
  Response: We will carefully revise and improve this section.

- "thermodynamical"
  Response: Corrected

Page 32:

- "19 years"
  Response: Corrected

- "The role of sulfide was not mentioned previously. Is sulfide generally an important player for thermodynamic calculations done here?"
  Sulfide influences AOM it appears in the formulation of F_T, which controls the AOM in the bioenergetic approach as shown in Eq. 11. Bicarbonate appears as well, but it is rarely a limiting factor.

Page 33:

- "The wording should be reversed. An AOM biomass accounts for an AOM filter, not the other way round"

Response: we agree but we wanted to stress that in order to have an efficient AOM filter a minimum AOM biomass is needed and this quantity has been estimated to be $> 10^{10}$ cells cm^{-3}, which is of the same order of magnitude as the value we found.

- "Overall, this is irrelevant. The supply from below is what counts for the Siberian shelf, not the in-situ production, which is negligible in almost all settings except for the Eastern East Siberian Sea and the Chukchi Sea. In addition, the statement is also irrelevant in a general sense. As the supply from below is increased, so must the proportional contribution of in-situ produced methane decrease. This is not worth mentioning."
  Response: We will edit this sentence accordingly in the final version of the paper.

- "typo here: from ... to.."
  Response: Corrected

- "I am getting lost with the abbreviations"
  $[CH_4]_-$ **is the methane concentration at the bottom of the sediment column.**

- "As stated this is not true and must be corrected. Never did you investigate ESAS shelf sediments in this study. Modeling scenarios were investigated, of which some conditions may apply to selected environmental setting on the ESAS. The passive/active terminology strictly applies to theoretical scenarios of system behavior.[...] Seriously, the authors have not investigated these sediments directly at all and should not make a claim to have investigate them."
  Response: This is a misunderstanding. The focus of this study is not a regional simulation of ESAS shelf sediments, but to develop a robust, quantitative framework that can be used to evaluate the potential for non-turbulent methane escape driven by thawing subsea permafrost and/or disintegrating methane gas hydrates on the warming Siberian shelf. We would again like to repeat our response to one of the general comments.

  "***This comment reflects a string of misunderstandings. We do not aim at quantifying, "with certainty" the exact evolution of present and future methane emissions from the Siberian shelf. As highlighted in the title, abstract, introduction, the presented study assesses the potential for non-turbulent methane escape (derived from deep sediment sources such as permafrost/gas hydrates) from Siberian shelf sediments. As pointed out in the results and conclusion section, it thus provides a robust, quantitative framework suitable to make first order estimates and draw conclusions with respect to present and potential future emissions, as well as methane gas emissions required to support previous estimates of Arctic Ocean methane emissions to the atmosphere. Given the urgent need to assess this potentially ticking***

time bomb, but the paucity of observational data, it represents a feasible and robust quantitative first step towards a better assessment of the threat methane emissions from thawing subsea permafrost/ disintegrating methane hydrates pose for our climate.

Therefore, we are convinced that the title, as well as the approach of the presented study adequately reflect its scope and do not give a false impression.

However, we also modified this section accordingly to avoid misunderstandings."

- "first or first-order?"
  Response: Actually both first and first-order. Modified accordingly.

References

Aloisi, Giovanni, Klaus Wallmann, RR Haese, and J-F Saliege (2004). "Chemical, biological and hydrological controls on the 14C content of cold seep carbonate crusts: numerical modeling and implications for convection at cold seeps". In: *Chemical Geology* 213.4, pp. 359–383.

Bohlen, Lisa, Andrew W Dale, and Klaus Wallmann (2012). "Simple transfer functions for calculating benthic fixed nitrogen losses and C: N: P regeneration ratios in global biogeochemical models". In: *Global Biogeochemical Cycles* 26.3.

Bourgeois, Solveig, Philippe Archambault, and Ursula Witte (2017). "Organic matter remineralization in marine sediments: A Pan-Arctic synthesis". In: *Global Biogeochemical Cycles* 31.1, pp. 190–213.

Bowles, Marshall W, José M Mogollón, Sabine Kasten, Matthias Zabel, and Kai-Uwe Hinrichs (2014). "Global rates of marine sulfate reduction and implications for sub–sea-floor metabolic activities". In: *Science* 344.6186, pp. 889–891.

Bröder, Lisa, Tommaso Tesi, August Andersson, Timothy I Eglinton, Igor P Semiletov, Oleg V Dudarev, Per Roos, and Örjan Gustafsson (2016). "Historical records of organic matter supply and degradation status in the East Siberian Sea". In: *Organic Geochemistry* 91, pp. 16–30.

Brüchert, Volker, Lisa Bröder, Joanna E Sawicka, Tommaso Tesi, Samantha P Joye, Xiaole Sun, Igor P Semiletov, and Vladimir A Samarkin (2018). "Carbon mineralization in Laptev and East Siberian sea shelf and slope sediment". In: *Biogeosciences* 15.2, pp. 471–490.

Capet, Arthur, Filip JR Meysman, Ioanna Akoumianaki, Karline Soetaert, and Marilaure Grégoire (2016). "Integrating sediment biogeochemistry into 3D oceanic models: a study of benthic-pelagic coupling in the Black Sea". In: *Ocean Modelling* 101, pp. 83–100.

Crémière, Antoine, Aivo Lepland, Shyam Chand, Diana Sahy, Daniel J Condon, Stephen R Noble, Tonu Martma, Terje Thorsnes, Simone Sauer, and Harald Brunstad (2016). "Timescales of methane seepage on the Norwegian margin following collapse of the Scandinavian Ice Sheet". In: *Nature communications* 7, p. 11509.

Crémière, Antoine, Aivo Lepland, Shyam Chand, Diana Sahy, Kalle Kirsimäe, Michael Bau, Martin J Whitehouse, Stephen R Noble, Tõnu Martma, Terje Thorsnes, et al. (2016). "Fluid source and methane-related diagenetic processes recorded in cold seep carbonates from the Alvheim channel, central North Sea". In: *Chemical Geology* 432, pp. 16–33.

Dale, Andrew W, Michelle Graco, and Klaus Wallmann (2017). "Strong and dynamic benthic-pelagic coupling and feedbacks in a coastal upwelling system (Peruvian shelf)". In: *Frontiers in Marine Science* 4, p. 29.

Dale, Andrew W, Levin Nickelsen, Florian Scholz, Christian Hensen, Andreas Oschlies, and Klaus Wallmann (2015). "A revised global estimate of dissolved iron fluxes from marine sediments". In: *Global Biogeochemical Cycles* 29.5, pp. 691–707.

Dudarev, Oleg Victorovich, Igor Petrovich Semiletov, Alexander Nikolaevich Charkin, and AI Botsul (2006). "Deposition settings on the continental shelf of the East Siberian Sea". In: *Doklady earth sciences*. Vol. 409. 2. Springer, pp. 1000–1005.

Gypens, Nathalie, Christiane Lancelot, and Karline Soetaert (2008). "Simple parameterisations for describing N and P diagenetic processes: Application in the North Sea". In: *Progress in oceanography* 76.1, pp. 89–110.

Karaca, Deniz, Christian Hensen, and Klaus Wallmann (2010). "Controls on authigenic carbonate precipitation at cold seeps along the convergent margin off Costa Rica". In: *Geochemistry, Geophysics, Geosystems* 11.8.

Luff, Roger, Jens Greinert, Klaus Wallmann, Ingo Klaucke, and Erwin Suess (2005). "Simulation of long-term feedbacks from authigenic carbonate crust formation at cold vent sites". In: *Chemical Geology* 216.1-2, pp. 157–174.

Marquardt, Mathias, Christian Hensen, Elena Pinero, Klaus Wallmann, and Matthias Haeckel (2010). "A transfer function for the prediction of gas hydrate inventories in marine sediments". In: *Biogeosciences* 7.9, pp. 2925–2941.

Meister, Patrick, Johanna Wiedling, Christian Lott, Wolfgang Bach, Hanna Kuhfuß, Gunter Wegener, Michael E Böttcher, Christian Deusner, Anna Lichtschlag, Stefano M Bernasconi, et al. (2018). "Anaerobic methane oxidation inducing carbonate precipitation at abiogenic methane seeps in the Tuscan archipelago (Italy)". In: *PloS one* 13.12, e0207305.

Pierre, Catherine, Marie-Madeleine Blanc-Valleron, Jérôme Demange, Omar Boudouma, Jean-Paul Foucher, Thomas Pape, Tobias Himmler, Noemi Fekete, and Volkhard Spiess (2012). "Authigenic carbonates from active methane seeps offshore southwest Africa". In: *Geo-Marine Letters* 32.5-6, pp. 501–513.

Regnier, Pierre, Andy W Dale, S Arndt, DE LaRowe, J Mogollón, and P Van Cappellen (2011). "Quantitative analysis of anaerobic oxidation of methane (AOM) in marine sediments: a modeling perspective". In: *Earth-Science Reviews* 106.1-2, pp. 105–130.

Strobl, C, V Schulz, S Vogler, S Baumann, Heidemarie Kassens, PW Kubik, M Suter, and A Mangini (1998). "Determination of depositional beryllium-10 fluxes in the area of the Laptev Sea and beryllium-10 concentrations in water samples of high northern latitudes". In: *Land-Ocean Systems in the Siberian Arctic*. Springer, pp. 515–532.

Tesi, Tommaso, Igor Semiletov, Gustaf Hugelius, Oleg Dudarev, Peter Kuhry, and Örjan Gustafsson (2014). "Composition and fate of terrigenous organic matter along the Arctic land–ocean continuum in East Siberia: Insights from biomarkers and carbon isotopes". In: *Geochimica et Cosmochimica Acta* 133, pp. 235–256.

Response to Review n.2: Volker Brüchert

May 17, 2020

General comment

"Puglini et al comments comments to revised version

1. The revised version has addressed the following points: The authors now consider a larger number of dated sediment cores as the basis for the extrapolation for their sedimentation rate map. The new model still considers sedimentation rate to be the main variant and not variation in sediment type. While the model makes clear that sedimentation is one of the most important driver in regulating AOM, the authors should still make reference to the uncertainties arising from variable sedimentary environments, in particular in the near-shore where the emissions are expected to be highest.

    - Porewater data from the Laptev Sea are now taken as reference instead of data from the Barents Sea.
    - More consideration is given to studies that investigated the reactivity of organic matter on the Siberian shelf, e.g., Wild, Tesi, Brüchert, Bröder, etc.) than in the first version.
    - The revised version explicitly considers transient response due to upward flow from gas hydrates and thawing permafrost simulating various potential scenarios."

Response: We would like to thank the reviewer for his comments which allowed us to better clarify and corroborate our findings.

"The authors use the same extrapolation of their data to the whole Laptev Sea that is based on a sedimentation rate map, but also calculate a Laptev Sea-wide transient seepage flux of 2.6 to 4.5Tg/yr-1 for the whole Laptev Sea without taking localized seepage into account. At least, this is my understanding from reading the section on the extrapolation. It is not clear, how the authors integrate the transient response into the spatial model." **Response: we did not include transient response in the spatial extrapolation which only relies on steady-state results.**

Specific comments

All the comments concerning the wording, typos and text extension/removal have been addressed and not listed below. If a different choice has been made the comment is reported below with a response.

Page 3:

- "wording: the shelf is not a basin, it is essentially a broad flat plain."
  Response: we follow the lines of use of this expression in literature, considering that a sedimentary basin like the Siberian shelf is basin which has been filled in with sediments. Examples of similar use are in Drachev, 2016; Franke et al., 2005; Gramberg et al., 1983; Herman, 1989; Malyshev et al., 2012.

- "wording: what is a typical sedimentation rate in the ocean?; shouldn't you use a typical shelf sedimentation rate, if at all?"
  Response: we mainly wanted to stress the difference in sedimentation rate on shelves with respect to other marine settings. As reported in Burwicz et al., 2011, the accumulation rate on shelves is of the order of 0.1 **cm yr**$^{-1}$**, 5-10 times faster than in the rest of the Ocean (**$<= 0.01$ **cm yr**$^{-1}$**), although highly spacial dependent.**

- "glacial interglacial changes do not affect the sulfate concentration significantly"
  Response: For sulfate we mean only the seasonal changes, not referring to interglacial states. We simply linked salinity to sulfate concentration employing the empirical relation provided in Dickson et al., 1994 and the seasonal salinity measured in Dmitrenko et al., 2011, which showed a seasonal variation in bottom salinity (20.68 ± 1.80 **psu in summer *vs.*** 26.61 ± 0.92 **psu in winter).**

Page 9:

- "I don't understand this. Fe(OH)3 and iron reduction is very apparent in these sediments in the upper 10 cm?"
  Response: we wanted to highlight all the reactions involving PO_4^{3-}**, and the sorption on** $Fe(OH)_3$ **among them. However, because of the small reaction constant and the amount of** $Fe(OH)_3$**, it is expected to be relevant only in the narrow horizon where iron reduction occurs.**

- "This is a very high value and unlikely found here, 2.2 - 2.4 g cm-3 are more realistic."
  Response: this is typo. The real value which has been used is reported in Table S6 and is 2.41 **g cm**$^{-3}$**.**

Page 10:

"I wonder why you didn't use the sedimentation rates given by BrÃűder et al 2016 or Vonk et al 2012 for the working area?"
Response: Sedimentation rates given by Bröder et al., 2016 (0.15 ± 0.04 cm yr^{-1} and 0.14 ± 0.03 cm yr^{-1}) and Vonk et al., 2012 ($0.11 - 0.16$ cm yr^{-1}) do not differ from the one we used in our baseline simulation, *i.e.* 0.123 cm yr^{-1}.

Page 12:

"There are distinct discrepancies that the model appears not to capture very well. I wonder whether forced concave CH4 profile of the model reflects reality. This model predicts very high CH4 cocentrations beyond the data domain, not in line with an extrapolated trend of the measured data."
Response: we do agree that there are species not well reproduced. Based on the results for NH_4^+ we try to give a plausible explanation for such discrepancies. A local change in organic matter quantity and/or reactivity beyond the data domain is the most plausible explanation for the disagreement in NH_4^+ profile, considering the reaction network implemented in BRNS. In fact, NH_4^+ is only affected by the degradation of the organic matter, nitrification (which occurs only in the upper and thin oxic layer) and adsorption. Even in case the adsorption process were misreproduced, it would mainly cause a horizontal shift in the profile which is however not compatible with the data profile. For such a reason a change in the OM reactivity and/or quantity remains as the most plausible interpretation.

Such a change in organic matter properties may cause also the disagreement in CH_4 profiles, especially concerning the concavity. The model well reproduces the other species (SO_4^{2-}, DIC, PO_4^{3-} and O_2) only if methane concentration gets high enough to oversaturate pore water at depth. A reduction of organic matter quantity and/or reactivity or a local dishomogeneity might account for a milder (linear) increase in CH_4 concentration with depth. It must also be stressed the crude and simplistic parametrization of gas biogeochemistry and physics in the sediments: a factor capable of altering the methane profile at depth. However, the qualitative behaviour in the upper part of the sediments, directly determining the diffusive flux into the water column, is grasped and this was the main aim of the section.

Page 18-19:

"this sentence is not clear to me. What other advection fluxes do you mean here? Bioirrigation? And this doesn't even account for the bubble flux? And what do you mean by both the advection and molecular diffusion flux to the total flux. Shouldn't this say the relative contribution of the molecular diffusion to the advection flux? The terminology is confusing."
Response: we made explicit the 4 mechanisms affecting the non-turbulent (*i.e.* non-bubble mediated) flux at the Sediment-Water Interface:

1. **molecular diffusion**
2. **bioturbation: described as a diffusion-like process**
3. **advection: due to the imbalance of the sedimentation rate ω and the flow velocities v_{up})**
4. **bioirrigation: described as a non-local transport of dissolved species, hence bubbles are not accounted.**

We refer to the section S1 for a thorough description of the mathematical modeling of these flux components, which are however at the base of most of the reactive-transport models (see Boudreau, 1997).

Page 20:

"at least for the range of OM degradation rate constnts chosen here. The chosen range is narrow, though."
The range of our investigations cover 4 orders of magnitude $[0.1 - 1000]$ yr. We disagree that the chosen range of investigation is narrow.

Page 27:

- "This manuscript comes to the conclusion that methanogensis from transported terrestrial organic matter and deposited on the ESAS as sediment can berce of methane. This is a new conclusion, because all previous work on the ESAS has focused on mobilisation of previous drowned in-situ terrestrially organic matter as methane source. This is a totally different mechanism, for which so far no field data exist to my knowledge. In fact, previous investigations, e.g., Koch et al. 2008; Overrduin et al., 2015; 2016; Thornton et al., 2015; shown that the interface with submarine permafrost is where AOM is prevalent. These data also show no signficant gradient in sulfate despite the near-shore locations of the drill cores. To some extent, the model results should also be consistent with these observations and not propose methanogenesis in Holocene sediments."
  Response: we disagree with such a conclusion, which is not in line with our statements. We would like to clarify that, although present, the methanogenesis in Holocene sediments (*i.e* those sediments above the drowned *in-situ* terrestrial organic matter) does not appear indeed to be the main source of methane according to our results. In fact, if we consider the simulations with zero input of methane from below, the flux of methane is generally almost negligible (see for reference Fig. 3). The only cases where the methane flux is relevant, even with 0 input of methane from below, and therefore the only cases where the methanogenesis occurring in upper sediments is crucial to have a sizable methane flux, are the simulations with a high upward flow velocity

($v_{up} > 5$ cm yr^{-1}) and/or a high sedimentation rate (roughly $\omega > 0.6$ cm yr^{-1} but very likley higher, looking again at Fig. 3). There is no evidence that either of these conditions could be found in the ESAS: considering that the highest sedimentation rate found is ~ 0.4 cm yr^{-1}, even if we cannot *a priori* exclude that on small scales they might be met, although we presume that currently they would not contribute largely enough to alter the methane flux we found. However, we have chosen to include the results of the simulations considering these "extreme" conditions in the discussion of the results for two reasons: i) they are genuine and plausible model results (supported in evidence for instance by similar results by Egger et al., 2016), ii) changes of the environmental conditions of Arctic coasts are quick and there is no reason to exclude that there might be regions or future scenarios where these conditions might be present, and this is exactly what we do not want to rule out in our conclusions.

- "do you have a reference for this?"
  Response: the most direct reference is Brüchert et al., 2018: "Evidence for bioturbation and bioirrigation based on multiple micro-electrode profile measurements per core was rare", "The good fit between the two methods also supports the notion that bioirrigation and bioturbation effects from meiofauna and macro-fauna were minor." and "For the other stations, optimal fits required no sediment mixing by bioturbation or advective pore-water transport by bioirrigation". But the lack of evidence and report of faunal activity in the description of other cores (Miller et al., 2017; Overduin et al., 2016; Shakhova, I. Semiletov, Gustafsson, et al., 2017; Shakhova, I. Semiletov, Leifer, et al., 2014; Wild et al., 2018) and the rough conditions due to ice scouring give indications in this direction.

Page 34

- "How is this number extrapolated? Simply by multiplying? But active seepage would be highly localized. How can one derive at this number?"
  Response: yes this is just a simple multiplication time the area of interest and it just offers an upper constraint to the transient flux to the water column

- "But transient scenarios where the SMTZ is closer to the SWI, would respond seasonally, I presume?"
  Response: based on our simulation there is no room to infer that this occurs. Looking for instance at Fig. S16 and S17 there is no sign of any seasonal variation affecting either the methane efflux or the SMTZ level. They seem to respond only to the longer trend. And this is actually also expected considering the shallowest SMTZ we found

($\ell_{SMTZ} \simeq 16$ cm) and the diffusivity of SO_4^{2-} ($D \simeq 174$ cm^2 yr^{-1}). A back-of-the-envelope calculation estimates that the time scale (τ) required for a variation of sulphate concentration at the sea bottom to propagate down to about 16 cm is roughly 1.5 year ($D \cdot \tau \simeq \ell^2_{SMTZ}$). The system is definitely responding on longer times than seasonal variations.

References

Boudreau, Bernard P (1997). *Diagenetic models and their implementation*. Vol. 505. Springer Berlin.

Bröder, Lisa, Tommaso Tesi, August Andersson, Timothy I Eglinton, Igor P Semiletov, Oleg V Dudarev, Per Roos, and Örjan Gustafsson (2016). "Historical records of organic matter supply and degradation status in the East Siberian Sea". In: *Organic Geochemistry* 91, pp. 16–30.

Brüchert, Volker, Lisa Bröder, Joanna E Sawicka, Tommaso Tesi, Samantha P Joye, Xiaole Sun, Igor P Semiletov, and Vladimir A Samarkin (2018). "Carbon mineralization in Laptev and East Siberian sea shelf and slope sediment". In: *Biogeosciences* 15.2, pp. 471–490.

Burwicz, Ewa B, LH Rüpke, and Klaus Wallmann (2011). "Estimation of the global amount of submarine gas hydrates formed via microbial methane formation based on numerical reaction-transport modeling and a novel parameterization of Holocene sedimentation". In: *Geochimica et Cosmochimica Acta* 75.16, pp. 4562–4576.

Dickson, Andrew G and Catherine Goyet (1994). *Handbook of methods for the analysis of the various parameters of the carbon dioxide system in sea water. Version 2*. Tech. rep. Oak Ridge National Lab., TN (United States).

Dmitrenko, Igor A, Sergey A Kirillov, L Bruno Tremblay, Heidemarie Kassens, Oleg A Anisimov, Sergey A Lavrov, Sergey O Razumov, and Mikhail N Grigoriev (2011). "Recent changes in shelf hydrography in the Siberian Arctic: Potential for subsea permafrost instability". In: *Journal of Geophysical Research: Oceans* 116.C10.

Drachev, Sergey S (2016). "Fold belts and sedimentary basins of the Eurasian Arctic". In: *arktos* 2.1, p. 21.

Egger, Matthias, Wytze Lenstra, Dirk Jong, Filip JR Meysman, Célia J Sapart, Carina van der Veen, Thomas Röckmann, Santiago Gonzalez, and Caroline P Slomp (2016). "Rapid sediment accumulation results in high methane effluxes from coastal sediments". In: *PloS one* 11.8, e0161609.

Franke, D and K Hinz (2005). "The structural style of sedimentary basins on the shelves of the Laptev Sea and western East Siberian Sea, Siberian Arctic". In: *Journal of Petroleum Geology* 28.3, pp. 269–286.

Gramberg, I S, Yu N Kulakov, Yu E Pogrebitsky, and D S Sorokov (1983). "Arctic oil and gas super basin". In: *X World Petroleum Congress*. Pp. 93–99.

Herman, Yvonne (1989). *The Arctic Seas. Climatology, Oceanography, Geology, and Biology*. Springer US.

Malyshev, NA, VA Nikishin, AM Nikishin, VV Obmetko, VN Martirosyan, LN Kleshchina, and Yu V Reydik (2012). "A new model of the geological structure and evolution of the North Kara Sedimentary Basin". In: *Doklady Earth Sciences*. Vol. 445. 1. Springer, pp. 791–795.

Miller, Clint M, Gerald R Dickens, Martin Jakobsson, Carina Johansson, Andrey Koshurnikov, Matt OfffdfffdfffdRegan, Francesco Muschitiello, Christian Stranne, and Carl-Magnus Mörth (2017). "Pore water geochemistry along continental slopes

north of the East Siberian Sea: inference of low methane concentrations". In: *Biogeosciences* 14, pp. 2929–2953.

Overduin, Paul, Sebastian Wetterich, Frank Günther, Mikhail N Grigoriev, Guido Grosse, Lutz Schirrmeister, Hans-Wolfgang Hubberten, and Aleksandr S Makarov (2016). "Coastal dynamics and submarine permafrost in shallow water of the central Laptev Sea, East Siberia". In: *Cryosphere* 10, pp. 1449–1462.

Shakhova, Natalia, Igor Semiletov, Orjan Gustafsson, Valentin Sergienko, Leopold Lobkovsky, Oleg Dudarev, Vladimir Tumskoy, Michael Grigoriev, Alexey Mazurov, Anatoly Salyuk, et al. (2017). "Current rates and mechanisms of subsea permafrost degradation in the East Siberian Arctic Shelf". In: *Nature communications* 8, p. 15872.

Shakhova, Natalia, Igor Semiletov, Ira Leifer, Valentin Sergienko, Anatoly Salyuk, Denis Kosmach, Denis Chernykh, Chris Stubbs, Dmitry Nicolsky, Vladimir Tumskoy, et al. (2014). "Ebullition and storm-induced methane release from the East Siberian Arctic Shelf". In: *Nature Geoscience* 7.1, p. 64.

Vonk, Jorien E, Laura Sánchez-García, BE Van Dongen, Vanja Alling, D Kosmach, A Charkin, Igor Petrovich Semiletov, Oleg Victorovich Dudarev, Natalia Shakhova, P Roos, et al. (2012). "Activation of old carbon by erosion of coastal and subsea permafrost in Arctic Siberia". In: *Nature* 489.7414, p. 137.

Wild, B., N. Shakhova, O. Dudarev, A. Ruban, D. Kosmach, V. Tumskoy, T. Tesi, H. Joß, H. Alexanderson, M. Jakobsson, A. Mazurov, I. Semiletov, and Ö. Gustafsson (2018). "Organic matter across subsea permafrost thaw horizons on the East Siberian Arctic Shelf". In: *The Cryosphere Discussions* 2018, pp. 1–26.

Assessing the potential for non-turbulent methane escape from the East Siberian Arctic Shelf

Matteo Puglini[1,2], Victor Brovkin[1,3], Pierre Regnier[2], and Sandra Arndt[2]

[1]Land in the Earth System, Max Planck Institute for Meteorology, Hamburg, Germany
[2]BGeosys, Department Geoscience, Environment & Society (DGES), Université Libre de Bruxelles, Brussels, Belgium
[3]CEN, Universität Hamburg, Hamburg, Germany

Correspondence: Matteo Puglini (matteo.puglini@mpimet.mpg.de)

Abstract. The East Siberian Arctic Shelf (ESAS) hosts large, yet poorly quantified reservoirs of subsea permafrost and associated gas hydrates. It has been suggested that the global-warming induced thawing and dissociation of these reservoirs is currently releasing methane (CH_4) to the shallow coastal ocean and ultimately the atmosphere. However, a major unknown in assessing the contribution of this CH_4 flux to the global CH_4 cycle and its climate feedbacks is the fate of CH_4 as it migrates towards the sediment-water interface. In marine sediments, (an)aerobic oxidation reactions generally act as a very efficient methane sink. Yet, a number of environmental conditions can reduce the efficiency of this biofilter. Here, we used a reaction-transport model to assess the efficiency of the benthic methane filter and, thus, the potential for benthic methane escape across a wide range of environmental conditions that could be encountered on the East Siberian Arctic Shelf. Results show that, under steady state conditions, anaerobic oxidation of methane (AOM) acts as an efficient biofilter. Yet, high CH_4 escape is simulated for rapidly accumulating and/or active sediments and can be further enhanced by the presence of organic matter with intermediate reactivity and/or intense local transport processes, such as bioirrigation. In addition, in active settings, the sudden onset of CH_4 flux triggered by, for instance, permafrost thaw or hydrate destabilization can also drives a high non-turbulent methane escape of up to 19 $\mu molCH_4$ cm^{-2} yr^{-1} during a transient, multi-decadal period. This "window of opportunity" arises due to delayed response of the resident microbial community to suddenly changing CH_4 fluxes. A first-order estimate of non-turbulent, benthic methane efflux from the Laptev Sea is derived as well. We find that, under present day conditions, non-turbulent methane efflux from Laptev Sea sediments does not exceed 1 $GgCH_4$ yr^{-1}. As a consequence, we conclude that previously published estimates of ocean-atmosphere CH_4 fluxes from the ESAS cannot be supported by non-turbulent, benthic methane escape.

1 Introduction

The Siberian Shelf represents the largest shelf on Earth ($\sim$ 3 millions km^2 Wegner et al. (2015)) and spreads from the Kara Sea to the Laptev, the East Siberian and the Chuckhi Sea. The East Siberian Arctic Shelf (ESAS) corresponds to the broad area beneath the shallow ($\sim$ 45 m water depth, James et al. (2016)) Laptev and East Siberian Arctic Sea (Romanovskii et al., 2004; Shakhova et al., 2010a) and represents the largest region on the Siberian Shelf (Romanovskii et al., 2005), covering about 25% of the total Arctic shelf (Shakhova et al., 2010a).

Although similar in many aspects to other shelf environments, a distinguishing feature of the ESAS is the presence of subsea permafrost and associated gas hydrates buried in the sediment (Sloan Jr and Koh, 2007; Romanovskii et al., 2005). Subsea permafrost is a terrestrial relict that mainly formed during glacial periods, when retreating sea levels (with a minimum of 120 m below the current level around the Last Glacial Maximum) exposed Arctic shelves (Fairbanks, 1989; Bauch et al., 2001). Under these conditions, permafrost aggraded on the shelf and was subsequently submersed (Romanovskii and Hubberten, 2001; Romanovskii et al., 2005) by rising sea levels during the Holocene sea transgression (12 and 5 kyr BP) (Bauch et al., 2001). Gas hydrates are solid, ~~methane concentrated states of matter,~~ methane-concentrated formations in which a gas molecule is trapped in a cage of water molecules (Ruppel and Kessler, 2017). They are thermodynamically stable under specific temperature-pressure-salinity ~~conditions~~ in the ocean floor including areas beneath the subsea permafrost (Sloan Jr and Koh, 2007).

Little is known about ~~he~~ the total amount of carbon stored in subsea permafrost ~~, as well as its partitioning between subsea permafrost itself, gas hydrates and free gas.~~ or its original extentPublished estimates of carbon reservoir sizes diverge by orders of magnitude. For instance Shakhova et al. (2010a) estimate that ~~1175 PgC~~ 1175 PgC are locked in subsea permafrost on the ESAS alone, while McGuire et al. (2009) calculate that, across the entire Arctic shelf, ~~9.4 PgC~~ 9.4 PgC reside in upper sediments and ~~1.5-49 PgC (2-65~~ $1.5 - 49$ PgC ($2 - 65$ $PgCH_4$) in methane gas hydrates. Thus, the size of the Arctic subsea permafrost reservoir, its spatial distribution, as well as its biogeochemical and physical characteristics remain poorly known.

These knowledge gaps are critical as climate change is amplified in polar regions. The Arctic is currently warming at a rate twice as fast as the global mean (Trenberth et al., 2007; Bekryaev et al., 2010; Jeffries and Richter-Menge, 2012; Christensen et al., 2013). Recent observations indicate that bottom water temperatures in the coastal and inner shelf regions of the ESAS (water depth < 30 m, Dmitrenko et al. (2011)) are rising, while the central shelf sea may be subject to intense episodic warming (Janout et al., 2016). The increasing influx of warmer Atlantic water into the Arctic Ocean - the so-called Atlantification (Polyakov et al., 2017; Barton et al., 2018) - will not only further enhance this warming, but will also influence circulation and salinity patterns on the shelf (Carmack et al., 1995; Zhang et al., 1998; Biastoch et al., 2011). At the same time, it has been long recognized that the Arctic is a potential hotspot for methane emissions. Extensive methane gas bubbling has been observed in the Laptev Sea and has been directly linked to these environmental changes (Shakhova et al., 2010b, 2014). Shakhova et al. (2014) suggest that warming induced subsea permafrost thaw and hydrate destabilization may support methane emissions of up to ~~17~~ 17 $TgCH_4$ yr^{-1} from the ESAS alone. Projected change in temperature (Shakhova et al., 2017, 2019) due to climate change is expected to further destabilize Arctic subsea permafrost and gas hydrate reservoirs and might thus enhance further methane emissions (Piechura and Walczowski, 1995; Westbrook et al., 2009; Reagan and Moridis, 2009; Biastoch et al., 2011; Hunter et al., 2013; Drake et al., 2015; Ruppel and Kessler, 2017). However, a number of recent studies have questioned the significance of subsea permafrost thaw and hydrate destabilization for methane efflux from Arctic sediment (Thornton et al., 2016; Ruppel and Kessler, 2017), for methane concentrations in Arctic Ocean waters (Overduin et al., 2015; Sapart et al., 2017) and, ultimately, for methane emissions from the Arctic waters (Ruppel and Kessler, 2017; Sparrow et al., 2018). Thus, the contribution of subsea permafrost thaw and gas hydrate destabilization to methane emissions from the warming Arctic shelf and, ultimately, methane-climate feedbacks remains poorly quantified (James et al., 2016; Saunois et al., 2016). As a consequence, it has not received much attention in the recent IPCC special report (Masson-Delmotte et al., 2018). At present,

a major unknown is the strength of methane sinks in Arctic sediments and waters and their influence on methane emissions (Ruppel and Kessler, 2017). Therefore, improved assessments of the present and future climate impact of permafrost thaw and hydrate destabilization require not only a better knowledge Arctic subsea permafrost and hydrates distribution, reservoir size and characteristics, but also a better quantitative understanding of Arctic methane sinks.

In marine sediments, upward migrating methane is generally efficiently consumed by the anaerobic oxidation of methane (AOM) and, to a lesser ~~extend~~extent, the aerobic oxidation of methane (AeOM) (Hinrichs and Boetius, 2002; Reeburgh, 2007; Knittel and Boetius, 2009). Although the exact AOM process has not been fully understood yet (James et al., 2016; McGlynn et al., 2015; Milucka et al., 2012; Wegener et al., 2015; Dean et al., 2018), it is thought that AOM is mediated by ~~methane oxidizing archea that use water (or bicarbonate) as electron acceptor (Hinrichs and Boetius, 2002; Dale et al., 2006) :~~

$$CH_4 + 3H_2O \rightarrow 4H_2 + HCO_3^- + H^+$$

~~The electrons are then shuttled (Krüger et al., 2003; Hinrichs and Boetius, 2002) , via H_2, to~~ a consortium of methane oxidizing Archaea and sulfate reducing bacteria ~~(eq. (??))~~

$$SO_4^{2-} + 4H_2 + H^+ \rightarrow HS^- + 4H_2O$$

~~the overall reaction being~~ (Boetius et al., 2000) according to the reaction (Hinrichs and Boetius, 2002; Krüger et al., 2003) :

$$CH_4 + SO_4^{2-} \rightarrow HCO_3^- + HS^- + H_2O. \quad (1)$$

~~The first catabolic step is thermodynamically favourable only under a limited range of environmental conditions, while the second step is subject to weaker thermodynamic constraints (LaRowe et al., 2008) .~~ A recent assessment indicates that, in global sediments, around ~~45-61~~ $45 - 61$ $TgCH_4$ yr^{-1} (Egger et al., 2018) are consumed by AOM, thus significantly reducing previously published estimates of ~~320-360~~ $320 - 360$ $PgCH_4$ yr^{-1} (Hinrichs and Boetius, 2002; Reeburgh, 2007).

AOM generally acts as a particularly efficient biofilter for upward migrating methane and oxidizes up to 100% of the methane flux coming from below (*e.g.* Regnier et al. (2011)). However, a number of environmental conditions can reduce the efficiency of this AOM biofilter, allowing methane to escape from the sediment (Iversen and Jorgensen, 1985; Piker et al., 1998; Jørgensen et al., 2001; Treude et al., 2005; Knab et al., 2008; Dale et al., 2008c; Thang et al., 2013; Egger et al., 2016). It has been shown that, in particular, high sedimentation rates (Egger et al., 2016), slow microbial growth (Dale et al., 2006, 2008c) or the accumulation of free gas can promote methane efflux from the sediment. These findings are particularly relevant for potential methane escape from Arctic shelf sediments. The Siberian shelf is the largest sedimentary basin in the world (Gramberg et al., 1983) and shelf areas close to the large Arctic rivers reveal sedimentation rates than can be up to 5 times faster than rates that are typically observed in the ocean (Leifer et al., 2017). In addition, the Arctic shelf is subject to large seasonal, as well as climate-induced longterm, changes in environmental conditions, namely SO_4^{2-} concentration in sea water and availability of CH_4 in the sediments coming from deeper strata. These factors may influence the efficiency of the AOM biofilter through their effect on microbial biomass dynamics. Finally, observations from the ESAS

also indicate that methane gas accumulates in the sediments. When free gas pockets grow enough, methane tends to migrate upwards along pathways with higher permeability or where fractures occur (Yakushev, 1989; Boudreau et al., 2005; Wright et al., 2008; Shakhova et al., 2014, 2015, 2017; Leifer et al., 2017) and might even crack the sediments themselves ~~(O'Connor et al., 2010; Overduin et al., 2016; Yao et al., 2019)~~ (O'Connor et al., 2010; Overduin et al., 2016; Yao et al., 2019; Stranne et
However, despite a wealth of AOM-related research, a holistic, quantitative evaluation of the most important environmental controls on the efficiency of the AOM biofilter and its impact on methane escape from marine sediments is currently lacking. Thus our ability to understand and quantify AOM sink in ESAS sediments and thus the climate impact of subsea permafrost thaw and gas hydrate destabilization is seriously compromised.

Therefore, we here use a 1-D reaction-transport model approach to understand and quantify the efficiency of the AOM biofilter and its influence on the potential benthic release of methane in response to a plausible range of upward migrating dissolved methane fluxes from thawing permafrost and/or dissociating methane gas hydrates on the wariming ESAS shelf. The developed model accounts for the most pertinent primary and secondary redox processes, as well as mineral precipitation, methane gas formation and fast equilibrium reactions. Both active sites (characterized by an upward water flow) and passive sites (without an upward water flow) are investigated. We limit our model analysis to non-turbulent methane efflux, because methane in gaseous form is not directly accessible for the AOM community. As a consequence, free gas bubbles are less prone to be consumed by AOM and methane gas either ~~sits~~ is trapped in the sediments or rapidly migrates ~~upcore~~ upwards through cracks, faults or fractures (Boudreau, 2012), bypassing the AOM biofilter.

The model is forced with a set of boundary conditions that are broadly representative of the conditions potentially encountered on the ESAS. It is applied to conduct a comprehensive one-at-a-time, steady-state sensitivity study over the entire plausible range of 1) sedimentation rates, 2) active fluid flow velocities, 3) AOM rate constants, 4) organic matter reactivity and 5) non-local transport activity encountered on the ESAS. In addition, we also evaluated the influence of 1) seasonal variability and 2) idealized, projected climate change on the efficiency of the AOM-biofilter and potential non-turbulent methane escape from the ESAS under transient conditions. For this purpose, the model is extended by adopting an explicit description of AOM biomass dynamics and a bioenergetic rate law for AOM (Dale et al., 2006, 2008c, b). Finally, the ~~the~~ results of all sensitivity study runs are used to identify the most important controls on methane efflux and derive a transfer function that allows establishing a first-order estimate of methane escape from the ESAS.

The specific aims of this work are thus: 1) to identify and quantitatively understand the most important environmental controls on the efficiency of the AOM biofilter, as well as 2) its significance in reducing upward migrating methane fluxes originating from thawing subsea permafrost or destabilizing methane gas hydrates under a plausible range of environmental conditions encountered on the present and future Siberian Shelf. Model results are then used to 3) identifying environmental conditions (and thus areas on the ESAS) that favour non-turbulent dissolved methane fluxes across the sediment-water interface and 4) derive transfer functions that allow estimating the potential for non-turbulent CH_4 escape from ESAS sediments, thus providing first order constraints on the Arctic methane budget.

2 Methods

2.1 BRNS: Reaction-transport model

The Biogeochemical Reaction Network Simulator (BRNS) (Regnier et al., 2002; Aguilera et al., 2005; Centler et al., 2010) - an adaptive simulation environment suitable for simulating large, mixed kinetic-equilibrium reaction networks in porous media (*e.g.* Jourabchi et al. (2005); Thullner et al. (2005); Dale et al. (2009)) - is used to quantitatively explore the fluxes and transformations of methane in a sediment column representative for ESAS conditions. For this purpose, we set-up a reaction network (~~table~~ Table S1, S2), model parameters (~~table~~ Table S6), as well as boundary conditions (~~table~~ Table S7) that cover the conditions encountered on the present-day Siberian shelf.

In the BRNS, the general mass conservation for each solid and dissolved species is described by a a set of coupled advection-diffusion-reaction equations in porous media which are solved simultaneously (*e.g.* Berner (1980); Boudreau (1997); note that dependencies on z and t have been omitted for simplicity):

$$\frac{\partial \xi C_i}{\partial t} = \frac{\partial}{\partial z}\left[(D_i + D_{b,i})\xi \frac{\partial C_i}{\partial z}\right] - \frac{\partial}{\partial z}(v \xi C_i) + \alpha_i \xi (C_i(0) - C_i) + \mathscr{S}_i. \tag{2}$$

C_i is the concentration of the species i (mass per porewater volume for dissolved species or mass per solid matrix volume for a solid species); ξ *i.e.* the porosity $\xi = \varphi$ for dissolved species and $\xi = \varphi_s = 1 - \varphi$ for solid species. D_i is the effective diffusion coefficient for species i and is affected by salinity, temperature and tortuosity (see Table S6). D_b denotes the bioturbation coefficient and v is the advective velocity. For solid species $v = \omega$ with ω being the burial rate, while the advective velocity for dissolved species is given by the sum of the burial rate and an advective flow velocity, v_{up}, *i.e.* $v = \omega + v_{up}$. A site where $v_{up} \neq 0$ is defined as an *active site*, while a site with no advective upward water flow is defined as *passive*. α_i is the bioirrigation coefficient ($\alpha_i = 0$ for solid species) and $C_i(0,t)$ is the concentration of the species i at the Sediment-Water Interface (SWI). The reaction term $\mathscr{S}_i$ is written as:

$$\mathscr{S}_i = \sum_j \lambda_{ij} R_j \tag{3}$$

where λ_{ij} are the stoichiometric coefficients of all reaction rates R_j that affect species i.

2.1.1 Transport

The effective diffusion coefficients D_i are determined by correcting the diffusion coefficients in free solution D_i^0 (Boudreau, 1997) for tortuosity θ and temperature. Tortuosity is calculated by means of porosity φ according to a modified Weissberg relation (Boudreau, 1997): $\theta = 1 - \ln(\varphi^2)$. Note that the effective diffusion coefficients used in the model neglect pressure effects. Following Dale et al. (2008a), migration of methane gas is simply parameterized via a pseudo-diffusive term, with an apparent gas diffusion coefficient, $D_{\mathrm{CH_4}}(g)$. Bioturbation in the upper decimeters of the sediment is simulated using a diffusive term (*e.g.*, Boudreau (1986)), with a constant bioturbation coefficient, D_b^0. The model assumes that bioturbation ceases at the

bioturbation depth, z_{bio} (Boudreau, 1997). Bioirrigation is included in the mass conservation equation as a source or a sink function analogous to a kinetic rate. It is calculated as the product of the irrigation intensity, α ($\alpha = 0$ for all solids), and the difference in concentration of species i relative to the concentration at the SWI, $C_i(0)$. The bioirrigation rate α, is evaluated from the bioirrigation coefficient at the sediment surface (α_0) and the bioirrigation attenuation depth (z_{irr}) and is given by eq. S9. Porosity is assumed to decrease with depth according to an exponential decay (Athy, 1930):

$$\varphi(z) = \varphi_0 e^{-c_0 z} \tag{4}$$

with φ_0: porosity at the Sediment-Water Interface (SWI) and c_0: typical length scale for compaction.

2.1.2 Biogeochemical network

The reaction network implemented here (33 species, 37 reactions) encompasses the most pertinent primary and secondary redox reactions, equilibrium reactions and mineral precipitation and adsorption reactions. A summary of the reactions, their stoichiometry and their rate formulations can be found in Table S2 and Table S3. The following section provides a short description of the implemented reaction network, as well as a more detailed description of the reactions that affect the production/consumption of methane. A complete description can be found in the supplementary information.

The BRNS model accounts for the degradation of organic matter by aerobic degradation, denitrification, manganese oxide reduction, iron reduction, sulfate reduction and methanogenesis (Table S2). Organic matter degradation is described by means of the reactive continuum model (RCM) (Aris, 1968; Ho and Aris, 1987; Boudreau and Ruddick, 1991) that describes compound-specific reactivities (Tesi et al., 2014) and, thus, captures the widely observed decrease in apparent organic matter reactivity with degradation state. The relative importance of each metabolic pathway is simulated through a series of kinetic limitation terms, reflecting their sequential utilization in the order of their decreasing Gibbs energy yields (Table S1). After all terminal electron acceptors (TEAs) are consumed, the remaining organic matter may be degraded by methanogenesis. The rates of secondary redox reactions (Table S3), are described by bimolecular rate laws (*e.g.* Wang and Van Cappellen (1996)). Adsorption reactions are considered as fast equilibrium processes (Table S3, R28-R30). Mineral precipitation rates are simulated according to kinetic-thermodynamic rate laws (Table S3, R16-R24).

As described above, methane is produced during organic matter degradation by methanogens in deeper sediment layers, once all TEAs are depleted (Table S2, R6). If the concentration of dissolved methane exceeds the saturation concentration $[\mathrm{CH_4}]^*$ methane gas forms. The transfer rate of methane between the dissolved and gaseous phase is linearly controlled by the departure of the simulated dissolved methane concentration from the saturation concentration (Haeckel et al., 2004; Hensen and Wallmann, 2005; Tishchenko et al., 2005; Mogollón et al., 2009; Graves et al., 2017). $[\mathrm{CH_4}]^*$ is calculated according to Dale et al. (2008a), derived from the formulation proposed by Duan et al. (1992) for which $[\mathrm{CH_4}]^*$ depends on *in situ* salinity, pressure and temperature. Here, we assume that the formed methane gas is inaccessible to microbial activity and hence bypasses anaerobic and/or aerobic oxidation zones. In contrast, dissolved methane can be consumed by anaerobic (AOM) or aerobic oxidation of methane (AeOM). Free gas can re-dissolve into porewater once porewater methane concentration fall below the saturation level and may then become available to methanotrophs. AeOM rate is simply described by a bimolecular

rate law (Table S3, R14). The description of AOM depends on the model scenario. For steady state simulations, we apply a simple bimolecular rate:

$$\text{rate}_{AOM} = k_{AOM}[\mathrm{CH_4}][\mathrm{SO_4^{2-}}]. \tag{5}$$

It is the simplest and most commonly used formulation of the AOM rate in reaction-transport models (*e.g.* Regnier et al. (2011)). It accounts for kinetic controls and assumes that, under steady state conditions, bioenergetic controls are negligible (Dale et al., 2006; Regnier et al., 2011).

For transient model simulations, we apply a bioenergetic rate law in combination with an explicit description of the AOM-performing biomass (Dale et al., 2006, 2008c). It has been shown that the rates of redox reactions, whose energy yield is used by micro-organisms to grow, can be coupled to biomass growth rates via a kinetic Monod term and a thermodynamic Boltzmann term (*e.g.* Rittmann and VanBriesen (2019)). Hence, the time derivative of AOM-performing biomass (B) can be written as:

$$\frac{dB}{dt} = \mu_g B \cdot F_K \cdot F_T - \mu_d B^2 \tag{6}$$

where μ_g is the growth rate and μ_d is the decay rate. F_K is the kinetic constraint given by:

$$F_K = \frac{[\mathrm{CH_4}]}{K_m^{\mathrm{CH_4}} + [\mathrm{CH_4}]} \cdot \frac{[\mathrm{SO_4^{2-}}]}{K_m^{\mathrm{SO_4^{2-}}} + [\mathrm{SO_4^{2-}}]} \tag{7}$$

with $K_m^{\mathrm{SO_4^{2-}}}$ half saturation constant of $\mathrm{SO_4^{2-}}$ and $K_m^{\mathrm{CH_4}}$ half saturation constant of $\mathrm{CH_4}$, according to a typical Michaelis-Menten for enzymatically-catalyzed reactions. F_T represent the thermodynamic limitation and is given by

$$\begin{cases} 1 - \exp\left(\frac{\Delta G_r + \Delta G_{BQ}}{\chi RT}\right), & \text{if } \frac{\Delta G_r + \Delta G_{BQ}}{\chi RT} < 0 \\ 0, & \text{if } \frac{\Delta G_r + \Delta G_{BQ}}{\chi RT} > 0 \end{cases} \tag{8}$$

where R is the gas constant, T is the absolute temperature, χ is the average number of electrons transferred per reaction per mole of ATP produced (Jin and Bethke, 2005), ΔG_r is the Gibbs free energy of the reaction and $\Delta G_{BQ} = 20$ kJ $(\text{mol e}^-)^{-1}$ is the minimum energy needed to support synthesis of $\sim \frac{1}{3} - \frac{1}{4}$ mol ATP (Dale et al., 2008c). In order to be thermodynamically favorable the total energy $\Delta G_r + \Delta G_{BQ}$ has to be negative, meaning ~~the~~ that Gibbs free energy provided by the catabolic reaction is sufficient to sustain the microbial biomass growth. ΔG_r is given by

$$\Delta G_r = \Delta G_r^0 + RT \ln\left(\gamma \frac{[\mathrm{HS^-}] \cdot [\mathrm{HCO_3^-}]}{[\mathrm{CH_4}] \cdot [\mathrm{SO_4^{2-}}]}\right) \tag{9}$$

with ΔG_r^0: standard free energy of the reaction, the second term: deviations from standard conditions (temperature and reaction quotient) on Gibbs free energy and γ: a parameter representing departure from ideal beahviour.

The link between substrate consumption and microbial growth (anabolism) is given by Dale et al. (2006):

$$13.8\mathrm{SD} \cdot \mathrm{SO_4^{2-}} + 14.3\mathrm{SD} \cdot \mathrm{CH_4} + 0.2\mathrm{SD} \cdot \mathrm{NH_4^+} + 0.3\mathrm{SD} \cdot \mathrm{H^+} \rightarrow 0.2\mathrm{B} + 13.3\mathrm{SD} \cdot \mathrm{HCO_3^-} + 13.8\mathrm{SD} \cdot \mathrm{HS^-} \tag{10}$$

Assuming that the cellular composition of the biomass B is equal to $C_5H_7O_2N$ (Bruce and Perry, 2001; Dale et al., 2006, 2008c; Rittmann and McCarty, 2012). $SD = (1-\varphi)/\varphi$ is the conversion factor between dissolved and solid species, here represented by microorganisms (which are assumed to be attached to the solid matrix). Catabolism is linked to biomass growth (anabolism) through the growth yield. We apply a yield of 0.0713 (Dale et al., 2006), which falls at the upper end of reported AOM growth yields, *i.e.* $0.05 - 0.07$ (Dale et al., 2006; Nauhaus et al., 2007).

2.1.3 Boundary conditions

Boundary conditions place the model in its environmental context. For dissolved species, constant bottom water concentrations (Dirichlet boundary conditions) are applied at the sediment-water interface, while a known flux condition (Neumann boundary condition) are applied for solid species. At the lower boundary, a zero gradient flux boundary condition ($\partial C/\partial z = 0$) is considered for all species except methane, for which a Dirichlet condition is specified to account for methane supplied from thawing permafrost and/or dissociating gas hydrates below.

2.2 Model evaluation

To evaluate the performance of the BRNS set-up in capturing the main diagenetic patterns observed in Arctic shelf sediments we run the model for two case study sites in the area of interest: 1) a site offshore Kotelny Island in the central region of the Laptev Sea, north of the Lena river delta (76.171°N, 129.333°E, 56 m water depth) collected during the SWERUS-C3 expedition in summer 2014 (Brüchert et al., 2018; Brüchert, 2020).

Although observations are merely available for the first 22 cm, the first 3 m of sediment are simulated to allow for the full development of the early diagenetic network, thus also accounting for biogeochemical processes (e.g. methanogenesis) in deeper sediment layers that potentially affect biogeochemical cycling in the shallower sediment. Observations at the site indicate the absence of active flow and the advective velocity v_{up} is thus set to zero. Upper boundary conditions and model parameters are constrained on the basis of the observations reported (Brüchert, 2020) (Table S4). The observed organic carbon profile is imposed in the first 19 cm (Table S5) and organic carbon contents in deeper sediments are calculated on the basis of the reactive continuum model for organic matter degradation (described in Sections S2 and S3) and the deepest observed value. In addition, the possibility of a source of methane is implemented at the bottom of the modelled sediment column by applying a Dirichlet boundary condition, thus taking into account the possible presence of methane seeping from deep sediments as results of destabilizing gas hydrates/subsea permafrost - a distinguishing feature of the ESAS sediments. The methane boundary condition is determined by model fitting (see below).

When evaluating model performance, particular attention is given to sulfate, methane, ammonium (NH_4^+), phosphates (PO_4^{3-}) and dissolved inorganic carbon (DIC) depth profiles. While the former two species are of main interest for evaluating simulated AOM dynamics, the remaining three serve as indicators for OM degradation dynamics since they are metabolic byproducts of degradation (see Table S2). Moreover NH_4^+ is only affected by nitrification (R7) and adsorption (R28). The latter, although important, acts homogeneously throughout the sediment (considering the slight variation in sediment porosity, LaRowe et al. (2017)). It can thus only cause uniform shifts in $[NH_4^+]$ profile, but does not affect the overall shape of the NH_4^+

depth profile. Similarly, PO_4^{3-} is only consumed by fluorapatite precipitation (R22) and adsorption processes (R29 and R31). Fluorapatite precipitation controls maximum dissolved PO_4^{3-} ~~)~~concentrations, while the mineral adsorption process (R29) exerts a homogeneous influence and the interaction with $Fe(OH)_3$ is expected to be minor and mainly affects PO_4^{3-} within the iron reduction zone.

OM reactivity parameters (a and ν), bottom methane concentration ($[CH_4]_-$) and reaction rates are varied to find the best fit between observed and simulated profiles. Methane concentrations at the bottom of the model domain can also exceed the saturation concentration $[CH_4]^* = 14$ mM (estimated according to the value reported in Dale et al. (2008a)) to include the possibility of methane in gaseous form.

2.3 Modeling strategy

2.3.1 Steady state sensitivity analysis:

To evaluate the main physical and biogeochemical controls on the efficiency of the AOM biofilter and its impact on non-turbulent methane emission from deep methane sources such as dissociating permafrost and/or disintegrating methane gas hydrates in ESAS sediments, we conduct a comprehensive, steady state sensitivity study. For this purpose, we design a set of two baseline scenarios that are broadly representative for environmental conditions encountered on the shallow ESAS:

1. a passive case, *i.e.* $v_{up} = 0$ cm yr^{-1};
2. an active case, *i.e.* with $v_{up} = 1$ cm yr^{-1}, a value which falls within the range of fluid flow velocities $v_{up} = 0.005 - 30$ cm yr^{-1} observed across a wide range of different active environments (Regnier et al., 2011).

For both baseline scenarios, we assume a water depth of 30 m, which is slightly shallower than the average water depth of the ESAS ~45 m (James et al., 2016), since we are here interested in the shallow, near-coastal part of the shelf that potentially hosts large subsea permafrost reservoirs and is most affected by the warming. Temperature is set equal to 0°C, and thus similar to the yearly average of -0.79°C observed in the Laptev Sea at a depth of about 30 m (Dmitrenko et al., 2011). The bioturbation coefficients D_b^0 and bioirrigation coefficients α_0 (Thullner et al., 2009) are then derived from global empirical relationships according to Middelburg et al. (1997) and Thullner et al. (2009), respectively. The methane saturation concentration $[CH_4]^*$ is calculated on the basis of the relationship proposed by Dale et al. (2008a) assuming a soil matrix density of ~~2.8~~ 2.41 g cm^{-3}. Values of φ_0 and c_0 (see eq. 4) are determined based on LaRowe et al. (2017). Boundary conditions are reported in Table S7 and informed by observations. They are chosen to be broadly representative of the wider Siberian shelf environment.

Each sensitivity study run is forced with a range of different dissolved $[CH_4]$ concentrations at the lower model boundary, mimicking different methane fluxes from thawing subsea permafrost and/or disintegrating methane gas hydrates at depth. The applied set of methane concentrations at the lower boundary range from zero to the methane gas saturation concentration $[CH_4]_- = 0 - 20 - 100 - 330 - 1169 - 5455$ μM and also include the highest methane concentration that has been to date observed in ESAS cores (Overduin et al., 2015) ($[CH_4]_- = 1.169$ mM).

Table 1 and Table S6 summarize the parameters applied in the baseline simulation and Table S7 provides an overview of the applied upper boundary conditions.

Table 1. Model parameters changed in the "one-at-time" sensitivity studies. Reported values are for the baseline simulations.

Quantity	Meaning	Value	Units	Reference
ω	Sedimentation rate	0.123	cm yr^{-1}	Burwicz et al. (2011)
$\mathbf{a}$	Average lifetime of reactive OM	10	yr	This study
$\mathbf{v_{up}}$	Upward water velocity	0, 1	cm yr^{-1}	This study
$\alpha_\mathbf{0}$	Bioirrigation coefficient	99.5	yr^{-1}	Thullner et al. (2009)
$\mathbf{k_{AOM}}$	AOM rate constant	$5.0 \cdot 10^3$	M^{-1} yr^{-1}	Regnier et al. (2011)
$[CH_4]_-$	CH_4 lower boundary condition	$0 - 5.455$	mM	This study

To assess the influence of environmental conditions on the efficiency of the AOM biofilter and its influence on non-turbulent methane emission from dissociating permafrost and/or disintegrating methane gas hydrates in ESAS sediments a set of five "one-at-time" parameter variation experiments is designed. It encompasses the most important controls on benthic methane cycling (Regnier et al., 2011; Meister et al., 2013; Egger et al., 2018) and parameter ~~varuation~~ variation experiments are performed for both the passive as well as active baseline scenario:

1. Sedimentation rate ω. The sedimentation rate is varied over two orders of magnitude ($0.03 - 0.123 - 0.17 - 1.5$ cm yr^{-1}). Maximum values are comparable to terrestrial sediment accumulation rates in the Lena river delta (Bolshiyanov et al., 2015), fast marine sedimentation rates during the early Holocene sea transgression (Bauch et al., 2001) and marine accumulation on subsea permafrost deposit in Buor Khaya Bay (~ 1.1 cm yr^{-1}, inferred from Overduin et al. (2015)), while minimum values are representative of sedimentation rates found in the East Siberian Arctic Sea (Stein et al. (2001) in Levitan and Lavrushin (2009)). The baseline value of ω is calculated based on the empirical global relationship proposed by Burwicz et al. (2011).

2. Active fluid flow v_{up}. Buoyancy-induced motion (Baker and Osterkamp, 1988), water streams channeled through fault lines or groundwater discharge (Charkin et al., 2017) can cause active fluid flow in Arctic shelf sediments underlain by subsea permafrost or gas hydrates (Judd and Hovland, 2009; Semenov et al., 2019). Therefore, v_{up} is varied from $0 - 0.3 - 0.5 - 1 - 3 - 7 - 10$ cm yr^{-1}. This interval falls in the range of reported upward advective water velocities in marine sediments $0.005 - 30$ cm yr^{-1} (Regnier et al., 2011).

3. AOM constant k_{AOM}. Rate constants implicitly account for factors that are not explicitly described in the model and thus tend to show a strong variability between sites. A comprehensive compilation of published model AOM rate constants (Regnier et al., 2011) reveals a variability of over 6 order of magnitudes ($10 - 10^7$ M^{-1} yr^{-1}). The AOM rate constant k_{AOM} (eq. 5) is thus varied over the range $k_{AOM} = 5 \cdot 10^2 - 5 \cdot 10^3 - 5 \cdot 10^4 - 5 \cdot 10^5 - 5 \cdot 10^6 - 5 \cdot 10^7$ M^{-1} yr^{-1}.

4. Organic matter reactivity (i.e. RCM parameter). Although the apparent OM reactivity is controlled by a combination of two parameters (a and ν), previous studies indicate a less pronounced variability in ν (Arndt et al., 2013; Sales de Freitas, 2018), as well as a strong control of a on the SMTZ depth (Regnier et al., 2011; Meister et al., 2013). Thus, ν was kept constant, while a was varied over the entire range of previously published values $a = 0.1 - 1 - 10 - 100 - 500 - 1000$ yr (Arndt et al., 2013). Studies about ESAS organic matter degradation shows a reactivity of deposited organic matter which is compatible with the RCM parameter we explored. For instance, Bröder et al. (2016) found an half life for the organic carbon in the East Siberian Arctic Shelf of $19 - 27$ yr, which would correspond to an $a = 3.4 - 4.8$ yr, with $\nu = 0.125$.

5. Bioirrigation coefficient α_0. Bioirrigation activity remains largely unconstrained on the Siberian shelf due to the scarcity of observational data (Teal et al., 2008). However, environmental stressors, such as ice scouring (*e.g.* Shakhova et al. (2017) and references therein) and trawling, which can dig furrows up to few meters (Shakhova et al., 2017) are detrimental to the local fauna, thus suggesting a low bioirrigation intensity. Yet, observations from other polar sites indicate that although biological diversity and activity is often low, it might be locally enhanced (Clough et al., 1997). In addition, ice scouring might also enhance non-local transport seasonally. We therefore, varied α_0 over the entire range of plausible values : $0 - 33 - 66 - 99.5 - 120 - 240$ yr^{-1} (Thullner et al., 2009).

2.3.2 Transient Sensitivity Study

Dale et al. (2008c) showed that temporally varying environmental conditions may reduce the efficiency of the benthic AOM filter and facilitate methane escape due to the delayed response of the microbial community to changing conditions. Therefore, in addition to the steady state sensitivity study, we also ~~perform~~ performed a series of transient simulations to explore the impacts of seasonal and projected climate change on benthic methane effluxes on the ESAS in ~~rresponse~~ response to changing upward methane fluxes from dissociating permafrost and/or disintegrating methane gas hydrates. Transient simulations ~~are~~ were run with a bioenergetic rate law for AOM (eq. 6) and an explicit description of AOM biomass. Simulation results from the passive steady state baseline run with $[CH_4]_- = 0$ mM ~~are~~ were used as initial conditions for the transient experiments. Four different transient environmental perturbation scenarios that reflect seasonal (1, 2), as well as idealized future (3, 4) environmental variability on the ESAS ~~are~~ were run with three different values of v_{up}=$0 - 1 - 5$ cm yr^{-1} over a period of 200 years:

1. *Seasonal* CH_4: seasonal change of methane supply from permafrost thaw and/or hydrate destabilization. CH_4 concentration at the bottom of the sediment column: null for 6 months, then increasing up to a peak of $[CH_4]_-$ ($20 - 100 - 330 - 1169 - 5455$ μM) for the remaining 6 months of the year and again back to null concentration.

2. *Seasonal* $CH_4 + SO_4^{2-}$: seasonal freshening of waters due to riverine discharge and sea ice melt. During winter, higher bottom salinity (Dmitrenko et al., 2011) results in higher sulfate concentration (Dickson and Goyet, 1994), while lower salinities and thus sulphate concentrations characterise the melt season. The bottom boundary condition for methane $[CH_4]_-$ follows an opposite trend: it is set to zero during the winter months and increases in Arctic summer.

3. *Linear* CH_4: slow increase in methane supply from permafrost thaw and/or hydrate destabilization. A linear increase of the bottom boundary methane concentration $[CH_4]_-$ (from 0 up to the peak) over 200 years is applied.

4. *Sudden* CH_4: abrupt increase of methane supply from permafrost thaw and/or hydrate destabilization. An instantaneous change of bottom boundary methane concentration - from 0 to one of the peak value $[CH_4]_-$ - is applied.

2.3.3 Analyzed output

For each simulation we evaluate the effect of the respective parameter change on:

1. the non-turbulent (i.e. not-ebullition driven) flux of methane from the sediments into the water column;

2. the depth of the SMTZ;

3. the efficiency (η) of the AOM biofilter (see Appendix A for the exact definition of AOM applied here).

In addition, fluxes of SO_4^{2-} and CH_4 at the SMTZ, the maximum and integrated AOM rate and the Damköhler number (D_a) for AOM and methanogenesis are also calculated. Damköhler number is defined as eq. B4 (see Appendix B) and sets the ratio between the typical transport time-scale and the typical reaction time-scale. If $D_a < 1$, the reaction time-scale is longer than transport time-scale (i.e. the reaction is slower) and the process is reaction-limited. If $D_a > 1$ the process is transport-limited. Finally, for transient simulations, the integrated AOM-perfoming biomass (ΣB) was also analyzed.

3 Results and discussion

3.1 Case study: sediment core on the Laptev Sea shelf

Fig. 1 compares simulated and observed depth profiles for site 14-3. Cores were retrieved during the SWERUS-C3 campaign (Miller et al., 2017; Brüchert et al., 2018; Brüchert, 2020). Simulation results show an overall good agreement with measurements, but also reveal a slight overestimation of NH_4^+. Data-model fitting reveals that, reconciling simulated and observed CH_4 and SO_4^{2-} depth profiles, requires a diffusive flux of CH_4 through the lower model boundary (i.e. a bottom boundary concentration of $[CH4]_- = 16$ mM). Neither higher marine OM contents in sediment layers below the first 22 cm for which observations are available, nor higher reactivities result can satisfactorily reproduce the observed sulfate depletion and observed gradients. Model-data fitting thus not only highlights the important role of AOM in controlling the sulfate-methane ~~transisition~~ transition zone (SMTZ), but also indicates that upward migrating methane from deep, pre-Holocene sources, such as subsea permafrost in the sediment might be an ubiquitous feature on the Siberian shelf.

The simulated PO_4^{3-} and DIC profiles are in good agreement with data, suggesting that the degradation dynamics of marine organic matter and adsorption are well captured by the model- although the maximum concentration of PO_4^{3-} at depth is mostly controlled by the saturation value of $[PO_4^{3-}]$. The largest discrepancy between data and modeling results are observed for NH_4^+. Observed NH_4^+ concentrations first increase to a maximum at about 6 cm depth and the slightly decrease in the

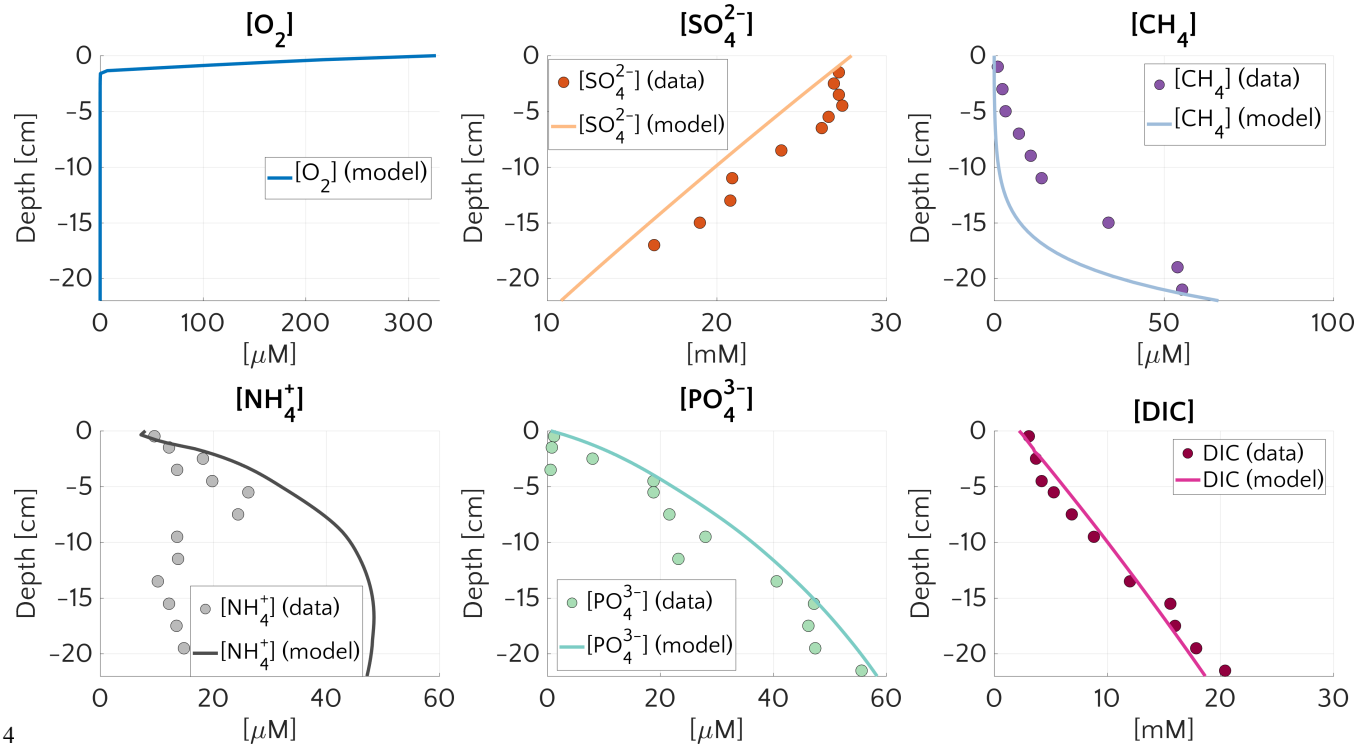

Figure 1. Pore water concentration profiles for O_2, SO_4^{2-}, CH_4, NH_4^+, PO_4^{3-} and DIC at site 14-3 on the Laptev Sea (76.171°N, 129.333°E, 56 m water depth). Dots represents the measurements and continuous lines the simulated results. The boundary conditions and model parameters employed in the model are reported in ~~table~~ Table S4, the measured organic carbon content in ~~table~~ Table S5. For O_2 no measured profile is available.

lower sediment layers, whereas simulated NH_4^+ show an asymptotic increase in NH_4^+ concentrations. The observed NH_4^+ profile might either indicate changes in OM reactivity and/or characteristics or spatially heterogeneous adsorption/desorption dynamics. Such ~~downcore~~ heterogenity is not incorporated in the model and accounting for such a heterogeneity would require additional information.

3.2 Main physical and biogeochemical controls on potential non-turbulent methane flux from ESAS sediments

3.2.1 General patterns of methane and sulfate cycling on the ESAS

The comprehensive ensemble of all sensitivity experiments allows exploring the general patterns of methane and sulfate cycling under a range of environmental conditions that is broadly representative for conditions encountered on the ESAS at present (Fig. 2). Model results confirm that AOM is an efficient sink for the diffusive CH_4 supply from below. For most of the investigated environmental conditions (95% of the runs), 95-99.9% of the upward diffusing CH_4 is consumed within the SMTZ, resulting in very small or negligible methane effluxes ($\leq 10^{-2}$ μmolCH_4 cm^{-2} yr^{-1}) from the sediment. If upscaled to the total area

of the ESAS ($\sim 1.485 \cdot 10^6$ km^2, Wegener et al. (2015)), for which methane outgassing estimates have been published, the smallest simulated non-turbulent methane flux (*i.e.* $1.4 \cdot 10^{-13}$ μmol cm^{-2} yr^{-1}, Fig. 2.*b*) would sum up to a total flux of 2.1 mmolCH_4 yr^{-1}, resulting in a negligible role of non-turbulent, benthic methane fluxes to the Arctic methane budget.

Yet, ~~model~~ results also show that, under a specific set of environmental conditions that lower the efficiency of the AOM biofilter (see detailed discussion below), non-turbulent CH_4 escape from ESAS sediments can reach values of up to 27 μmolCH_4 cm^{-2} yr^{-1}. Simulation ~~results show~~ analysis shows that these high effluxes and, thus, low AOM biofilter efficiencies are generally ~~simulated~~ obtained for environmental conditions that cause a shallow location of the SMTZ (< 18 cm) and that they are very sensitive to changes in environmental conditions that would cause a deepening of the SMTZ. For instance, a deepening of the SMTZ from 18 to 26 cm results in a rapid increase in AOM efficiency from 1% to 98% (Fig. 2.*a*). Furthermore, results indicate that, for SMTZ depths larger than 26 cm, AOM remains an efficient barrier across the full spectrum of investigated environmental conditions (Fig. 2). The observed link between AOM filter efficiency and SMTZ is reflected in the strong (semilog) linear relationship between methane flux at the SWI and the SMTZ depth (Fig.2.*b*). Such a relationship reveals the pivotal connections between these two quantities and mirrors the empirically found linear log-log relationship between measured CH_4 fluxes at the SMTZ and the SMTZ depths (Fig. ~~S4~~S5) by Egger et al. (2018). Maximum simulated CH_4 effluxes are thus comparable in magnitude to fluxes reported from other settings potentially sensible for CH_4 emissions. These include mud-volcanoes, *e.g.* in the Gulf of Cadiz: 2.1-40.7 μmolCH_4 cm^{-2} yr^{-1} (Niemann et al., 2006a); Håkon Mosby mud-volcano in the Barents Sea: 0.03 μmolCH_4 cm^{-2} yr^{-1} (Niemann et al., 2006b) and coastal settings, *e.g.* a Dutch coastal reservoir (20-80 μmolCH_4 cm^{-2} yr^{-1}, Egger et al. (2016)) or tidal flats (4-800 μmolCH_4 cm^{-2} yr^{-1} Borges and Abril (2011)). Upscaling the highest simulated non-turbulent flux (27.48 μmolCH_4 cm^{-2} yr^{-1}) to the ESAS results in a total efflux of 0.408 TmolCH_4 yr^{-1} = 6.52 TgCH_4 yr^{-1}. This value represents an estimated upper limit which, for comparison, equals $\sim 10\%$ of global marine seepage at seabed level (Saunois et al., 2016) and is in magnitude similar to the global methane efflux that has been estimated for upper continental slope sediments on a centennial timescale (4.73 TgCH_4 yr^{-1}, Kretschmer et al. (2015)).

Further insights into the general drivers that control methane dynamics in ESAS sediments are provided by Damköhler numbers. Damköhler numbers for simulated methanogenesis ($D_{a_{MG}}$) and AOM ($D_{a_{AOM}}$) are reported in Fig. S2. $D_{a_{MG}}$ (purple circles) are < 1 , span a range of $\sim 0.0021 - 0.43$ and are thus comparable to previously reported $D_{a_{MG}}$ of 0.22 for methane gas hydrate bearing sites, such as Hydrate Ridge and Kithley Canyon (Chatterjee et al., 2011). They reveal that methanogenesis is always slower than methane transport and that CH_4 dynamics driven by methanogenesis are thus reaction-limited. This result is consistent with the fact that methanogenesis rates are merely supported by the slow influx and transport of OM by burial and bioturbation.

In contrast, high $D_{a_{AOM}}$ values ($D_{a_{AOM}}$ =32-2.78 $\cdot 10^5$ - Fig. S2, orange circles), show that AOM is transport-limited, suggesting a sensitive role of transport parameters in determining AOM efficiency and in controlling methane flux across the SMTZ and subsequently the SWI.

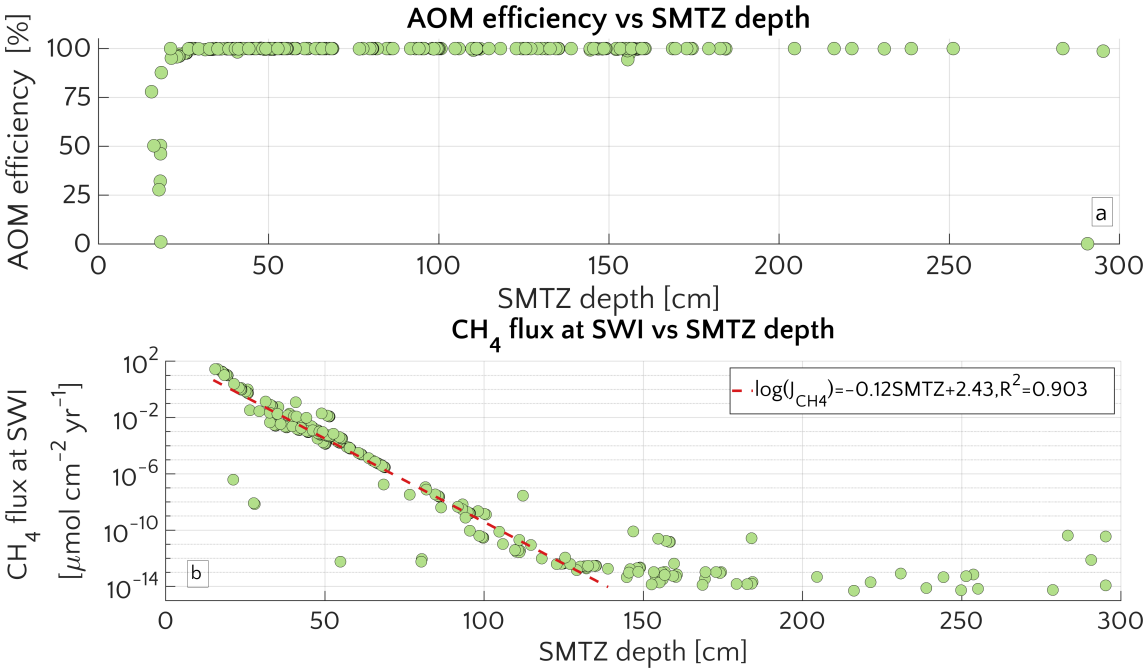

Figure 2. Aggregation of all the simulation performed for the "one-at-time" sensitivity study. *a*. AOM efficiency versus the depth of the SMTZ. *b*. Scatter plot and semi-log fit of the methane flux (J_{CH4}) at the SWI versus SMTZ depth.

3.2.2 Environmental controls and mechanisms of methane escape from ESAS sediments

The simulated general patterns of methane and sulfate cycling on the ESAS broadly corroborate previous findings regarding the dominant environmental controls on AOM biofilter efficiency and SMTZ depth (Regnier et al., 2011; Egger et al., 2018; Meister et al., 2013; Winkel et al., 2018). Yet, they also challenge intuitive views on the factors that favour high CH_4 escape through the SWI. In particular, they highlight the essential link between AOM efficiency and SMTZ depth and the central importance of environmental conditions that control the depth of the SMTZ. In addition, they suggest that transport processes play a dominant role for non-turbulent methane effluxes from ESAS sediments. The following sections explore the role of each of the investigated environmental conditions on methane efflux in more detail. They also shed light on the mechanisms behind non-turbulent methane escape from ESAS sediments.

3.2.3 Role of advective transport

Fig. 3.*a* illustrates the effects of sedimentation rate ω on the flux of methane across the SWI. For both active ($v_{up} = 1$ cm yr^{-1}) and passive ($v_{up} = 0$ cm yr^{-1}) settings, simulated CH_4 effluxes increase exponentially with sedimentation rate (log-log linear, see fig. 3.*c*) from $5.5 \cdot 10^{-15}$ μmolCH_4 cm^{-2} yr^{-1} for low sedimentation rates ($\omega = 0.03$ cm yr^{-1}) to values as high as 27.5 μmolCH_4 cm^{-2} yr^{-1} for high sedimentation rates ($\omega = 1.5$ cm yr^{-1}). Accordingly AOM acts as an efficient

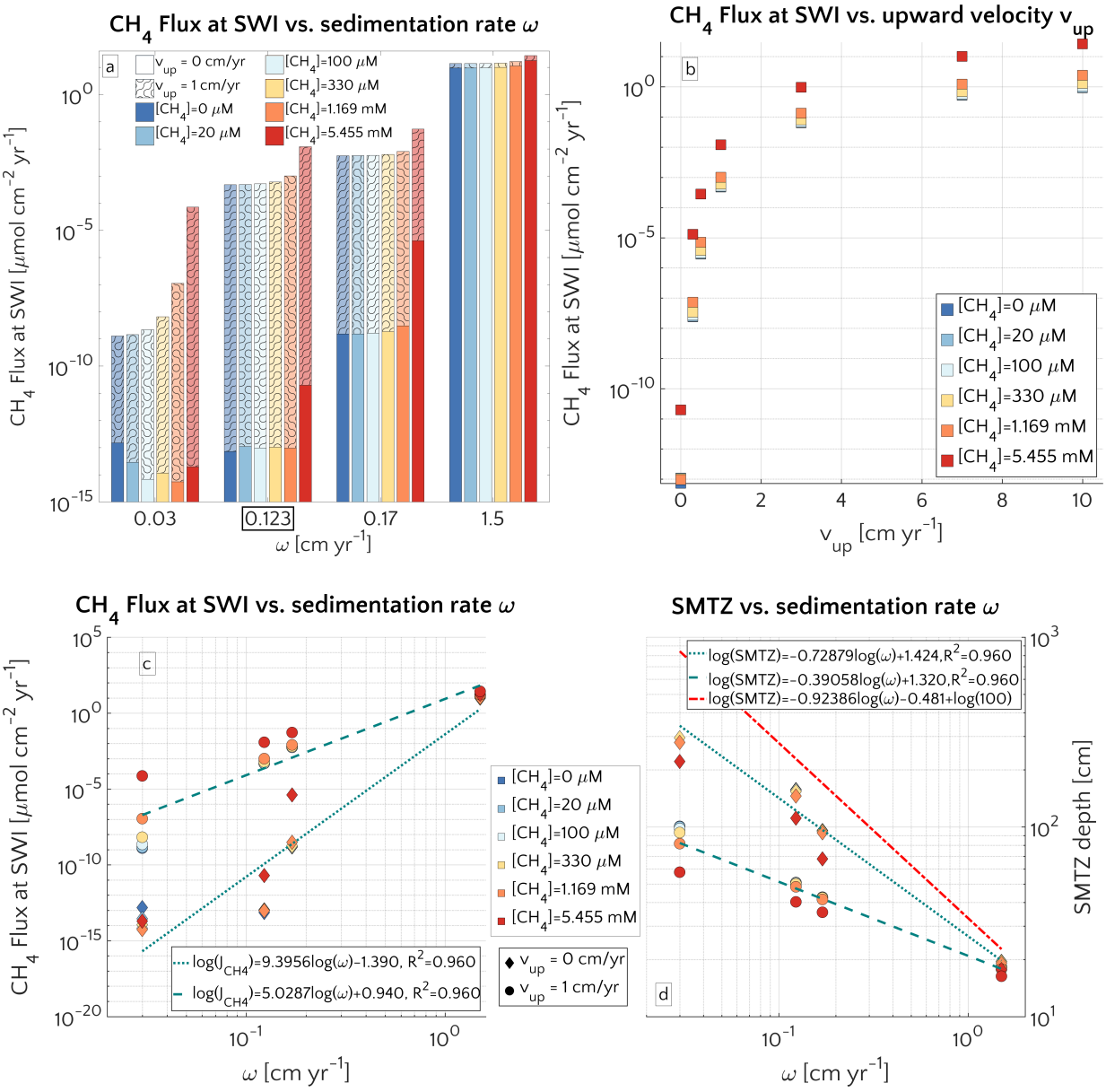

Figure 3. *a*. Barplot of the methane flux at the SWI versus ω for passive case (plain style) and active case (pattern style) and the $[CH_4]_-$ reported in the text. The squared value of ω is the reference value. *b*. Semilog plot of methane flux at SWI versus v_{up} for the different $[CH_4]_-$ reported in the text. *c*. Log-log plot of methane efflux at SWI versus ω for passive case (diamonds) and active case (circle). The log-log fit is also displayed. *d*. Log-log plot of SMTZ depth versus ω for passive case (diamonds) and active case (circle) with log-log fit. The red line is the trend found by Egger et al, 2018 (the term log(100) is to take into account unit conversion).

filter for upward diffusing methane (with $\eta \sim 100\%$, see Fig. S3S4), in slowly accumulating sediments. Integrated AOM rates (ΣAOM), for both active and passive settings, are in agreement with these findings. They range from $0.04 - 3.7$ mol m^{-2} yr^{-1} and are, thus, comparable to values that are typically observed in sediments characterised by an efficient AOM biofilter (*e.g.* Albert et al. (1998); Martens et al. (1998); Regnier et al. (2011)). In contrast, the efficiency of the AOM biofilter drops to $50 - 0\%$ for high sedimentation rates. The main driver behind the simulated high CH_4 fluxes and low AOM efficiencies in these rapidly accumulating sediments, are enhanced methanogenesis rates. High sedimentation rates facilitate not only the supply of organic matter to the methanogenic zone of the sediment, but also reduce residence times in the upper sediment layer, resulting in a lower OM age (see eq. S13, S15S14, S16)/degradation state (see eq. S11S12) within the methanogenic zone. The enhanced supply of reactive OM to anoxic sediment layers supports higher methanogenesis rates, resulting in higher methane porewater concentrations and an upward shift of the SMTZ.

In addition, the presence of active fluid flow further enhances methane efflux. The CH_4 fluxes from below adds complexity to the overall methane dynamics and this effect is investigated further by contrasting Damköhler numbers for passive and active settings on the shelf. Table ?? S8 shows that for low to intermediate sedimentation rates, $D_{a_{AOM}}$ values significantly decrease with v_{up}, indicating that less and less methane consumption occurs within the typical transport time scale τ_T, thus, leading to a reduction in AOM biofilter efficiency. For instance, for $\omega = 0.123$ cm yr^{-1}, τ_T is about three orders of magnitude slower than τ_R without the presence of active fluid flow, while for $v_{up} = 10$ cm yr^{-1} τ_T accelerates and is only one order of magnitude slower than τ_R, resulting in a reduced consumption within the SMTZ. Accordingly, the decrease in $D_{a_{AOM}}$ coincides with an increase in CH_4 effluxes (Fig. 3. The trend in $D_{a_{AOM}}$ is reversed for high sedimentation rates ($\omega > 1.5$ cm yr^{-1}, *i.e.* $D_{a_{AOM}}$ increases with increasing v_{up}, while CH_4 efflux remains constant. This increase in $D_{a_{AOM}}$ can be explained with a simple increase in AOM rates due to the build-up of methane gas in deeper sediment layers and its partial re-dissolution with in the AOM zone where porewater methane concentrations decrease (also see Fig. 4 below).

AOM Damköhler number for $\omega = 0.123$ cm yr^{-1} and $\omega = 1.5$ cm yr^{-1}. The two values are for the maximum and minimum values among the simulations with different bottom methane concentration. Missing values are because simulations were not run with the corresponding pair of parameters. ω 1206 1124 683 327 120 52 32 [cm yr^{-1}] 1521 1473 772 409 139 57 42 470 - - 1408 - - - 518 1630

Maximum simulated flux differences between active and passive settings can reach up to 10 orders of magnitude. Yet, flux differences quickly decrease with increasing sedimentation rates. Rapidly accumulating sediments show almost no difference in efflux between active and passive sites (Fig. 3.*a*). In contrast to sedimentation rates, the mechanism behind the control of v_{up} on non-turbulent methane efflux is straightforward and self-evident. Active flow enhances the upcore upward transport of CH_4, shifting the SMTZ upcore upwards and, thus, increasing CH_4 concentrations at shallow sediment depths (see Fig. 3.*d*). The apparent paradox of the CH_4 efflux insensitive to fluid flow in fast accumulating sediments can be resolved by examining the dissolved CH_4 depth profiles (Fig. 4). Simulated depth profiles are nearly identical and reveal CH_4 concentrations at or near the saturation concentration. In fast accumulating sediments, high methanogenesis rates result in an over-saturation of porewaters directly below the generally shallow SMTZ. High methanogenesis rates thus support the build up of methane gas. Methane gas formation also explains why, in for these cases, integrated methanogenesis exceed no-turbulent non-turbulent CH_4 fluxes by

up to 6 times. In rapidly accumulating, active and passive sediments, non-turbulent CH_4 fluxes are thus essentially identical. However, active settings will be characterised by the additional build-up of gaseous CH_4 and its potential escape through the sediment-water interface- a process not simulated in the present study.

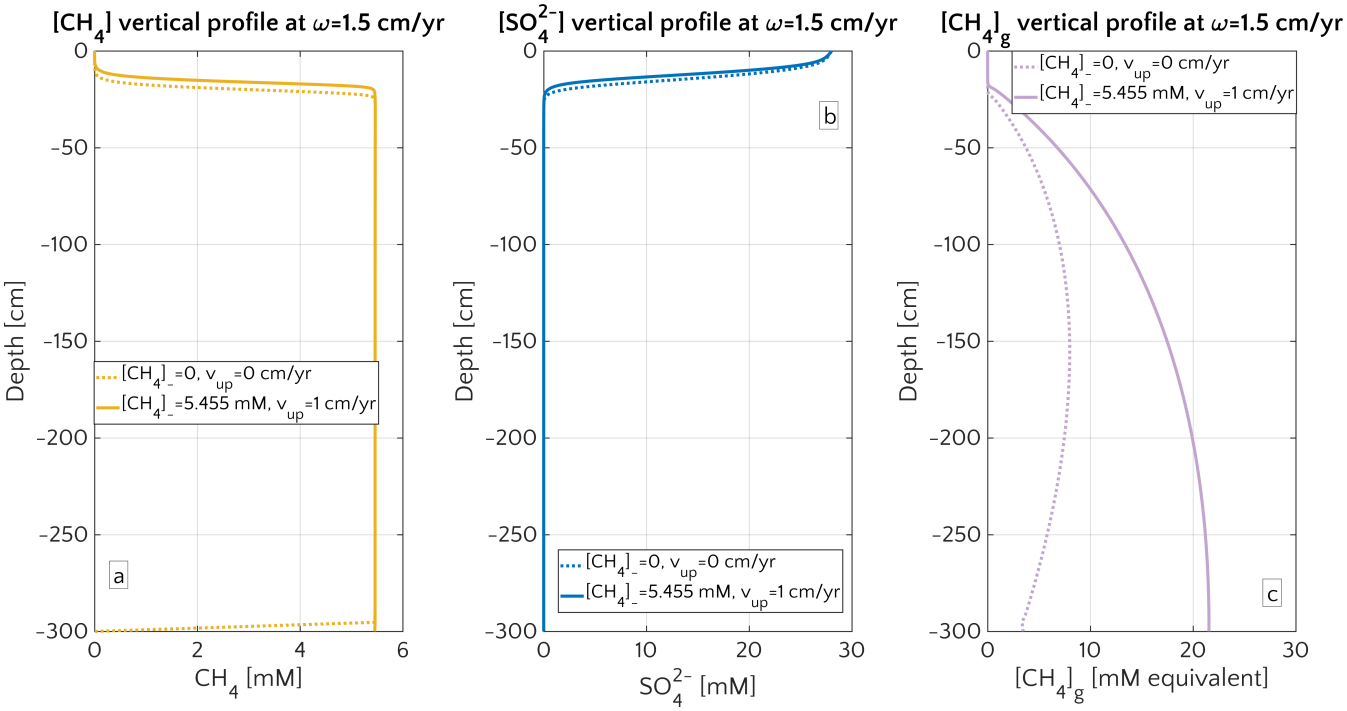

Figure 4. Porewater profiles in case of $\omega = 1.5$ cm yr^{-1} for CH_4 (*a*), SO_4^{2-} (*b*) and gaseous CH_4 (*c*). Dashed lines are simulation in passive scenario with $[CH_4]_- = 0$ mM, while continuous lines simulations display active scenario with $[CH_4]_- = 5.455$ mM, corresponding to the saturation concentration in the environmental conditions considered for the representative profile.

Model results thus show that the dominant mechanism behind the observed transport-control on non-turbulent CH_4 efflux is an overall increase in CH_4 concentration and an ~~upcore~~ upward shift of the SMTZ rather than an increasing relative contribution of advective transport processes to the total efflux. In fact, a comparison of the different methane transport processes across the SWI (~~Fig. ??~~*i.e* molecular diffusion, bioturbation-induced diffusion, bioirrigation and advective transport, as explained in section S1) shows that the relative contribution of both the advection and molecular diffusion flux to the total flux is small and further decreases with increasing v_{up} (Fig. S3). High non-turbulent methane effluxes in rapidly accumulating and/or active settings are thus largely driven by the non-local irrigation flux (see section 3.2.5 for more details on the role of irrigation). With increasing ω or v_{up}, the SMTZ shifts ~~upcore~~upwards, resulting in higher methane concentrations at shallow sediment depths and thereby reinforcing the relative contribution of non-local transport for CH_4 fluxes, as well as lowering the efficiency of the AOM barrier from $\eta \sim 100\%$ to $\eta \sim 78\%$. The important role of the SMTZ location as a key control on CH_4 efflux is further confirmed by the observed exponential relationship between the location of the SMTZ and ω (Fig. 3.*d*). This result is

qualitatively in agreement with the global compilation of empirical data by Egger et al. (2018), which reveals the same log-log decreasing trend between SMTZ and sedimentation rate. Our results are also consistent with observations from brackish sediments that show that sedimentation rates > 10 cm yr^{-1} give rise to high non-turbulent CH_4 fluxes ($20 - 80$ μmolCH_4 cm^{-2} yr^{-1}) and a high OM burial efficiency ($\sim 78\%$, Egger et al. (2016)). Egger and co-workers explained these findings by the slow growth of AOM microorganisms and the resulting inability of the microbial community to consume all of the CH_4 produced. Yet, our results show that the same pattern can be observed without having to invoke a low AOM efficiency. Our simulations thus indicate that the rapid burial of reactive organic matter to deeper sediment layers in rapidly accumulating sediments is sufficient to explain high CH_4 effluxes.

~~Relative contribution of transport process to the methane flux at the SWI: the advective component (blue) and the bioirrigation component (red). ω is set to the baseline value of 0.123 cm yr^{-1}. For each value of v_{up} and a specific flux component each dot corresponds to a simulation with a different value of bottom CH_4 concentration. Diffusive component of the flux is always $< 10^{-10}$.~~

3.2.4 Role of organic matter quality

The quality of organic matter deposited onto the sediment exerts an additional control on CH_4 efflux. Fig. 5 illustrates the influence of organic matter quality (as a function of OM degradation model parameter a, see eq. ~~S11~~S12) and sedimentation rate ω on non-turbulent methane efflux for both active and passive settings, as well as different methane fluxes from below. Results corroborate the dominant influence of sedimentation rates on methane efflux, while organic matter quality exerts a secondary control. This also means that, in order to assess the main features of possible CH_4 efflux in terms of modeling, capturing the details of organic matter quality is not fundamental. Maximum fluxes are generally simulated for rapidly accumulating sediments $\omega > 0.5$ cm yr^{-1} that receive organic matter of intermediate quality ($a = 10 - 100$ yr).

These findings are in agreement with previously published studies (Regnier et al., 2011; Meister et al., 2013) and can be explained with the fact that high methanogenesis rates require a supply of reactive OM to the methanogenic zone. If organic matter quality is high ($a < 10$ yr), methanogenesis becomes substrate limited due to the rapid degradation of organic matter through energetically more favourable degradation pathways in the shallow sediments. In turn, if organic matter quality is low ($a > 100$ yr), methanogenesis becomes reactivity limited. ~~The~~ And this is especially true for ESAS sediments at depth. Therefore, the ideal combinations of organic matter reactivity and sedimentation rate that result in maximum methane effluxes correspond to conditions ~~characterised~~ characterized by OM that is i) sufficiently reactive to support enhanced methanogenesis rates and thus an accumulation of CH_4 at depth, but ii) sufficiently unreactive (in comparison to the burial rate) to escape the complete degradation in non-methanogenic sediments. ~~Model results~~ BRNS outcomes show that the onset of active fluid flow and an enhanced methane supply from below (i.e. higher CH_4 concentration at the lower boundary) increase the CH_4 efflux through the SWI without altering the overall patterns (see Fig. 5.*a-b* vs 5.*c-d*).

3.2.5 Role of non-local transport

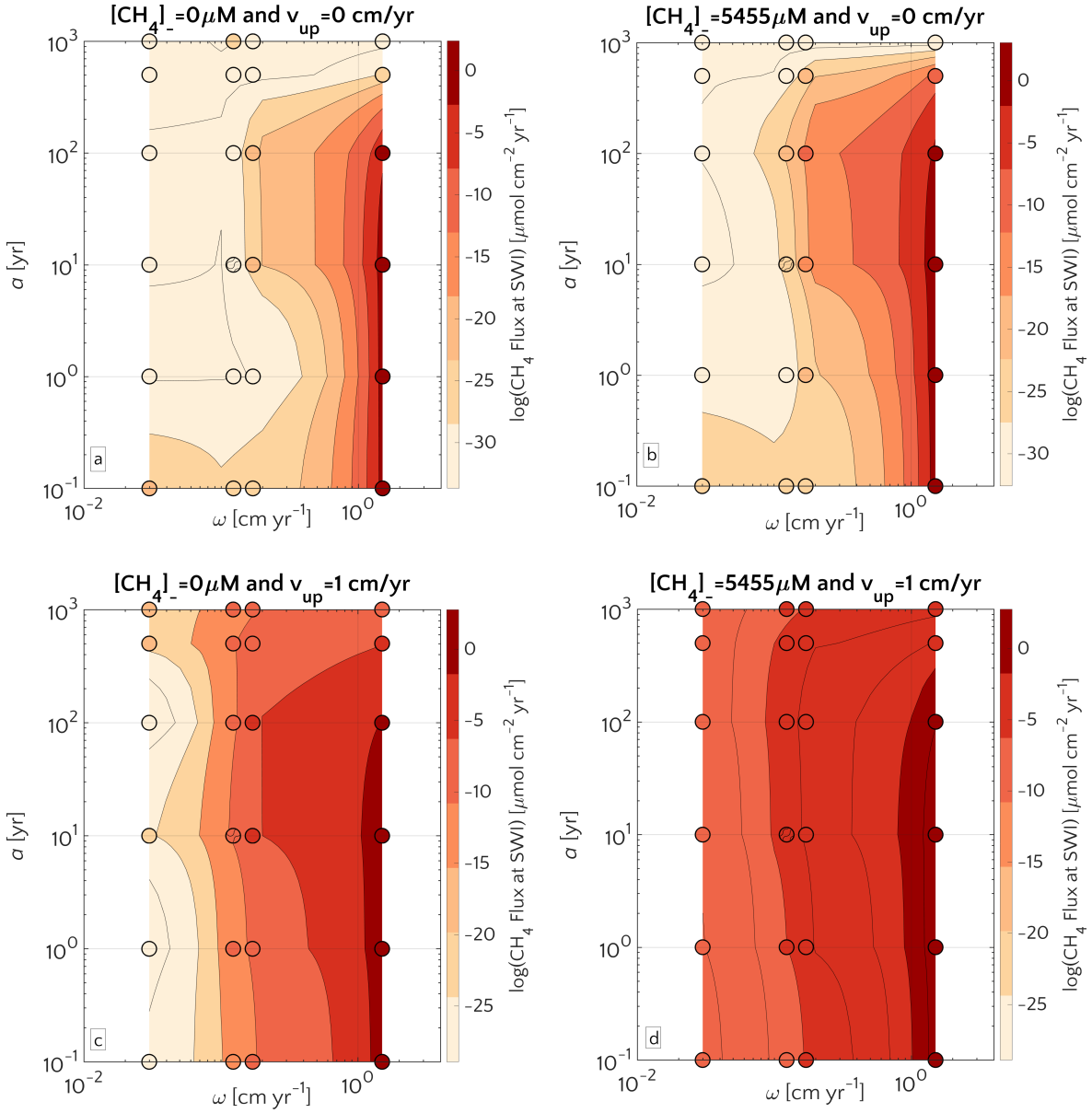

Figure 5. Flux of methane at the SWI as dependent on a and ω. For $[CH_4]$=0 mM (*left*) and $[CH_4]$=5.455 mM (*right*), and passive (*top*) and active (*bottom*) case. The circle with pattern corresponds to the baseline simulation.

~~Fig. ?? further investigates~~ The analysis of the influence of bioirrigation on non-turbulent CH_4 efflux from the ESAS ~~. It~~ (Fig. S12) shows that such a process enhances methane efflux in sediments that are ~~characterised~~ characterized by a shallow SMTZ~~, for instance, due to high sedimentation rates, active fluid flow and//or methane flux from below~~. Yet, bioirrigation exerts a limited effect under a range of environmental conditions that favour a deep or shallow SMTZ location respectively.

In passive settings, changes in bioirrigation coefficient ~~,~~ (α_0~~,~~) exert a limited ~~influence~~ control on CH_4 effluxes. For most ~~model~~ passive scenarios, the SMTZ is located well below the sediment layer affected by bioirrigation ($z_{irr} = 3.5$ cm, ~~hence~~ which implies that bioirrigation is strongly suppressed below ~~15~~ 15 cm) and, thus, changes in α_0 have no effect on methane efflux. ~~Changes in bioirrigation intensity only exert a noticeable effect on methane efflux when methane concentrations at the lower boundary exceed $[CH_4]_- = 5.455$ mM. Under these conditions, a decrease in methane efflux is observed with increasing α_0, because the increasing bioirrigation activity supports an enhanced downcore transport of SO_4^{2-}, leading to a deepening of the SMTZ and a reduction in methane efflux. Model results thus partly support previously published findings by Cordes et al. (2005) and Niemann et al. (2006a) , who argued that bioirrigation increases methane consumption due to the enhanced downcore electron acceptors transport. However, model results also show that this effect is only observed under environmental conditions that result in a shallow SMTZ and that methane consumption and efflux remain largely unaffected by changes in bioirrigation intensity if the SMTZ is located deeper in the sediment.~~

~~Barplot of the methane flux at the SWI versus α_0 for passive case (plain style) and active case (pattern style) and the $[CH_4]_-$ reported in the text.~~

In contrast to passive settings, active settings reveal a rapid increase in methane efflux with the onset of bioirrigation activity. Methane effluxes first increase by up to 5 orders of magnitude from α_0=0 yr^{-1} to α_0=5 yr^{-1}, reaching maximum effluxes of ~ 0.02 $\mu molCH_4$ cm^{-2} yr^{-1}, before remaining almost constant with a further increase in bioirrigation coefficients (up to 240 yr^{-1}). The simulated increase in methane efflux is a direct effect of the transport process itself, which enhances the ~~upcore~~ upward transport of methane accumulating in the upper sediment layers, including layers below the generally shallow SMTZ. ~~The subsequently simulated constant methane effluxes with increasing bioirrigation intensity in combination with the fact that bioirrigation represents the largest flux term at SWI (Fig.6) suggest that concentration differences close the the sediment-water interface remain broadly similar for all $\alpha_0 > 5$ yr^{-1}.~~

These results are corroborated by the concomitant analysis of CH_4 dynamics over the 3-dimensional transport coefficient ω, v_{up} and α_0 space shown in Fig.6.

A comparison between simulations with $\alpha_0 = 0$ yr^{-1} and $\alpha_0 \neq 0$ yr^{-1} ($\alpha_0 = 5$ yr^{-1}, $\alpha_0 = 10$ yr^{-1} and $\alpha_0 = 33$ yr^{-1}) shows that irrigation increases the CH_4 efflux at low to intermediate sedimentation rates and/or high v_{up} (lower-left corner of the phase space in both plots). Yet, maximum methane effluxes that are simulated for high sedimentation rates or v_{up} are almost identical between bioirrigated and non-irrigated sites despite the differences in dominant transport mechanism (diffusion when $\alpha_0 = 0$ yr^{-1}; irrigation when $\alpha_0 \neq 0$ yr^{-1}). Under these conditions (i.e. high v_{up} and/or high ω), the SMTZ is located close to the SWI. ~~Under these conditions~~In such settings, non-local transport becomes the dominant transport process in bioirrigated sediments (see section 3.2.3 and Fig. S3) because it weakens concentration gradients near the SWI and, thus, contributes to a substantial reduction in the gradient-driven, diffusive transport terms. As a consequence, simulated CH_4 efflux at the SWI are ~~are~~ broadly similar for all of the investigated $\alpha_0 \neq 0$ yr^{-1} (Fig. 6.*b,c,d*). It is worth noticing that, independently on the α_0, CH_4 efflux for $\omega = 0.03$ cm yr^{-1} and $v_{up} = 10$ cm yr^{-1} is ~ 1 $\mu molCH_4$ cm^{-2} yr^{-1}- a value almost identical to the one reported in Luff and Wallmann (2003) - 1.4 $\mu molCH_4$ cm^{-2} yr^{-1} - for a sediments characterised by $v_{up} = 10$ cm yr^{-1} and $\omega = 0.0275$ cm yr^{-1}.

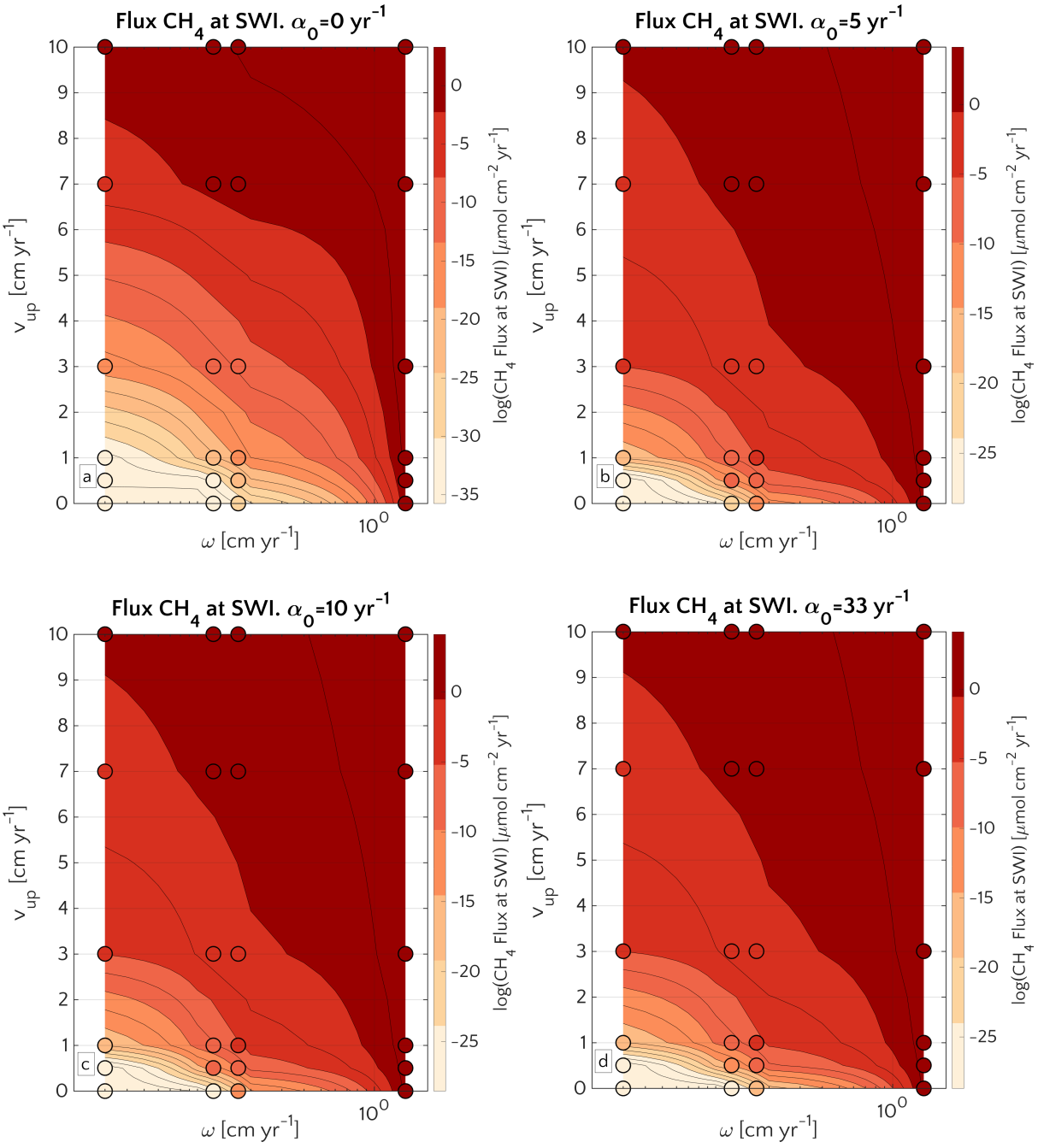

Figure 6. Efflux of methane at the SWI as dependent on v_{up} and ω for $\alpha_0 = 0$ yr^{-1} (*a*), $\alpha_0 = 5$ yr^{-1} (*b*), $\alpha_0 = 10$ yr^{-1} (*c*) and $\alpha_0 = 33$ yr^{-1} (*d*). Circles represent simulations outcomes. Results for $\alpha_0 \neq 0$ yr^{-1} are almost the same. The lower boundary condition for methane is $[CH_4]_- = 1.169$ mM. A 3D version of the plot is reported in Fig. S13.

3.2.6 AOM rate constant

Given its crucial role in AOM biogeochemistry, one would expect a pronounced influence of the kinetic rates constant, k_{AOM}, on non-turbulent methane effluxes. However, ~~simulation results reveal~~ modeling reveals that k_{AOM} only plays a minor role for non-turbulent methane fluxes across the SWI (see Fig. ~~S11, S12~~S14, S15). An increase in k_{AOM} can reduce methane effluxes from passive shelf sediments by up to 5 ~~order~~ orders of magnitude. Still, its effect remains small compared, for instance, to the response to variations in sedimentation rate, which can change methane efflux by up to 14 orders of magnitude. The most important effect of increasing k_{AOM} is the increasing linearity of the $[CH_4]$ and $[SO_4^{2-}]$ profiles around the SMTZ and the concurrent narrowing and ~~downcore~~ downward movement of the SMTZ, which can result in a reduction in methane efflux. ~~Model results~~ Simulations thus show that the AOM biofilter and, as a consequence, non-turbulent methane effluxes from sediments, are not affected by the exact value of the kinetic rate constant, at least in the range we analyzed. This is in disagreement with results by Dale et al. (2008c), which show that, in dynamic settings subject to large methane fluxes, an increase of 3 orders of magnitude in k_{AOM} (from 10^2 M^{-1} yr^{-1} to 10^5 M^{-1} yr^{-1}) leads to a reduction in steady state methane fluxes below 10^{-2} $\mu molCH_4$ cm^{-2} yr^{-1}. However this discrepancy might be ascribable to the high water flow velocity employed in their simulation ($v_{up} = 10$ cm yr^{-1}), ten times higher than the one we considered in our active simulations. Finally, on the shallow ESAS, dissolved methane concentrations are limited by the comparably low gas saturation concentration, resulting in a minor influence of k_{AOM} on methane fluxes (as the AOM rate is proportional to the CH_4 concentration). An indirect support to our findings regarding the secondary role of k_{AOM} on the AOM itself comes from Luff and Wallmann (2003). They showed that, as long as not null, the actual value of k_{AOM} is unimportant for the precipitation of authigenic carbonate. Since the authigenic carbonate precipitation is largely driven by alkalinity produced during AOM (*e.g.* Aloisi et al. (2004); Luff et al. (2005); Karaca et al. (2010); Pierre et al. (2012); Crémière et al. (2016b, a); Meister et al. (2018)), the observed independence of precipitation rates from k_{AOM} bolsters our conclusion.

3.2.7 Summary of steady state experiments

The results of the steady state sensitivity study indicate that, under environmental conditions that are broadly representative for the ESAS, low AOM efficiencies and thus high non-turbulent CH_4 effluxes from thawing subsea permafrost and/or dissociating methane gas hydrates (larger than 4 $\mu molCH_4$ cm^{-2} yr^{-1}) are promoted by intense advective transport (sedimentation rate $\omega > 1$ cm yr^{-1}, active fluid flow $v_{up} > 7$ cm yr^{-1}). Under these conditions, CH_4 efflux can be further enhanced by moderate OM reactivity ($a = 10 - 10^2$ yr) and intense non-local transport processes, such as bioirrigation (irrigation constant $\alpha_0 > 0$ yr^{-1}). Overall, non-turbulent benthic escape of CH_4 from deep sources appears to be mainly controlled by the concurrent effects of ω, v_{up} and α_0. In contrast, maximum AOM rates, k_{AOM}, exert no influence on the AOM filter efficiency.

3.2.8 Geographic pattern and potential for non-turbulent methane emissions from Laptev Sea sediments

One strength of ~~a~~ models is that ~~it~~ they can provide the explorative means to assess dynamics at spatial/temporal scales that cannot easily be assessed by observations alone. In particular, transfer functions, simple look-up tables and ~~/or~~ neural networks

that are derived from, or trained on, a large ensemble of individual model simulations over a broad range of plausible boundary conditions have been frequently and successfully used to investigate regional and even global dynamics (Gypens et al., 2008; Marquardt et al., 2010; Dale et al., 2015; Capet et al., 2016; Dale et al., 2017; Bowles et al., 2014). Such a quantitative framework in which first-order estimates of potential non-turbulent methane escape from ESAS sediments can also be derived from the results of the model sensitivity study.

Model results indicate that sedimentation rate exerts the dominant control on benthic escape of methane from thawing subsea permafrost and/or dissociating methane gas hydrates on the ESAS. The functional relationship between sedimentation rate and methane flux across the SWI reported in Fig. 3.*c* thus allows estimating a potential non-turbulent, benthic methane efflux derived from deep sources for a given sedimentation rate. Thus, if the spatial distributions of these environmental controls on methane efflux are known, a first-order geographical distribution of potential non-turbulent methane escape from the Siberian Shelf can be derived. However, the availability of observational data from the Siberian Shelf is extremely scarce. Therefore, we here focus on the Laptev Sea - a comparable well studied part of the Siberian Shelf. The Laptev Sea is well-known for its subsea permafrost and gas hydrate content and subject to large riverine inputs from the Lena river. To derive a map of sedimentation rates for Laptev Sea shelf sediments, we use published linear sedimentation rates (Table ~~S8~~S9) and extrapolate these values to the entire region by applying a simple 3D kriging method (see Fig. 7.*a*), using the International Bathymetric Chart of Arctic Ocean (IBCAO) (Jakobsson et al., 2012) and employing longitude, latitude and water depth as predictors for ω.

Observations indicate that sedimentation rates are highest ($\omega = 0.45$ cm yr^{-1}) close to the mouth of the Lena river and Moustakh Island in the Buor-Khaya Gulf. As a consequence, the vicinity of the river mouth, as well as the area along the shallow bathymetric profile towards the NE of the Lena delta are characterized by comparably high sedimentation rates ($\omega = 0.27 - 0.42$ cm yr^{-1}). The relatively shallow areas (~ 10 m deep) around the New Siberian islands reveal intermediate values ($\omega = 0.06 - 0.12$), while minimum sedimentation rates ($\sim 0.002 - 0.03$ cm yr^{-1}) roughly follow the 55 m isobath down to the continental slope at 100 m. Deeper shelf areas are characterized by a more homogeneous distribution of sedimentation rates with values around $0.03 - 0.06$ cm yr^{-1}.

Table 2. Estimated flux of CH_4 at SWI in mol yr^{-1} for different depth regions of Laptev Sea in a passive ($v_{up} = 0$ cm yr^{-1}) and active ($v_{up} = 1$ cm yr^{-1}) case.

	v_{up}	
Region (water depth, area)	0	1
$0 - 10$ m, $7.7 \cdot 10^4$ km^2	6.5	$8.9 \cdot 10^5$
$10 - 80$ m, $4.5 \cdot 10^5$ km^2	296.2	$8.5 \cdot 10^6$

Estimated non-turbulent methane effluxes corresponding to the highest measured sedimentation rates close to the Lena mouth do not exceed $1.57 \cdot 10^{-1}$ μmolCH_4 cm^{-2} yr^{-1} assuming the presence of active fluid flow and $2.25 \cdot 10^{-5}$ μmolCH_4 cm^{-2} yr^{-1} for passive settings. These findings are not surprising as steady state sensitivity results indicate that high CH_4 efflux requires sedimentation rates of $\omega > 1$ cm yr^{-1}. The regional non-turbulent CH_4 efflux budget for different depth sections of

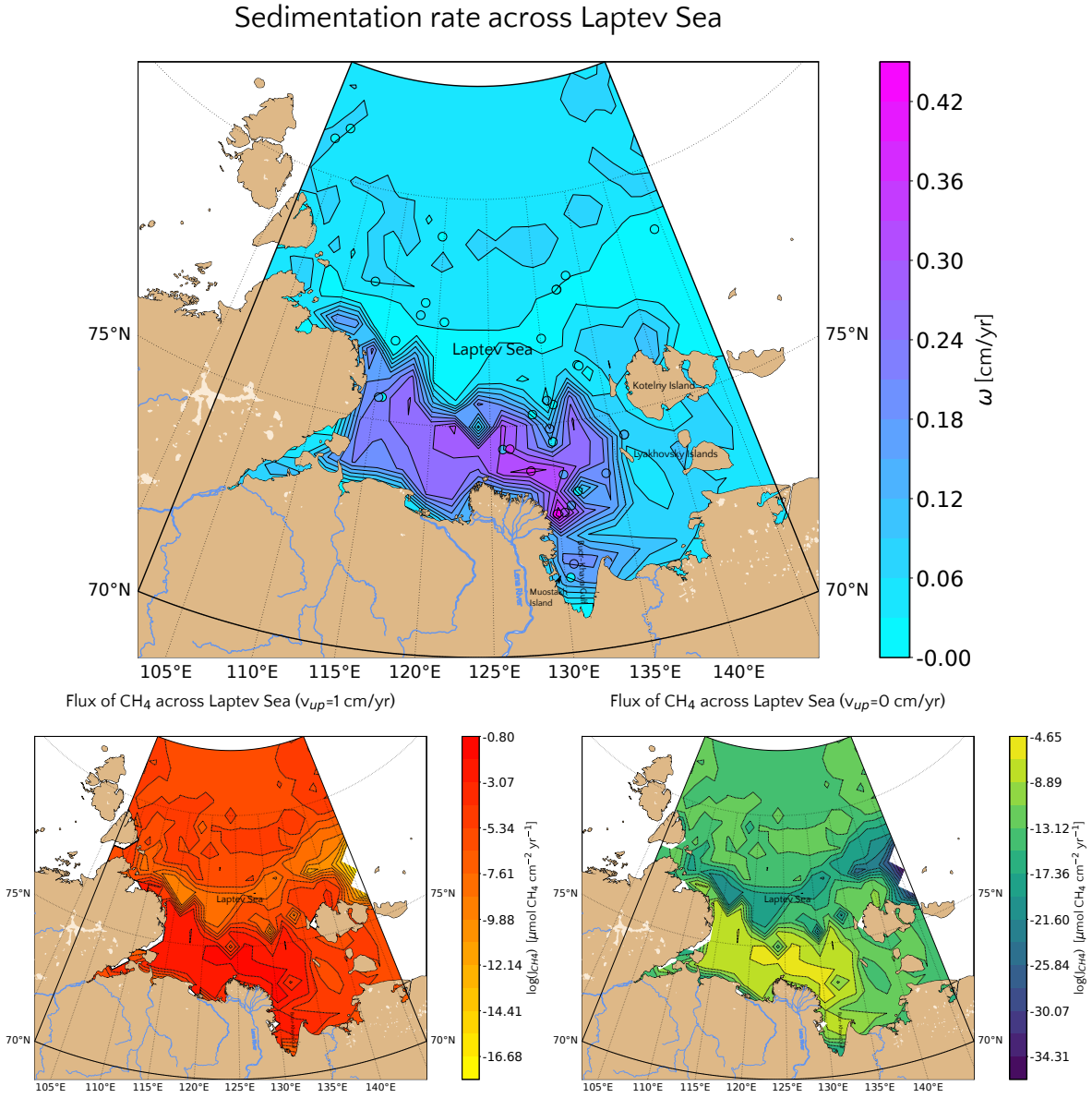

Figure 7. *a*. values of the sedimentation rate extrapolated for the whole Laptev Sea via a simple kriging method. The reference values (circles) are the ones reported in Table ~~S8~~S9. *Bottom* (Log) Values of the potential non-turbulent dissolved methane emissions at the SWI considering the relationship presented in Fig. 3.*c* for passive (*b*) and active (*c*) cases.

the Laptev Sea assuming the absence of active fluid flow in Laptev Sea shelf sediments (see Table 2) thus indicates that non-turbulent CH_4 efflux is negligible. Even if we assume the omnipresence of an active fluid flow of $v_{up} = 1$ cm yr^{-1}, the estimated non-turbulent methane efflux merely sums up to $9.39 \cdot 10^6$ molCH_4/yr (~ 0.1 GgCH_4/yr) over the entire Laptev Sea

area of $527.4 \cdot 10^3$ km^2. Such small effluxes would most likely be subject to further oxidation in the water column, thus limiting any potential impact on atmospheric methane concentrations and climate.

Higher advective fluid flow velocities, intermediate organic matter reactivity and/or a more intense macrobenthic biological activity could increase these estimates of non-turbulent methane escape from the Laptev Sea shelf. Higher advective fluid flow velocities (i.e. $v_{up} > 1$ cm yr^{-1}), possibly in connection with active seepages, groundwater discharges and fault lines (the latter follow parallel pattern in Laptev Sea (Drachev et al., 1998) on the direction SW-NE from the west of Lena delta up to the little Lyakhovsky and Kotelny island), could result in methane effluxes of up to $10 - 10^{1.3}$ μmolCH$_4$ cm^{-2} yr^{-1} (see Fig. 5 and Fig. 6). However, such high fluid flow velocities would be only found locally and would thus merely give rise to a number of methane emission hot spots that would not change the overall non-turbulent methane flux budget. In addition, intermediate organic matter reactivity, in particular in the fast accumulating sediments close to the coastline and the Lena River Delta that receive more reactive organic matter from thawing terrestrial permafrost (Wild, 2019) could result in a higher estimated non-turbulent methane escape . However, our sensitivity study results show that OM reactivity merely plays a secondary role, suggesting that changes in OM reactivity would only change efflux by less than an order of magnitude assuming both $a = 100$ yr or $a = 1$ yr. Changes in bioirrigation intensity would exert merely a limited effect on efflux estimates, as bioirrigation has already been included in the estimate calculations. The absence of bioirrigation, which is known to be patchy in Arctic sediments, could act both in the direction of further reducing (limiting the bioirrigated flux from the sediments) or increasing (by limiting the flux of TEAs from the seawater and therefore oxidation) the estimated non-turbulent methane efflux. Additional physical reworking, such as ice scouring or dredging, may also have such an opposite effect: it could reduce the methane efflux (by enhancing the flux of TEAs into the sediments) but it could also intensify it (by removal of the upper sediment layer).

Model results thus show that, under present-day, steady state environmental conditions, AOM acts as an efficient biofilter for potential non-turbulent methane fluxes in Laptev Sea sediments. The estimated non-turbulent methane escape from Laptev Sea shelf sediments cannot support previously estimated methane outgassing fluxes of few teragrams of CH$_4$ yr^{-1} ~~(Berchet et al., 2016)~~ (Berchet et al., 2016; Thornton et al., 2020) or even tens of teragrams of CH$_4$ yr^{-1} (Shakhova et al., 2014). If such outgassing were to be supported by methane efflux from Laptev Sea sediments, it would require the build-up of CH$_4$ gas reservoirs in Laptev Sea sediments of at least similar or larger size than the evaded amount, as well as the preferential and rapid transport of this CH$_4$ gas to the atmosphere. Nevertheless, model results also suggest that projected trends of terrestrial permafrost thawing and coastal permafrost degradation (Vonk et al., 2012) might increase the importance of non-turbulent methane escape for the Arctic's methane budget by potentially increasing sedimentation rates through coastal erosion (vast amount of debris and terrigenous material) and increased riverine inputs (Guo et al., 2007); active fluid flow through permafrost and methane gas hydrate degradation (James et al., 2016; Ruppel and Kessler, 2017); organic matter reactivity through an enhanced delivery of more reactive permafrost organic matter (Wild et al., 2019) and/or an enhanced macrobenthic activity through warming and Atlantification. However, the magnitude of these projected environmental changes and thus their effect on non-turbulent methane escape from ESAS sediments is difficult to assess.

3.3 Methane efflux dynamics in response to seasonal and long term environmental variability

The steady state sensitivity results ~~reveals~~ reveal that, under steady state conditions, AOM represents an efficient biofilter for upward migrating methane from thawing permafrost and/or dissociating methane gas hydrates on the ESAS. Yet, transient dynamics induced by, for instance, seasonally or climate change driven variability in environmental conditions, may weaken the efficiency of the AOM biofilter. Therefore, we additionally explore the potential for non-turbulent methane escape from thawing subsea permafrost ~~tand~~and/or dissociating methane gas hydrate in ESAS sediments under transient conditions. Table 3 summarizes the maximum ~~, simulated ,~~ simulated non-turbulent methane fluxes for two ~~seasonal~~ kinds of environmental change scenarios~~(~~: seasonal and long-term. With the former, we explore seasonal changes in deep methane flux ~~,~~ and seasonal freshening of bottom waters~~), as well as for two longterm environmental change scenarios (~~. With the latter instead, we investigate the impacts of a slow linear increase and a sudden maximum increase in deep methane flux ~~)~~(see Section 2.3.2).

Table 3. Maximum of methane fluxes (in μmol cm^{-2} yr^{-1}) at SWI for the 4 analyzed transient scenarios. Values in round parenthesis indicate the year after the beginning of simulation corresponding to the reported maximum.

		[*1.Seasonal* CH_4]			[*2.Seasonal* $CH_4 + SO_4^{2-}$]		
		v_{up} (cm yr^{-1})			v_{up} (cm yr^{-1})		
		0	1	5	0	1	5
CH_4 (μM)	20	0.030 (200)	0.550 (50)	12.7 (17.5)	0.059 (200)	0.772 (51)	13.7 (18)
	100	0.029 (200)	0.550 (50)	12.7 (17.5)	0.058 (200)	0.753 (51)	13.7 (18)
	330	0.030 (200)	0.552 (49.5)	12.8 (18)	0.058 (200)	0.775 (51)	13.8 (18)
	1169	0.031 (200)	0.558 (49.5)	12.9 (18)	0.059 (200)	0.783 (51)	14.0 (18)
	5455	0.034 (200)	0.577 (49)	14.0 (19)	0.062 (200)	0.832 (50)	15.2 (19)
		[*3.Linear* CH_4]			[*4.Sudden* CH_4]		
		v_{up} (cm yr^{-1})			v_{up} (cm yr^{-1})		
		0	1	5	0	1	5
CH_4 (μM)	20	0.029 (200)	0.550 (50)	11.7 (20)	0.029 (200)	0.550 (50)	12.7 (18)
	100	0.030 (200)	0.550 (50)	11.7 (20)	0.030 (200)	0.552 (50)	12.7 (18)
	330	0.030 (200)	0.550 (50)	11.7 (20)	0.031 (200)	0.557 (50)	12.9 (18)
	1169	0.032 (200)	0.550 (50)	11.7 (20)	0.033 (200)	0.565 (49.5)	13.4 (18)
	5455	0.036 (200)	0.560 (50)	11.8 (20)	0.040 (200)	0.639 (47)	18.8 (23)

~~Model results~~ Results reveal that the transient response of simulated non-turbulent methane efflux is similar for all environmental scenarios, but instead significantly differs for passive and active sites. In general, passive settings do not allow for significant methane escape (Fig. ~~S14~~S17). Although transient methane efflux monotonously increases over the simulated

period, ~~they merely reach small, maximum fluxes of 0.03-0.05~~ it only reaches a maximum value of $0.03-0.05$ μmolCH$_4$ cm^{-2} yr^{-1} (Fig. ~~S14~~S17). Similarly, the simulated SMTZ depth merely migrates $11.5-29$ cm ~~upcore~~ upwards (Fig. ~~S15~~S18). Over the simulated 200 years, the integrated non-turbulent methane escape from passive settings for all environmental change scenarios barely reaches 3-4 μmolCH$_4$ cm^{-2}.

In contrast, active settings (i.e. $v_{up} = 1$ cm yr^{-1}) ~~show~~ exhibit an initial increase in CH$_4$ fluxes to maxima of 0.55-0.83 μmolCH$_4$ cm^{-2} yr^{-1} over the first 50 years~~that~~. This growth coincides with a rapid upward shift of the SMTZ by 100 cm. Methane escape then temporarily ~~decreases~~ drops by 17-20% until year 70-75, ~~followed by a monotonous increase (i.e. onset of a new steady-state)~~ when it begins to increase again until the end of the ~~simulated period~~simulation. During this second ~~period (i.e.~~ phase (*i.e.* after the first 50 years), the SMTZ remains stationary. Temporally integrated methane efflux (over 200 years) increases with active fluid flow rate rate from 66-121 μmolCH$_4$ cm^{-2} for $v_{up} = 1$ cm yr^{-1} to $\sim 0.95-1.154$ mmolCH$_4$ cm^{-2} for $v_{up} = 5$ cm yr^{-1}. A large fraction of these emissions (30% and 48-87%, respectively) ~~of these emissions~~ occurs in the first 100 years after the perturbation.

Model results thus indicate that the exact temporal character of environmental changes does not exert an important influence on non-turbulent methane efflux. ~~Instead,~~ Conversely, both microbial growth dynamics ~~, as well as~~ and the presence/absence of active fluid flow (Table 3) largely control the transient response ~~of non-turbulent methane effluxes~~ to environmental change. The reasons for this are twofold. First, the response time of the resident AOM community is longer than the characteristic timescales ~~of the investigated environmental variability~~ under investigation, thus smoothing out the impact of environmental perturbations. ~~Furthermore~~Second, active fluid flow ~~initially~~ enhances the impact of the perturbation by triggering a significant ~~upcore~~ upward shift of the SMTZ.~~The~~ In particular, the initial movement of the SMTZ prevents the establishment of an efficient AOM community at the SMTZ~~and, thus,~~: this creates a "window of ~~opportunity~~opportunity" for methane escape. In contrast, the comparably slow and limited movements of the SMTZ in passive settings (Fig. ~~S15~~S18) enables the efficient establishment of an AOM community that acts as an efficient biofilter for upward migrating methane.

The following sections explore the factors that control the creation of such a window of opportunity and discusses the mechanisms behind the simulated methane escape. Given the overall similar transient response of non-turbulent methane fluxes to different environmental scenarios (Fig. S17, S18), we will ~~focus~~ base the following discussion on scenario 4~~(*i.e.* ~~, namely a step-like CH$_4$ forcing ~~)~~ with $v_{up} = 1$ cm yr^{-1} and a specific bottom concentration ~~, *e.g.*~~ ($[\mathrm{CH_4}]_- = 1.169$ mM). The reason for selecting this scenario is simple. In contrast to the other scenarios, scenario 4 allows for a straightforward definition of the initial and final state, which facilitates the attribution of a typical response time-scale for the system.

3.3.1 Window of opportunity

Fig. 8 illustrates the temporal evolution of the simulated (a) filter efficiency and AOM rate, (b) CH$_4$ efflux, (c) SMTZ depth and (d) AOM biomass for the ~~sudden methane flux~~ scenario 4 ~~(~~in case of $v_{up} = 1$ cm yr^{-1} ~~,~~ and $[\mathrm{CH_4}]_- = 1.169$ mM~~)~~. The onset of a sudden ~~, maximum~~ methane flux from thawing permafrost and/or dissociating methane gas hydrates below the sediment column triggers the rapid movement of the SMTZ. Simulation ~~results~~ outputs show that velocity ~~with~~ at which the SMTZ moves upward (v_{SMTZ}) is solely controlled by v_{up}~~as indicated by the constant $v_{SMTZ} \sim 11.4$~~ , as evident from the constant

$v_{SMTZ} \sim 2.46$ cm yr^{-1} ~~in all~~ for all the transient scenarios with $v_{up} = 1$ cm yr^{-1} (Fig. ~~S15~~S18). The initial ~~upward~~ upwards movement of the SMTZ delays the microbial response since the transient dynamics inhibits the establishment of a resident AOM community ~~that is~~ sufficiently large to consume upward migrating methane. The AOM rate~~and thus filter efficiency are controlled by~~ , and thus the filter efficiency, is controlled by the AOM biomass dynamics (~~Eq~~eq. 6), which in turn is determined by the kinetic (F_K, eq. 7) and thermodynamic (F_T, eq. 8) constraints. Fig. 10 illustrates the depth profiles of the thermodynamic and kinetic terms in the bioenergetic AOM formulation (eq. 6), as well as their evolution in response to the onset of a sudden methane flux from below. Initially, although kinetically possible (i.e. $F_K \neq 0$~~, eq. 7~~), AOM is inhibited by thermodynamic constraints (i.e. $F_T = 0$~~, eq. 8~~). During the ~~initial~~ first 23 years, AOM biomass thus remains largely constant (Fig. ~~S18.a~~S21.*a*) and, as a consequence, AOM rate and filter efficiency are zero. ~~During~~ In this period, aerobic methane oxidation represents the only barrier ~~for~~ to upward diffusing methane. However, ~~because of~~ this barrier is weak due to the limited availability of oxygen and the competition with aerobic organic matter degradation ~~and~~ as well as additional secondary redox reactions that also consume oxygen (see Table S3)~~, this barrier is weak~~. As a consequence, CH_4 efflux increases. The initial methane efflux is largely supported by ~~in-situ production of methane~~ *in situ* methanogenesis since the advective transport of methane (~~$\bar{v} = v_{up} - \omega = 0.877$~~ occurring at $v_{up} - \omega = 0.877$ cm yr^{-1}, corresponding to ~~20.2 cm in 24~~ 20.17 cm in 23 years) is too slow to allow methane from below ~~3~~ 3 m to reach the sediment-water interface.

After the first 23 years, thermodynamic constraints ease and AOM begins to efficiently consume upward migrating methane at the SMTZ by 40% (Fig. 8.*a*). ~~At that point, favourable conditions are encountered and the increasing AOM filter efficiency reduces methane efflux (Fig. 10.*b*). However, because~~ However, as consumption occurs at the SMTZ (~~i.e.~~ for the specific case at a sediment depth of 100.4 cm), it does not immediately affect the methane efflux at the SWI. The time required for the consumption signal to propagate to the SWI ~~amounts to~~ with velocity $\bar{v} = v_{SMTZ} + v_{up} - \omega = 3.337$ cm yr^{-1} is therefore $\frac{100.4\,\text{cm}}{3.337\,\text{cm yr}^{-1}} = 30.1$ yr. ~~As a consequence~~Consequently, methane efflux further increases~~typically peak 2-3 decades after the onset of methane supply~~. This methane efflux is now also supported from deep sources such as thawing permafrost and/or dissociating methane gas hydrates, which have started to contribute to methane efflux ~~around~~ between years 7 ~~to~~ and 20 ~~years~~ (assuming typical values of v_{up} reported for active marine sediments of 0.5-5 cm yr^{-1}). Methane ~~effluxes typically peak~~ efflux typically peaks 2-3 decades after the onset of methane supply. Maximum methane efflux increases with v_{up}: from $0.5 - 0.6$ μmolCH_4 cm^{-2} yr^{-1} for $v_{up} = 1$ cm yr^{-1} to $11 - 19$ μmolCH_4 cm^{-2} yr^{-1} for $v_{up} = 5$ cm yr^{-1}. Yet, the duration of this initial "window of opportunity" for methane escape decreases with increasing v_{up}. In general, simulated maximum methane fluxes ~~, as well as long-term methane efflux~~ fall within the range of previous ~~model methane effluxes from a range of~~ models applied to different environments (Sommer et al., 2006; Dale et al., 2008c) but do not reach the high values measured in other settings (Linke et al., 2005; Regnier et al., 2011).

After ~~this~~ the initial "window of opportunity" (i.e. $23 + 30.1 = 53.1$ years), the effect of ~~the~~ an efficient methane consumption at the SMTZ starts to reduce the non-turbulent methane efflux at the SWI (Fig. 8.*b*). This reduction ~~in methane efflux~~ lasts until the upward movement of the SMTZ slows down. At this point, the AOM filter efficiency reaches a quasi-stationary level of ~85% (as Fig. 8.*a*). Meanwhile, *in situ* methanogenesis continues to produce methane, which is not entirely consumed by the

AOM community that already reached its full capacity. As a consequence, methane fluxes at SWI increase again ~~and~~ until a new steady state is reached.

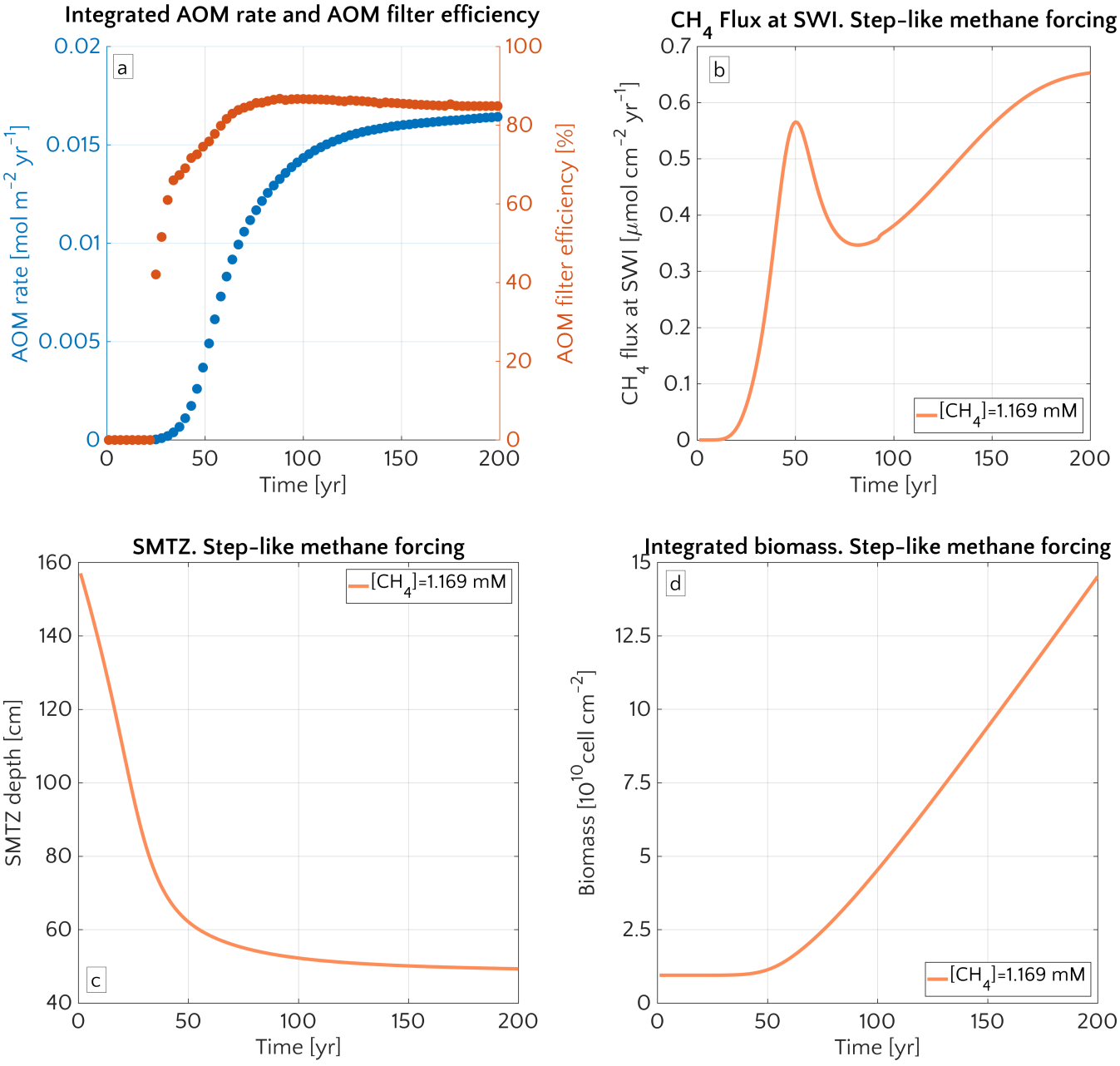

Figure 8. Time evolution over 200 years for the case of an active setup with $v_{up} = 1$ cm yr^{-1} and a step-like methane forcing from below from 0 to $[CH_4]_- = 1.169$ mM. *a.* AOM vertically integrated rate (blue) and AOM efficiency (red). *b.* CH_4 flux at SWI. *c.* SMTZ depth. *d.* Vetically integrated biomass (number of cells).

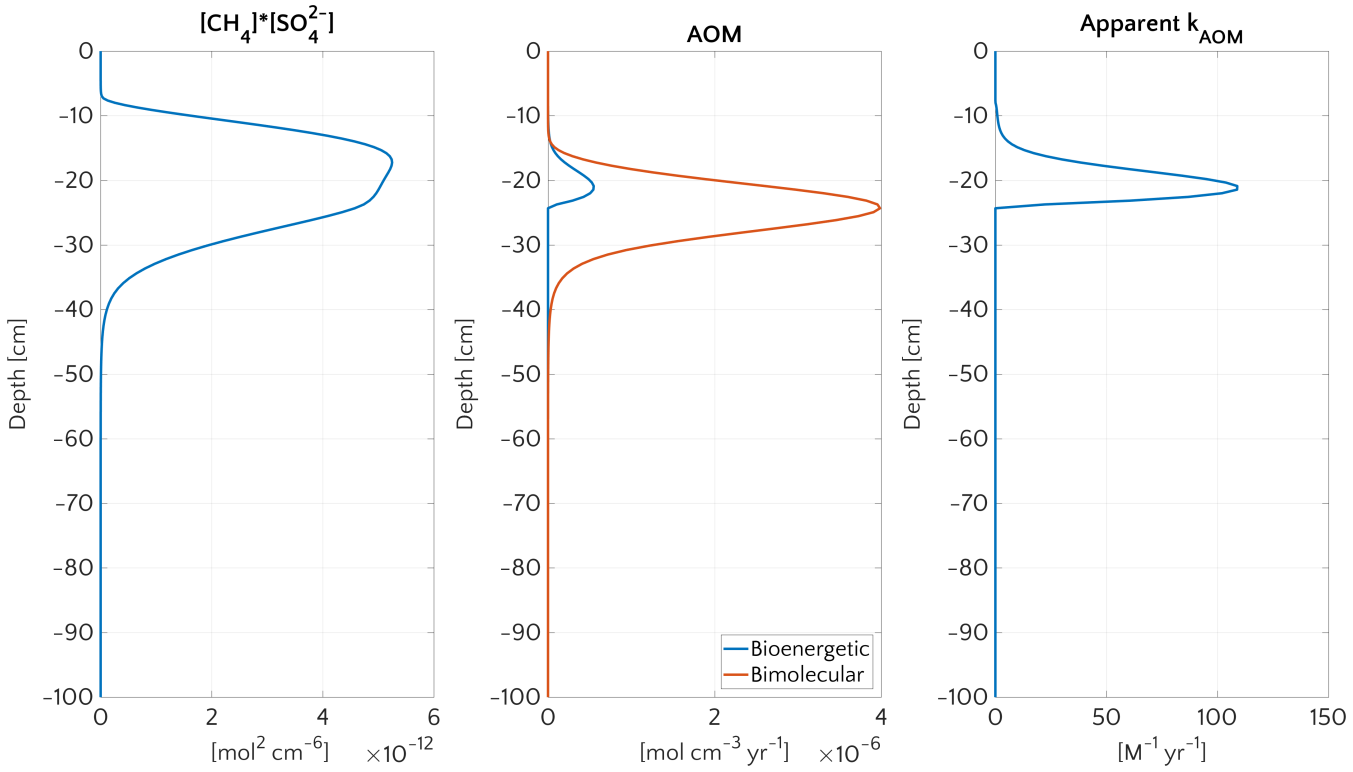

Figure 9. Vertical profiles at the end of transient simulation (after 200 years) with bioenergetic AOM fomulation for the case $[CH_4]_- = 1.169$ mM and $v_{up} = 5$ cm yr^{-1}. *a.* Bimolecular product $[CH_4] \cdot [SO_4^{2-}]$. *b.* AOM rate according to the bioenergetic formulation (blue) and, for comparison, according to bimolecular formulation used for the steady-state simulations (red). *c.* Apparent k_{AOM}, estimated from eq. 5.

3.3.2 Final new steady state

The ~~simulated~~ final new steady state ~~CH_4~~ value of methane efflux (Fig. 10.*b*, ~~S14 and S16~~S17 and S19) is generally in good agreement with Dale et al. (2008c), who reported an efflux of the same order of magnitude (3 μmolCH_4 cm^{-2} yr^{-1}) for the new steady state at the end of a transient run with $v_{up} = 10$ cm yr^{-1} and $[CH_4]_- = 70$ mM. ~~A better understanding can be obtained looking for instance at results of simulations~~ Simulations with $v_{up} = 5$ cm yr^{-1}, $\omega = 0.123$ cm yr^{-1} and $[CH_4]_- = 1.169$ mM (Fig. ~~S16) . In such a case~~S19) offer a better understanding of the model. In this case, the final new steady state is ~~roughly two order~~ about two orders of magnitude larger than the efflux of ~ 0.1 μmolCH_4 cm^{-2} yr^{-1} simulated in the steady state simulations~~(~~, with bimolecular rate law~~)~~, under identical environmental conditions (inferred from Fig. 6).

The reason for this discrepancy can be ~~found when~~ clarified by plotting the apparent k_{AOM} for transient simulations~~(*i.e.* extracting~~ . Such a value is calculated by computing an apparent bimolecular rate constant k_{AOM} (as in eq. 5) from the transient bioenergetic ~~simulation results for the~~ simulations for the new final steady state~~)~~. Results are shown in Fig. 9. Panel 9.*a* illustrates that the concentration product $[CH_4] \cdot [SO_4^{2-}]$ is wider than the AOM rate profile (panel 9.*b*, blue curve). Fig. 9.*c*

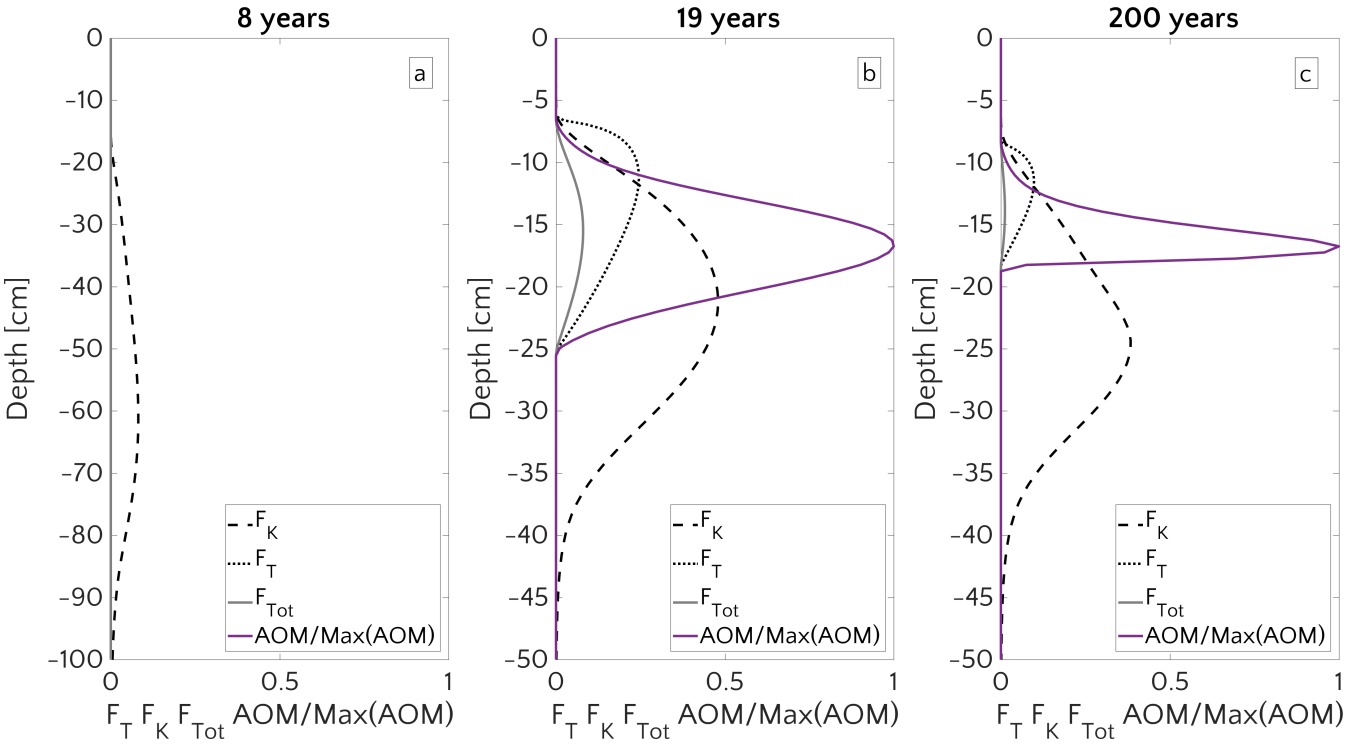

Figure 10. Vertical profile of F_T, F_K, $F_{Tot} = F_K \cdot F_T$ and the AOM (scaled to the maximum) for three instant in times. 8 years (a), 19 years (b)and 200 years ((c) of simulation, for the case $[CH_4]_- = 1.169$ mM and $v_{up} = 5$ cm yr^{-1}.

also shows that the apparent k_{AOM} is not uniform: it reaches a maximum value of 109 M^{-1} yr^{-1}, but remains well below 100 M^{-1} yr^{-1} at most depths. Compared to the values typically applied for bimolecular rate laws (i.e. $k_{AOM} = 10^2 - 10^7$ M^{-1} yr^{-1}), these values are rather low and reflect the ongoing thermodynamic limitation of AOM. F_T remains the main constraint on AOM throughout the simulation (Fig. 10.c). A more uniform sulfide concentration - $[HS^-]$ enters in defining F_T - in lower sediments ~~together~~ combined with the upward movement of the SMTZ pushes the maximum of F_T upwards, thus limiting the zone where AOM is thermodynamically favourable ($\sim$ 13 cm deep).

Integrated biomass ΣB ranges from $\sim 1.2 \cdot 10^{10}$ to $3.5 \cdot 10^{11}$ cells cm^{-2} (except for simulation with $v_{up} = 5$ cm yr^{-1} and $[CH_4]_- = 5.455$ mM, whose ΣB$= 1.2 \cdot 10^{12}$). These values are comparable with AOM biomass reported in Treude et al. (2003) ($1.5 - 1.8 \cdot 10^{10}$ cells cm^{-2}) or with values simulated in Dale et al. (2008c) ($3.7 \cdot 10^{11}$ cells cm^{-2} for $v_{up} = 5$ cm yr^{-1}). In addition, the maximum simulated biomass for active settings ($0.5 - 2.5 \cdot 10^{10}$ cells cm^{-3}) agrees well with previously reported values, ranging from 0.27 to $7.4 \cdot 10^{10}$ cells cm^{-3} (Dale et al., 2008c). ~~However, integrated~~ Integrated AOM rates (ΣAOM) are instead smaller then previously published rates for shallow, active sites above the shelf break (Boetius et al., 2000; Haese et al., 2003; Luff and Wallmann, 2003; Linke et al., 2005; Wallmann et al., 2006b; Dale et al., 2008c), but comparable to those observed in active sites below the shelf break (Aloisi et al., 2004; Wallmann et al., 2006a; Maher et al., 2006) or in passive settings (Borowski et al., 1996; Martens et al., 1998; Fossing et al., 2000; Jørgensen et al., 2001; Dale et al., 2008c).

The discrepancy ~~is likely~~ may be due to different environmental conditions encountered at these sites. For instance, Dale et al. (2008c) applied an advective velocity of $v_{up} = 10$ cm yr^{-1} and $[CH_4]_- = 60$ mM. While differences in v_{up} affect the ΣAOM, its effect on ΣB is negligible since an efficient AOM microbial filter ~~is known~~ has to account for at least $> 10^{10}$ cells cm^{-3} (Lösekann et al., 2007; Knittel and Boetius, 2009).

4 Conclusions

In this study, we evaluate the potential for non-turbulent, benthic methane escape from thawing subsea permafrost and/or dissociating methane gas hydrates in both passive as well as active settings and under a range of environmental conditions that are broadly representative for conditions encountered on the present and future East Siberian Arctic Shelf (ESAS). We identify the most important biogeochemical and physical controls on non-turbulent methane escape from those sediments under steady state conditions, as well as in response to environmental variability on seasonal and centennial timescales. Based on model results, we derive a simple transfer function that allows establishing a first-order regional estimate of (not-turbulent) methane efflux and of potential methane consumption in Laptev Sea sediments.

Model results reveal that AOM is an efficient sink for upward migrating, dissolved methane in ESAS sediments. Simulated non-turbulent methane effluxes are negligible for a broad range of environmental conditions under both steady state and transient conditions. Since AOM is a transport-limited process, transport parameters exert a dominant control on the efficiency of the AOM biofilter and, ultimately, on the methane efflux at the SWI. Both steady state and transient model results confirm the key role of advective transport (mainly sedimentation and active fluid flow) in supporting methane escape from Arctic shelf sediments. Under steady state conditions, high methane effluxes (up to 27.5 μmol cm^{-2} yr^{-1}) are generally found for sediments that are characterized by high sedimentation rates and/or active fluid flow (sedimentation rate $\omega > 0.7$ cm yr^{-1}, active fluid flow $v_{up} > 6$ cm yr^{-1}). Under these conditions, methane efflux can be further enhanced by intermediate organic matter reactivity (RCM model parameter $a = 10 - 10^2$ yr) even though the control exerted by organic matter is only secondary with respect to the transport parameters. Finally intense local transport processes, such as bioirrigation (irrigation constant $\alpha_0 > 1$ yr^{-1}), do also contribute to larger methane effluxes. Our results indicate therefore that present methane efflux from ESAS sediments can be supported by methane gas escape and non-turbulent CH_4 efflux from rapidly accumulating and/or active sediments (*e.g.* coastal settings, portions close to river mouths or submarine slumps). In particular, active sites sediments may release methane in response to the onset or increase of permafrost thawing or CH_4 gas hydrate destabilization.

High methane escape (up to 11-19 μmolCH_4 cm^{-2} yr^{-1} corresponding to 2.6-4.5 TgCH_4 yr^{-1} if upscaled to the ESAS) can occur during a transient period following the onset of methane flux from the deep sediments. Under these conditions, substantial methane escape from sediments requires the presence of active fluid flow that supports a significant and rapid upward migration of the SMTZ in response to the onset of CH_4 flux from below. Such rapid and pronounced movements create a window of opportunity for non-turbulent methane escape by inhibiting the accumulation of AOM-performing biomass within the SMTZ - mainly through thermodynamic constraints - thereby perturbing the efficiency of the AOM biofilter. The magnitude of methane effluxes, as well as the duration of this window of opportunity, is largely controlled by the active flow

velocity. In addition, results of transient scenario runs indicated that the characteristic response time of the AOM biofilter is of the order of few decades (20-30 years), thus exceeding seasonal-interannual variability. Consequently, seasonal variation of bottom methane and sea water sulfates exert a negligible effect on methane escape through the sediment-water interface.

AOM generally acts as an efficient biofilter for upward migrating CH_4 under environmental conditions that are representative for the present-day ESAS with potentially important, yet unquantified implications for the Arctic ocean's alkalinity budget and, thus, CO_2 fluxes. Our results thus suggest that previously published fluxes estimated from ESAS waters to atmosphere cannot be supported by non-turbulent methane efflux alone.

A regional upscaling of non-turbulent methane efflux for the Laptev Sea Shelf using a model-derived transfer function that relates sedimentation rate and methane efflux merely sums up to ~ 0.1 $GgCH_4$ yr^{-1}. Nevertheless, it also suggests that the evaluation of methane efflux from Siberian Shelf sediments should pay particular attention to the dynamic and rapidly changing Arctic coastal areas close to big river mouths, as well as areas that may favor preferential methane gas release (*e.g.* rapidly eroding coastlines, fault lines or shallow sea floors, *i.e* <30 m). In addition, our findings call for more data concerning sedimentation and active fluid flow rates, as well as the reactivity of depositing organic matter and bioirrigation rates in Arctic shelf sediments.

In conclusion, we argue that the evaluation of projected subsea permafrost thaw and/or hydrate destabilization impacts on the Arctic environment requires models that include an explicit description of 1) methane gas, 2) AOM biomass, as well as 3) the entire network of the most pertinent biogeochemical reactions. Such approaches, valid globally for all the shelves underlain by methane reservoirs (*e.g.* continental slopes), are even more recommended in order to enable a robust quantification of methane escape from the Arctic shelf to the Arctic ocean, settings even more sensible to the rapidly changing environmental conditions. Finally such refined modeling will also help evaluate the impact of subsea permafrost thaw and methane destabilization on Arctic alkalinity and biogeochemical cycling.

Code and data availability. Primary data needed to reproduce the analyses presented in this study are archived by the MaxPlanck Institute for Meteorology are available upon request (publications@mpimet.mpg.de)

Appendix A: AOM efficiency η

If we identify the SMTZ region as the portion of the sediment column where the rate of AOM is 1% of the maximum, we can define the efficiency of the AOM filter η as

$$\eta(\%) = \left(1 - \frac{J^{+}_{CH4}}{J^{-}_{CH4}}\right) \cdot 100 \tag{A1}$$

where J^{+}_{CH4} is the methane flux at the shallowest point where the AOM rate is 1% of the maximum (upper dashed line in Fig. A1), and J^{-}_{CH4} is methane flux at the deepest point where the AOM rate is 1% of the maximum (lower dashed line in Fig. A1).

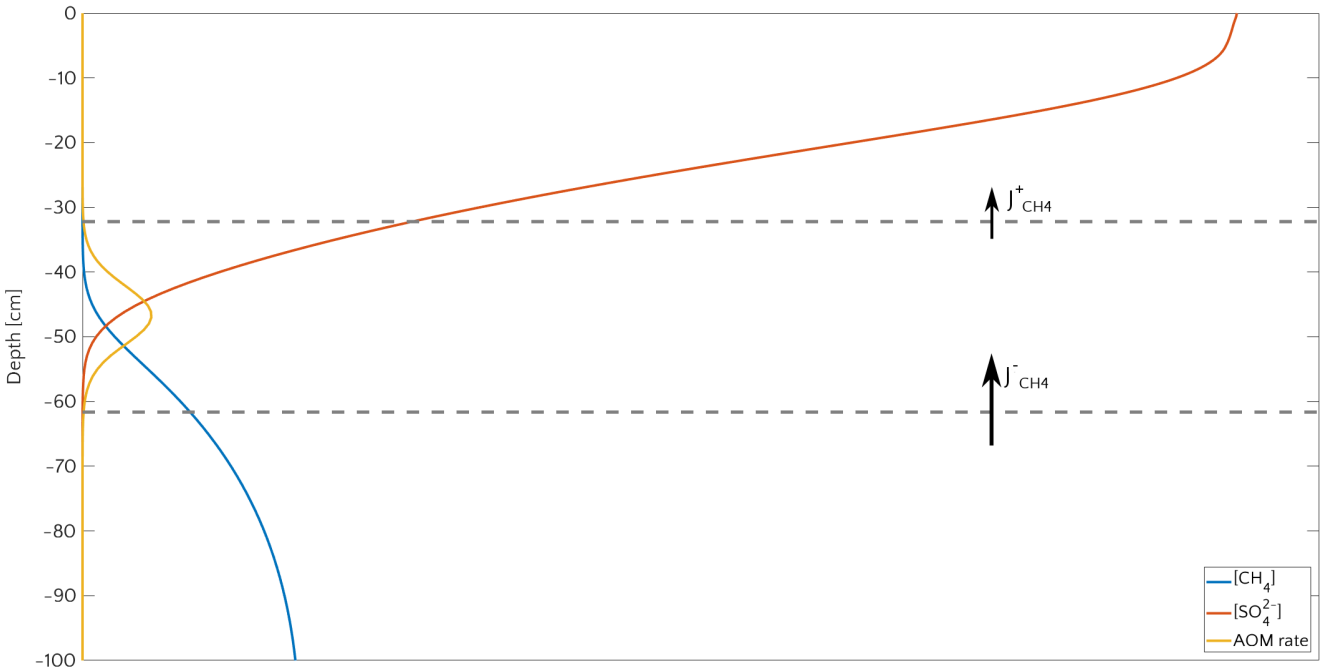

Figure A1. Typical sediment profile of $[SO_4^{2-}]$, $[CH_4]$ and AOM rate. Units are mM for concentration and mM yr^{-1} for rate. The region between the two dashed lines represents the zone where AOM rate is larger than 1% of it its maximum and defines the Sulfate Methane Transition Zone (SMTZ). The fluxes J^-_{CH4} and J^+_{CH4} are the fluxes used in the definition of η of eq. (A1).

Appendix B: Damköhler number

The Damköhler number $D_a$is a dimensionless quantity which relates time scales typical of transport processes to time scales typical of chemical reactions. It compares the consumption/production rate with the advective transport and is defined as

$$D_a = \tau_T/\tau_R \tag{B1}$$

where τ_T is the advective timescale and τ_R is the reaction timescale. τ_R is defined as $1/K_R$ where K_R is the reaction rate of AOM or methanogenesis. If we call R the reaction rate then K_R reads:

$$K_R = \frac{1}{\mathcal{L}} \int_{\mathcal{L}} \frac{R}{[\mathrm{CH_4}]} dz \tag{B2}$$

where $\mathcal{L}$ is the width where the reaction rate is larger than 1% of the maximum rate. τ_T is instead defined as

$$\tau_T = \frac{\mathcal{L}}{|v_{up} - \omega|} \tag{B3}$$

where $v_{up} - \omega$ is the effective advective velocity. D_a can be the expressed by:

$$D_a = \frac{\tau_T}{\tau_R} = \frac{1}{|v_{up} - \omega|} \int_{\mathcal{L}} \frac{R}{[\mathrm{CH_4}]} dz. \tag{B4}$$

Competing interests. All contributing authors declare that no competing interests are present.

Acknowledgements. We would like to thank Prof. Volker Brüchert (Department of Geological Sciences at Stockholm University and Bolin Centre for Climate Research) for his constructive criticism during the reviewing process and for having shared the data of Laptev Sea sediment cores. The research leading to these results has received funding from the European Union's Horizon 2020 research and innovation programme under the Marie Skłodowska-Curie grant agreement No 643052 (C-CASCADES project).

References

Aguilera, D., Jourabchi, P., Spiteri, C., and Regnier, P.: A knowledge-based reactive transport approach for the simulation of biogeochemical dynamics in Earth systems, Geochemistry, Geophysics, Geosystems, 6, 2005.

Albert, D. B., Martens, C. S., and Alperin, M. J.: Biogeochemical processes controlling methane in gassy coastal sediments—part 2: Groundwater flow control of acoustic turbidity in Eckernförde Bay Sediments, Continental Shelf Research, 18, 1771–1793, 1998.

Aloisi, G., Wallmann, K., Haese, R., and Saliege, J.-F.: Chemical, biological and hydrological controls on the 14C content of cold seep carbonate crusts: numerical modeling and implications for convection at cold seeps, Chemical Geology, 213, 359–383, 2004.

Aris, R.: Prolegomena to the rational analysis of systems of chemical reactions II. Some addenda, Archive for Rational Mechanics and Analysis, 27, 356–364, 1968.

Arndt, S., Jørgensen, B. B., LaRowe, D. E., Middelburg, J., Pancost, R., and Regnier, P.: Quantifying the degradation of organic matter in marine sediments: a review and synthesis, Earth-science reviews, 123, 53–86, 2013.

Athy, L. F.: Density, porosity, and compaction of sedimentary rocks, AAPG Bulletin, 14, 1–24, 1930.

Baker, G. and Osterkamp, T.: Implications of salt fingering processes for salt movement in thawed coarse-grained subsea permafrost, Cold regions science and technology, 15, 45–52, 1988.

Barton, B. I., Lenn, Y.-D., and Lique, C.: Observed Atlantification of the Barents Sea causes the Polar Front to limit the expansion of winter sea ice, Journal of Physical Oceanography, 48, 1849–1866, 2018.

Bauch, H. A., Mueller-Lupp, T., Taldenkova, E., Spielhagen, R. F., Kassens, H., Grootes, P. M., Thiede, J., Heinemeier, J., and Petryashov, V.: Chronology of the Holocene transgression at the North Siberian margin, Global and Planetary Change, 31, 125–139, 2001.

Bekryaev, R. V., Polyakov, I. V., and Alexeev, V. A.: Role of polar amplification in long-term surface air temperature variations and modern Arctic warming, Journal of Climate, 23, 3888–3906, 2010.

Berchet, A., Bousquet, P., Pison, I., Locatelli, R., Chevallier, F., Paris, J.-D., Dlugokencky, E. J., Laurila, T., Hatakka, J., Viisanen, Y., et al.: Atmospheric constraints on the methane emissions from the East Siberian Shelf, Atmospheric Chemistry and Physics, 16, 4147–4157, 2016.

Berner, R. A.: Early diagenesis: a theoretical approach, 1, Princeton University Press, 1980.

Biastoch, A., Treude, T., Rüpke, L. H., Riebesell, U., Roth, C., Burwicz, E. B., Park, W., Latif, M., Böning, C. W., Madec, G., et al.: Rising Arctic Ocean temperatures cause gas hydrate destabilization and ocean acidification, Geophysical Research Letters, 38, 2011.

Boetius, A., Ravenschlag, K., Schubert, C. J., Rickert, D., Widdel, F., Gieseke, A., Amann, R., Jørgensen, B. B., Witte, U., and Pfannkuche, O.: A marine microbial consortium apparently mediating anaerobic oxidation of methane, Nature, 407, 623, 2000.

Bolshiyanov, D., Makarov, A., and Savelieva, L.: Lena River delta formation during the Holocene, Biogeosciences, 12, 579–593, 2015.

Borges, A. and Abril, G.: 5.04-Carbon dioxide and methane dynamics in estuaries, Treatise on Estuarine and Coastal Science, Volume 5: Biogeochemistry, pp. 119–161, 2011.

Borowski, W. S., Paull, C. K., and Ussler III, W.: Marine pore-water sulfate profiles indicate in situ methane flux from underlying gas hydrate, Geology, 24, 655–658, 1996.

Boudreau, B. P.: Mathematics of tracer mixing in sediments: I. Spatially-dependent, diffusive mixing, Am. J. Sci, 286, 161–198, 1986.

Boudreau, B. P.: Diagenetic models and their implementation, vol. 505, Springer Berlin, 1997.

Boudreau, B. P.: Boudreau, Bernard P. "The physics of bubbles in surficial, soft, cohesive sediments, Marine and Petroleum Geology, 38, 1–18, 2012.

Boudreau, B. P. and Ruddick, B. R.: On a reactive continuum representation of organic matter diagenesis, American Journal of Science, 291, 507–538, 1991.

Boudreau, B. P., Algar, C., Johnson, B. D., Croudace, I., Reed, A., Furukawa, Y., Dorgan, K. M., Jumars, P. A., Grader, A. S., and Gardiner, B. S.: Bubble growth and rise in soft sediments, Geology, 33, 517–520, 2005.

Bowles, M. W., Mogollón, J. M., Kasten, S., Zabel, M., and Hinrichs, K.-U.: Global rates of marine sulfate reduction and implications for sub–sea-floor metabolic activities, Science, 344, 889–891, 2014.

Bröder, L., Tesi, T., Andersson, A., Eglinton, T. I., Semiletov, I. P., Dudarev, O. V., Roos, P., and Gustafsson, Ö.: Historical records of organic matter supply and degradation status in the East Siberian Sea, Organic Geochemistry, 91, 16–30, 2016.

Bruce, E. R. and Perry, L. M.: Environmental biotechnology: principles and applications, New York: McGrawHill, 400, 2001.

Brüchert, V.: Unpublished raw data, 2020.

Brüchert, V., Bröder, L., Sawicka, J. E., Tesi, T., Joye, S. P., Sun, X., Semiletov, I. P., and Samarkin, V. A.: Carbon mineralization in Laptev and East Siberian sea shelf and slope sediment, Biogeosciences, 15, 471–490, 2018.

Burwicz, E. B., Rüpke, L., and Wallmann, K.: Estimation of the global amount of submarine gas hydrates formed via microbial methane formation based on numerical reaction-transport modeling and a novel parameterization of Holocene sedimentation, Geochimica et Cosmochimica Acta, 75, 4562–4576, 2011.

Capet, A., Meysman, F. J., Akoumianaki, I., Soetaert, K., and Grégoire, M.: Integrating sediment biogeochemistry into 3D oceanic models: a study of benthic-pelagic coupling in the Black Sea, Ocean Modelling, 101, 83–100, 2016.

Carmack, E. C., Macdonald, R. W., Perkin, R. G., McLaughlin, F. A., and Pearson, R. J.: Evidence for warming of Atlantic water in the southern Canadian Basin of the Arctic Ocean: Results from the Larsen-93 expedition, Geophysical Research Letters, 22, 1061–1064, 1995.

Centler, F., Shao, H., De Biase, C., Park, C.-H., Regnier, P., Kolditz, O., and Thullner, M.: GeoSysBRNS—A flexible multidimensional reactive transport model for simulating biogeochemical subsurface processes, Computers & Geosciences, 36, 397–405, 2010.

Charkin, A. N., Rutgers van der Loeff, M., Shakhova, N. E., Gustafsson, Ö., Dudarev, O. V., Cherepnev, M. S., Salyuk, A. N., Koshurnikov, A. V., Spivak, E. A., Gunar, A. Y., et al.: Discovery and characterization of submarine groundwater discharge in the Siberian Arctic seas: a case study in the Buor-Khaya Gulf, Laptev Sea, The Cryosphere, 11, 2305–2327, 2017.

Chatterjee, S., Dickens, G. R., Bhatnagar, G., Chapman, W. G., Dugan, B., Snyder, G. T., and Hirasaki, G. J.: Pore water sulfate, alkalinity, and carbon isotope profiles in shallow sediment above marine gas hydrate systems: A numerical modeling perspective, Journal of Geophysical Research: Solid Earth, 116, 2011.

Christensen, J., Krishna Kumar, K., Aldrian, E., An, S., Cavalcanti, I., de Castro, M., Dong, W., Goswami, A., Hall, A., Kanyanga, J., et al.: Climate change 2013: the physical scientific basis, Contribution of Working Group I to the Fifth Assessment Report of the Intergovernmental Panel on Climate Change, 2013.

Clough, L. M., Ambrose Jr, W. G., Cochran, J. K., Barnes, C., Renaud, P. E., and Aller, R. C.: Infaunal density, biomass and bioturbation in the sediments of the Arctic Ocean, Deep Sea Research Part II: Topical Studies in Oceanography, 44, 1683–1704, 1997.

Cordes, E. E., Arthur, M. A., Shea, K., Arvidson, R. S., and Fisher, C. R.: Modeling the mutualistic interactions between tubeworms and microbial consortia, PLoS Biology, 3, e77, 2005.

Crémière, A., Lepland, A., Chand, S., Sahy, D., Condon, D. J., Noble, S. R., Martma, T., Thorsnes, T., Sauer, S., and Brunstad, H.: Timescales of methane seepage on the Norwegian margin following collapse of the Scandinavian Ice Sheet, Nature communications, 7, 11 509, 2016a.

Crémière, A., Lepland, A., Chand, S., Sahy, D., Kirsimäe, K., Bau, M., Whitehouse, M. J., Noble, S. R., Martma, T., Thorsnes, T., et al.: Fluid source and methane-related diagenetic processes recorded in cold seep carbonates from the Alvheim channel, central North Sea, Chemical Geology, 432, 16–33, 2016b.

Dale, A. W., Regnier, P., and Van Cappellen, P.: Bioenergetic controls on anaerobic oxidation of methane (AOM) in coastal marine sediments: a theoretical analysis, American Journal of Science, 306, 246–294, 2006.

Dale, A. W., Aguilera, D., Regnier, P., Fossing, H., Knab, N., and Jørgensen, B. B.: Seasonal dynamics of the depth and rate of anaerobic oxidation of methane in Aarhus Bay (Denmark) sediments, Journal of Marine Research, 66, 127–155, 2008a.

Dale, A. W., Regnier, P., Knab, N., Jørgensen, B. B., and Van Cappellen, P.: Anaerobic oxidation of methane (AOM) in marine sediments from the Skagerrak (Denmark): II. Reaction-transport modeling, Geochimica et Cosmochimica Acta, 72, 2880–2894, 2008b.

Dale, A. W., Van Cappellen, P., Aguilera, D., and Regnier, P.: Methane efflux from marine sediments in passive and active margins: Estimations from bioenergetic reaction–transport simulations, Earth and Planetary Science Letters, 265, 329–344, 2008c.

Dale, A. W., Brüchert, V., Alperin, M., and Regnier, P.: An integrated sulfur isotope model for Namibian shelf sediments, Geochimica et Cosmochimica Acta, 73, 1924–1944, 2009.

Dale, A. W., Nickelsen, L., Scholz, F., Hensen, C., Oschlies, A., and Wallmann, K.: A revised global estimate of dissolved iron fluxes from marine sediments, Global Biogeochemical Cycles, 29, 691–707, 2015.

Dale, A. W., Graco, M., and Wallmann, K.: Strong and dynamic benthic-pelagic coupling and feedbacks in a coastal upwelling system (Peruvian shelf), Frontiers in Marine Science, 4, 29, 2017.

Dean, J. F., Middelburg, J. J., Röckmann, T., Aerts, R., Blauw, L. G., Egger, M., Jetten, M. S., Jong, A. E., Meisel, O. H., Rasigraf, O., et al.: Methane feedbacks to the global climate system in a warmer world, Reviews of Geophysics, 2018.

Dickson, A. G. and Goyet, C.: Handbook of methods for the analysis of the various parameters of the carbon dioxide system in sea water. Version 2, Tech. rep., Oak Ridge National Lab., TN (United States), 1994.

Dmitrenko, I. A., Kirillov, S. A., Tremblay, L. B., Kassens, H., Anisimov, O. A., Lavrov, S. A., Razumov, S. O., and Grigoriev, M. N.: Recent changes in shelf hydrography in the Siberian Arctic: Potential for subsea permafrost instability, Journal of Geophysical Research: Oceans, 116, 2011.

Drachev, S. S., Savostin, L. A., Groshev, V. G., and Bruni, I. E.: Structure and geology of the continental shelf of the Laptev Sea, Eastern Russian Arctic, Tectonophysics, 298, 357–393, 1998.

Drake, T. W., Wickland, K. P., Spencer, R. G., McKnight, D. M., and Striegl, R. G.: Ancient low–molecular-weight organic acids in permafrost fuel rapid carbon dioxide production upon thaw, Proceedings of the National Academy of Sciences, 112, 13 946–13 951, 2015.

Duan, Z., Møller, N., Greenberg, J., and Weare, J. H.: The prediction of methane solubility in natural waters to high ionic strength from 0 to 250 C and from 0 to 1600 bar, Geochimica et Cosmochimica Acta, 56, 1451–1460, 1992.

Egger, M., Lenstra, W., Jong, D., Meysman, F. J., Sapart, C. J., van der Veen, C., Röckmann, T., Gonzalez, S., and Slomp, C. P.: Rapid sediment accumulation results in high methane effluxes from coastal sediments, PloS one, 11, e0161 609, 2016.

Egger, M., Riedinger, N., Mogollón, J. M., and Jørgensen, B. B.: Global diffusive fluxes of methane in marine sediments, Nature Geoscience, 11, 421, 2018.

Fairbanks, R. G.: A 17,000-year glacio-eustatic sea level record: influence of glacial melting rates on the Younger Dryas event and deep-ocean circulation, Nature, 342, 637, 1989.

Fossing, H., Ferdelman, T. G., and Berg, P.: Sulfate reduction and methane oxidation in continental margin sediments influenced by irrigation (South-East Atlantic off Namibia), Geochimica et Cosmochimica Acta, 64, 897–910, 2000.

Gramberg, I. S., Kulakov, Y. N., Pogrebitsky, Y. E., and Sorokov, D. S.: Arctic oil and gas super basin, X World Petroleum Congress., pp. 93–99, 1983.

Graves, C. A., James, R. H., Sapart, C. J., Stott, A. W., Wright, I. C., Berndt, C., Westbrook, G. K., and Connelly, D. P.: Methane in shallow subsurface sediments at the landward limit of the gas hydrate stability zone offshore western Svalbard, Geochimica et Cosmochimica Acta, 198, 419–438, 2017.

Guo, L., Ping, C.-L., and Macdonald, R. W.: Mobilization pathways of organic carbon from permafrost to arctic rivers in a changing climate, Geophysical Research Letters, 34, 2007.

Gypens, N., Lancelot, C., and Soetaert, K.: Simple parameterisations for describing N and P diagenetic processes: Application in the North Sea, Progress in oceanography, 76, 89–110, 2008.

Haeckel, M., Suess, E., Wallmann, K., and Rickert, D.: Rising methane gas bubbles form massive hydrate layers at the seafloor, Geochimica et Cosmochimica Acta, 68, 4335–4345, 2004.

Haese, R. R., Meile, C., Van Cappellen, P., and De Lange, G. J.: Carbon geochemistry of cold seeps: methane fluxes and transformation in sediments from Kazan mud volcano, eastern Mediterranean Sea, Earth and Planetary Science Letters, 212, 361–375, 2003.

Hensen, C. and Wallmann, K.: Methane formation at Costa Rica continental margin—constraints for gas hydrate inventories and cross-décollement fluid flow, Earth and Planetary Science Letters, 236, 41–60, 2005.

Hinrichs, K.-U. and Boetius, A.: The anaerobic oxidation of methane: new insights in microbial ecology and biogeochemistry, in: Ocean margin systems, pp. 457–477, Springer, 2002.

Ho, T. and Aris, R.: On apparent second-order kinetics, AIChE journal, 33, 1050–1051, 1987.

Hunter, S., Goldobin, D., Haywood, A., Ridgwell, A., and Rees, J.: Sensitivity of the global submarine hydrate inventory to scenarios of future climate change, Earth and Planetary Science Letters, 367, 105–115, 2013.

Iversen, N. and Jorgensen, B. B.: Anaerobic methane oxidation rates at the sulfate-methane transition in marine sediments from Kattegat and Skagerrak (Denmark) 1, Limnology and Oceanography, 30, 944–955, 1985.

Jakobsson, M., Mayer, L., Coakley, B., Dowdeswell, J. A., Forbes, S., Fridman, B., Hodnesdal, H., Noormets, R., Pedersen, R., Rebesco, M., et al.: The international bathymetric chart of the Arctic Ocean (IBCAO) version 3.0, Geophysical Research Letters, 39, 2012.

James, R. H., Bousquet, P., Bussmann, I., Haeckel, M., Kipfer, R., Leifer, I., Niemann, H., Ostrovsky, I., Piskozub, J., Rehder, G., et al.: Effects of climate change on methane emissions from seafloor sediments in the Arctic Ocean: A review, Limnology and oceanography, 61, 2016.

Janout, M., Hölemann, J., Juhls, B., Krumpen, T., Rabe, B., Bauch, D., Wegner, C., Kassens, H., and Timokhov, L.: Episodic warming of near-bottom waters under the Arctic sea ice on the central Laptev Sea shelf, Geophysical Research Letters, 43, 264–272, 2016.

Jeffries, M. and Richter-Menge, J.: State of the climate in 2011: The Arctic, Bull. Am. Meteorol. Soc, 93, S127–S148, 2012.

Jin, Q. and Bethke, C. M.: Predicting the rate of microbial respiration in geochemical environments, Geochimica et Cosmochimica Acta, 69, 1133–1143, 2005.

Jørgensen, B. B., Weber, A., and Zopfi, J.: Sulfate reduction and anaerobic methane oxidation in Black Sea sediments, Deep Sea Research Part I: Oceanographic Research Papers, 48, 2097–2120, 2001.

Jourabchi, P., Van Cappellen, P., and Regnier, P.: Quantitative interpretation of pH distributions in aquatic sediments: A reaction-transport modeling approach, American Journal of Science, 305, 919–956, 2005.

Judd, A. and Hovland, M.: Seabed fluid flow: the impact on geology, biology and the marine environment, Cambridge University Press, 2009.

Karaca, D., Hensen, C., and Wallmann, K.: Controls on authigenic carbonate precipitation at cold seeps along the convergent margin off Costa Rica, Geochemistry, Geophysics, Geosystems, 11, 2010.

Knab, N., Cragg, B. A., Hornibrook, E., Holmkvist, L., Borowski, C., Parkes, R., and Jørgensen, B. B.: Regulation of anaerobic methane oxidation in sediments of the Black Sea, Biogeosciences Discussions, 5, 2305–2341, 2008.

Knittel, K. and Boetius, A.: Anaerobic oxidation of methane: progress with an unknown process, Annual review of microbiology, 63, 311–334, 2009.

Kretschmer, K., Biastoch, A., Rüpke, L., and Burwicz, E.: Modeling the fate of methane hydrates under global warming, Global Biogeochemical Cycles, 29, 610–625, 2015.

Krüger, M., Meyerdierks, A., Glöckner, F. O., Amann, R., Widdel, F., Kube, M., Reinhardt, R., Kahnt, J., Böcher, R., Thauer, R. K., et al.: A conspicuous nickel protein in microbial mats that oxidize methane anaerobically, Nature, 426, 878, 2003.

LaRowe, D., Dale, A. W., and Regnier, P.: A thermodynamic analysis of the anaerobic oxidation of methane in marine sediments, Geobiology, 6, 436–449, 2008.

LaRowe, D. E., Burwicz, E., Arndt, S., Dale, A. W., and Amend, J. P.: Temperature and volume of global marine sediments, Geology, 45, 275–278, 2017.

Leifer, I., Chernykh, D., Shakhova, N., and Semiletov, I.: Sonar gas flux estimation by bubble insonification: application to methane bubble flux from seep areas in the outer Laptev Sea, The Cryosphere, 11, 1333–1350, 2017.

Levitan, M. A. and Lavrushin, Y. A.: Sedimentation history in the Arctic Ocean and Subarctic Seas for the last 130 kyr, vol. 118, Springer Science & Business Media, 2009.

Linke, P., Wallmann, K., Suess, E., Hensen, C., and Rehder, G.: In situ benthic fluxes from an intermittently active mud volcano at the Costa Rica convergent margin, Earth and Planetary Science Letters, 235, 79–95, 2005.

Lösekann, T., Knittel, K., Nadalig, T., Fuchs, B., Niemann, H., Boetius, A., and Amann, R.: Diversity and abundance of aerobic and anaerobic methane oxidizers at the Haakon Mosby Mud Volcano, Barents Sea, Appl. Environ. Microbiol., 73, 3348–3362, 2007.

Luff, R. and Wallmann, K.: Fluid flow, methane fluxes, carbonate precipitation and biogeochemical turnover in gas hydrate-bearing sediments at Hydrate Ridge, Cascadia Margin: numerical modeling and mass balances, Geochimica et Cosmochimica Acta, 67, 3403–3421, 2003.

Luff, R., Greinert, J., Wallmann, K., Klaucke, I., and Suess, E.: Simulation of long-term feedbacks from authigenic carbonate crust formation at cold vent sites, Chemical Geology, 216, 157–174, 2005.

Maher, K., Steefel, C. I., DePaolo, D. J., and Viani, B. E.: The mineral dissolution rate conundrum: Insights from reactive transport modeling of U isotopes and pore fluid chemistry in marine sediments, Geochimica et Cosmochimica Acta, 70, 337–363, 2006.

Marquardt, M., Hensen, C., Pinero, E., Wallmann, K., and Haeckel, M.: A transfer function for the prediction of gas hydrate inventories in marine sediments, Biogeosciences (BG), 7, 2925–2941, 2010.

Martens, C. S., Albert, D. B., and Alperin, M. J.: Biogeochemical processes controlling methane in gassy coastal sediments—Part 1. A model coupling organic matter flux to gas production, oxidation and transport, Continental Shelf Research, 18, 1741–1770, 1998.

Masson-Delmotte, V., Zhai, P., Pörtner, H. O., Roberts, D., Skea, J., Shukla, P., Pirani, A., Moufouma-Okia, W., Péan, C., Pidcock, R., Connors, S., Matthews, J. B. R., Chen, Y., Zhou, X., Gomis, M. I., Lonnoy, E., Maycock, T., Tignor, M., and Waterfield, T.: IPCC, 2018: Global warming of 1.5°C. An IPCC Special Report on the impacts of global warming of 1.5°C above pre-industrial levels and related global greenhouse gas emission pathways, in the context of strengthening the global response to the threat of climate change, sustainable development, and efforts to eradicate poverty, Tech. rep., 2018.

McGlynn, S. E., Chadwick, G. L., Kempes, C. P., and Orphan, V. J.: Single cell activity reveals direct electron transfer in methanotrophic consortia, Nature, 526, 531, 2015.

McGuire, A. D., Anderson, L. G., Christensen, T. R., Dallimore, S., Guo, L., Hayes, D. J., Heimann, M., Lorenson, T. D., Macdonald, R. W., and Roulet, N.: Sensitivity of the carbon cycle in the Arctic to climate change, Ecological Monographs, 79, 523–555, 2009.

Meister, P., Liu, B., Ferdelman, T. G., Jørgensen, B. B., and Khalili, A.: Control of sulphate and methane distributions in marine sediments by organic matter reactivity, Geochimica et Cosmochimica Acta, 104, 183–193, 2013.

Meister, P., Wiedling, J., Lott, C., Bach, W., Kuhfuß, H., Wegener, G., Böttcher, M. E., Deusner, C., Lichtschlag, A., Bernasconi, S. M., et al.: Anaerobic methane oxidation inducing carbonate precipitation at abiogenic methane seeps in the Tuscan archipelago (Italy), PloS one, 13, 2018.

Middelburg, J. J., Soetaert, K., and Herman, P. M.: Empirical relationships for use in global diagenetic models, Deep Sea Research Part I: Oceanographic Research Papers, 44, 327–344, 1997.

Miller, C. M., Dickens, G. R., Jakobsson, M., Johansson, C., Koshurnikov, A., O'Regan, M., Muschitiello, F., Stranne, C., and Mörth, C.-M.: Pore water geochemistry along continental slopes north of the East Siberian Sea: inference of low methane concentrations, Biogeosciences, 14, 2929–2953, 2017.

Milucka, J., Ferdelman, T. G., Polerecky, L., Franzke, D., Wegener, G., Schmid, M., Lieberwirth, I., Wagner, M., Widdel, F., and Kuypers, M. M.: Zero-valent sulphur is a key intermediate in marine methane oxidation, Nature, 491, 541, 2012.

Mogollón, J. M., L'Heureux, I., Dale, A. W., and Regnier, P.: Methane gas-phase dynamics in marine sediments: A model study, American Journal of Science, 309, 189–220, 2009.

Nauhaus, K., Albrecht, M., Elvert, M., Boetius, A., and Widdel, F.: In vitro cell growth of marine archaeal-bacterial consortia during anaerobic oxidation of methane with sulfate, Environmental Microbiology, 9, 187–196, 2007.

Niemann, H., Duarte, J., Hensen, C., Omoregie, E., Magalhaes, V., Elvert, M., Pinheiro, L., Kopf, A., and Boetius, A.: Microbial methane turnover at mud volcanoes of the Gulf of Cadiz, Geochimica et Cosmochimica Acta, 70, 5336–5355, 2006a.

Niemann, H., Lösekann, T., De Beer, D., Elvert, M., Nadalig, T., Knittel, K., Amann, R., Sauter, E. J., Schlüter, M., Klages, M., et al.: Novel microbial communities of the Haakon Mosby mud volcano and their role as a methane sink, Nature, 443, 854, 2006b.

O'Connor, F. M., Boucher, O., Gedney, N., Jones, C., Folberth, G., Coppell, R., Friedlingstein, P., Collins, W., Chappellaz, J., Ridley, J., et al.: Possible role of wetlands, permafrost, and methane hydrates in the methane cycle under future climate change: A review, Reviews of Geophysics, 48, 2010.

Overduin, P., Wetterich, S., Günther, F., Grigoriev, M. N., Grosse, G., Schirrmeister, L., Hubberten, H.-W., and Makarov, A. S.: Coastal dynamics and submarine permafrost in shallow water of the central Laptev Sea, East Siberia, Cryosphere, 10, 1449–1462, 2016.

Overduin, P. P., Liebner, S., Knoblauch, C., Günther, F., Wetterich, S., Schirrmeister, L., Hubberten, H.-W., and Grigoriev, M. N.: Methane oxidation following submarine permafrost degradation: Measurements from a central Laptev Sea shelf borehole, Journal of Geophysical Research: Biogeosciences, 120, 965–978, 2015.

Piechura, J. and Walczowski, W.: The Arctic Front: structure and dynamics, Oceanologia, 37, 47–73, 1995.

Pierre, C., Blanc-Valleron, M.-M., Demange, J., Boudouma, O., Foucher, J.-P., Pape, T., Himmler, T., Fekete, N., and Spiess, V.: Authigenic carbonates from active methane seeps offshore southwest Africa, Geo-Marine Letters, 32, 501–513, 2012.

Piker, L., Schmaljohann, R., and Imhoff, J. F.: Dissimilatory sulfate reduction and methane production in Gotland Deep sediments (Baltic Sea) during a transition period from oxic to anoxic bottom water (1993-1996), Aquatic Microbial Ecology, 14, 183–193, 1998.

Polyakov, I. V., Pnyushkov, A. V., Alkire, M. B., Ashik, I. M., Baumann, T. M., Carmack, E. C., Goszczko, I., Guthrie, J., Ivanov, V. V., Kanzow, T., et al.: Greater role for Atlantic inflows on sea-ice loss in the Eurasian Basin of the Arctic Ocean, Science, 356, 285–291, 2017.

Reagan, M. T. and Moridis, G. J.: Large-scale simulation of methane hydrate dissociation along the West Spitsbergen Margin, Geophysical research letters, 36, 2009.

Reeburgh, W. S.: Oceanic methane biogeochemistry, Chemical reviews, 107, 486–513, 2007.

Regnier, P., O'kane, J., Steefel, C., and Vanderborght, J.-P.: Modeling complex multi-component reactive-transport systems: towards a simulation environment based on the concept of a Knowledge Base, Applied Mathematical Modelling, 26, 913–927, 2002.

Regnier, P., Dale, A. W., Arndt, S., LaRowe, D., Mogollón, J., and Van Cappellen, P.: Quantitative analysis of anaerobic oxidation of methane (AOM) in marine sediments: a modeling perspective, Earth-Science Reviews, 106, 105–130, 2011.

Rittmann, B. and VanBriesen, J. M.: Microbiological processes in reactive modeling, in: Reactive Transport in Porous Media, pp. 311–334, Walter de Gruyter GmbH, 2019.

Rittmann, B. E. and McCarty, P. L.: Environmental biotechnology: principles and applications, Tata McGraw-Hill Education, 2012.

Romanovskii, N., Hubberten, H.-W., Gavrilov, A., Tumskoy, V., and Kholodov, A.: Permafrost of the east Siberian Arctic shelf and coastal lowlands, Quaternary Science Reviews, 23, 1359–1369, 2004.

Romanovskii, N., Hubberten, H.-W., Gavrilov, A., Eliseeva, A., and Tipenko, G.: Offshore permafrost and gas hydrate stability zone on the shelf of East Siberian Seas, Geo-marine letters, 25, 167–182, 2005.

Romanovskii, N. N. and Hubberten, H.-W.: Results of permafrost modelling of the lowlands and shelf of the Laptev Sea region, Russia, Permafrost and periglacial processes, 12, 191–202, 2001.

Ruppel, C. D. and Kessler, J. D.: The interaction of climate change and methane hydrates, Reviews of Geophysics, 55, 126–168, 2017.

Sales de Freitas, F.: Deciphering the relationships between reactivity and sources of organic matter in marine sediments: a coupled large-scale model and lipid biomarker analysis, Ph.D. thesis, School on Earth Sciences, University of Bristol, 2018.

Sapart, C. J., Shakhova, N., Semiletov, I., Jansen, J., Szidat, S., Kosmach, D., Dudarev, O., Van Der Veen, C., Egger, M., Sergienko, V., et al.: The origin of methane in the East Siberian Arctic Shelf unraveled with triple isotope analysis, Biogeosciences, 14, 2283–2292, 2017.

Saunois, M., Bousquet, P., Poulter, B., Peregon, A., Ciais, P., Canadell, J. G., Dlugokencky, E. J., Etiope, G., Bastviken, D., Houweling, S., et al.: The global methane budget 2000–2012, Earth System Science Data, 8, 697–751, 2016.

Semenov, P., Portnov, A., Krylov, A., Egorov, A., and Vanshtein, B.: Geochemical evidence for seabed fluid flow linked to the subsea permafrost outer border in the South Kara Sea, Geochemistry, 2019.

Shakhova, N., Semiletov, I., Leifer, I., Salyuk, A., Rekant, P., and Kosmach, D.: Geochemical and geophysical evidence of methane release over the East Siberian Arctic Shelf, Journal of Geophysical Research: Oceans, 115, 2010a.

Shakhova, N., Semiletov, I., Salyuk, A., Yusupov, V., Kosmach, D., and Gustafsson, Ö.: Extensive methane venting to the atmosphere from sediments of the East Siberian Arctic Shelf, Science, 327, 1246–1250, 2010b.

Shakhova, N., Semiletov, I., Leifer, I., Sergienko, V., Salyuk, A., Kosmach, D., Chernykh, D., Stubbs, C., Nicolsky, D., Tumskoy, V., et al.: Ebullition and storm-induced methane release from the East Siberian Arctic Shelf, Nature Geoscience, 7, 64, 2014.

Shakhova, N., Semiletov, I., Sergienko, V., Lobkovsky, L., Yusupov, V., Salyuk, A., Salomatin, A., Chernykh, D., Kosmach, D., Panteleev, G., et al.: The East Siberian Arctic Shelf: towards further assessment of permafrost-related methane fluxes and role of sea ice, Philosophical Transactions of the Royal Society A: Mathematical, Physical and Engineering Sciences, 373, 20140 451, 2015.

Shakhova, N., Semiletov, I., Gustafsson, O., Sergienko, V., Lobkovsky, L., Dudarev, O., Tumskoy, V., Grigoriev, M., Mazurov, A., Salyuk, A., et al.: Current rates and mechanisms of subsea permafrost degradation in the East Siberian Arctic Shelf, Nature communications, 8, 15 872, 2017.

Shakhova, N., Semiletov, I., and Chuvilin, E.: Understanding the permafrost–hydrate system and associated methane releases in the east Siberian Arctic Shelf, Geosciences, 9, 251, 2019.

Sloan Jr, E. D. and Koh, C.: Clathrate hydrates of natural gases, CRC press, 2007.

Sommer, S., Pfannkuche, O., Linke, P., Luff, R., Greinert, J., Drews, M., Gubsch, S., Pieper, M., Poser, M., and Viergutz, T.: Efficiency of the benthic filter: Biological control of the emission of dissolved methane from sediments containing shallow gas hydrates at Hydrate Ridge, Global Biogeochemical Cycles, 20, 2006.

Sparrow, K. J., Kessler, J. D., Southon, J. R., Garcia-Tigreros, F., Schreiner, K. M., Ruppel, C. D., Miller, J. B., Lehman, S. J., and Xu, X.: Limited contribution of ancient methane to surface waters of the US Beaufort Sea shelf, Science advances, 4, eaao4842, 2018.

Stein, R., Boucsein, B., Fahl, K., de Oteyza, T. G., Knies, J., and Niessen, F.: Accumulation of particulate organic carbon at the Eurasian continental margin during late Quaternary times: controlling mechanisms and paleoenvironmental significance, Global and Planetary Change, 31, 87–104, 2001.

Stranne, C., O'Regan, M., Jakobsson, M., Brüchert, V., and Ketzer, M.: Can anaerobic oxidation of methane prevent seafloor gas escape in a warming climate?, Solid Earth, 10, 1541–1554, 2019.

Teal, L., Bulling, M. T., Parker, E., and Solan, M.: Global patterns of bioturbation intensity and mixed depth of marine soft sediments, Aquatic Biology, 2, 207–218, 2008.

Tesi, T., Semiletov, I., Hugelius, G., Dudarev, O., Kuhry, P., and Gustafsson, Ö.: Composition and fate of terrigenous organic matter along the Arctic land–ocean continuum in East Siberia: Insights from biomarkers and carbon isotopes, Geochimica et Cosmochimica Acta, 133, 235–256, 2014.

Thang, N. M., Brüchert, V., Formolo, M., Wegener, G., Ginters, L., Jørgensen, B. B., and Ferdelman, T. G.: The impact of sediment and carbon fluxes on the biogeochemistry of methane and sulfur in littoral Baltic Sea sediments (Himmerfjärden, Sweden), Estuaries and Coasts, 36, 98–115, 2013.

Thornton, B. F., Geibel, M. C., Crill, P. M., Humborg, C., and Mörth, C.-M.: Methane fluxes from the sea to the atmosphere across the Siberian shelf seas, Geophysical Research Letters, 43, 5869–5877, 2016.

Thornton, B. F., Prytherch, J., Andersson, K., Brooks, I. M., Salisbury, D., Tjernström, M., and Crill, P. M.: Shipborne eddy covariance observations of methane fluxes constrain Arctic sea emissions, Science Advances, 6, eaay7934, 2020.

Thullner, M., Van Cappellen, P., and Regnier, P.: Modeling the impact of microbial activity on redox dynamics in porous media, Geochimica et Cosmochimica Acta, 69, 5005–5019, 2005.

Thullner, M., Dale, A. W., and Regnier, P.: Global-scale quantification of mineralization pathways in marine sediments: A reaction-transport modeling approach, Geochemistry, geophysics, geosystems, 10, 2009.

Tishchenko, P., Hensen, C., Wallmann, K., and Wong, C. S.: Calculation of the stability and solubility of methane hydrate in seawater, Chemical geology, 219, 37–52, 2005.

Trenberth, K., Jones, P., Ambenje, P., Bojariu, R., Easterling, D., Klein Tank, A., Parker, D., Rahimzadeh, F., Renwick, J., Rusticucci, M., et al.: Observations: surface and atmospheric climate change. Chapter 3, Climate change, pp. 235–336, 2007.

Treude, T., Boetius, A., Knittel, K., Wallmann, K., and Jørgensen, B. B.: Anaerobic oxidation of methane above gas hydrates at Hydrate Ridge, NE Pacific Ocean, Marine Ecology Progress Series, 264, 1–14, 2003.

Treude, T., Krüger, M., Boetius, A., and Jørgensen, B. B.: Environmental control on anaerobic oxidation of methane in the gassy sediments of Eckernförde Bay (German Baltic), Limnology and oceanography, 50, 1771–1786, 2005.

Vonk, J. E., Sánchez-García, L., Van Dongen, B., Alling, V., Kosmach, D., Charkin, A., Semiletov, I. P., Dudarev, O. V., Shakhova, N., Roos, P., et al.: Activation of old carbon by erosion of coastal and subsea permafrost in Arctic Siberia, Nature, 489, 137, 2012.

Wallmann, K., Aloisi, G., Haeckel, M., Obzhirov, A., Pavlova, G., and Tishchenko, P.: Kinetics of organic matter degradation, microbial methane generation, and gas hydrate formation in anoxic marine sediments, Geochimica et Cosmochimica Acta, 70, 3905–3927, 2006a.

Wallmann, K., Drews, M., Aloisi, G., and Bohrmann, G.: Methane discharge into the Black Sea and the global ocean via fluid flow through submarine mud volcanoes, Earth and Planetary Science Letters, 248, 545–560, 2006b.

Wang, Y. and Van Cappellen, P.: A multicomponent reactive transport model of early diagenesis: Application to redox cycling in coastal marine sediments, Geochimica et Cosmochimica Acta, 60, 2993–3014, 1996.

Wegener, G., Krukenberg, V., Riedel, D., Tegetmeyer, H. E., and Boetius, A.: Intercellular wiring enables electron transfer between methanotrophic archaea and bacteria, Nature, 526, 587, 2015.

Wegner, C., Bennett, K. E., de Vernal, A., Forwick, M., Fritz, M., Heikkilä, M., Łącka, M., Lantuit, H., Laska, M., Moskalik, M., et al.: Variability in transport of terrigenous material on the shelves and the deep Arctic Ocean during the Holocene, Polar Research, 34, 24 964, 2015.

Westbrook, G. K., Thatcher, K. E., Rohling, E. J., Piotrowski, A. M., Pälike, H., Osborne, A. H., Nisbet, E. G., Minshull, T. A., Lanoisellé, M., James, R. H., et al.: Escape of methane gas from the seabed along the West Spitsbergen continental margin, Geophysical Research Letters, 36, 2009.

Wild, B., Andersson, A., Bröder, L., Vonk, J., Hugelius, G., McClelland, J. W., Song, W., Raymond, P. A., and Gustafsson, Ö.: Rivers across the Siberian Arctic unearth the patterns of carbon release from thawing permafrost, Proceedings of the National Academy of Sciences, p. 201811797, 2019.

Winkel, M., Mitzscherling, J., Overduin, P. P., Horn, F., Winterfeld, M., Rijkers, R., Grigoriev, M. N., Knoblauch, C., Mangelsdorf, K., Wagner, D., et al.: Anaerobic methanotrophic communities thrive in deep submarine permafrost, Scientific reports, 8, 1291, 2018.

Wright, J., Taylor, A., and Dallimore, S.: Thermal Impact of Holocene Lakes on a Permafrost Landscape, Mackenzie Delta, Canada, in: Proceedings of the Ninth international conference on Permafrost, Fairbanks, AK, 2008.

Yakushev, V. S.: Gas hydrates in cryolithozone, 11, 100–105, 1989.

Yao, H., Hong, W.-L., Panieri, G., Sauer, S., Torres, M. E., Lehmann, M. F., Gründger, F., and Niemann, H.: Fracture-controlled fluid transport supports microbial methane-oxidizing communities at Vestnesa Ridge, Biogeosciences, 16, 2221–2232, 2019.

Zhang, J., Rothrock, D. A., and Steele, M.: Warming of the Arctic Ocean by a strengthened Atlantic inflow: Model results, Geophysical Research Letters, 25, 1745–1748, 1998.